37th International Conference on Solution Chemistry

25th - 29th July, 2022

BOOK OF ABSTRACTS

Universidad de los Andes Colombia

37 I C S C

INTERNATIONAL UNION OF PURE AND APPLIED CHEMISTRY

Fundación Universidad de América

37th INTERNATIONAL CONFERENCE OF SOLUTION CHEMISTRY

BOOK OF ABSTRACTS

25th – 29th July, 2022

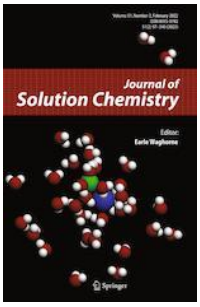

Committees

Academic Chairman
Edgar F. Vargas (Universidad de los Andes-Colombia)

General secretaries
Diana Madelen Galindres (Universidad de América--Colombia)
Valeria Eslava (MSD)

International Steering Committee
Prof. Dr. Toshio Yamaguchi (Fukuoka, Japan, Chairman)
Prof. Dr. Bešter Rogač (Slovenia)
Prof. Dr. G. Hefter (Murdoch, Australia)
Prof. Dr. Jalel Mhalla (Monastir, Tunisia)
Prof. Dr. I. Nezbed (Prague, Czech Republic)
Prof. Dr, Pál Sipos (Szeged, Hungary)
Prof. Dr. Yongquan Zhou (Xining, China)
Prof. Edgar F. Vargas (Bogotá, Colombia)
Prof. B. Gill* (Leeds, UK)
*Honorary member

Organizing Committee
Prof. Dr. Jhon Zapata Rivera (Universidad de los Andes-Colombia)
Prof. Dr. Maria Teresa Cortés (Universidad de los Andes-Colombia)
Prof. Dr. Fleming Martinez (Universidad Nacional de Colombia)
Maricell De la Hoz V. (Universidad de los Andes-Colombia)
Nicolas Espitia Galindo (Universidad de los Andes-Colombia)
Gerson Dirceu Lopez M. (Universidad de los Andes-Colombia)
Santiago Jose Mongua N. (Universidad de los Andes-Colombia)
Karen Gissela Segura A. (Universidad de los Andes-Colombia)
Juan Andres Gomez G. (Universidad de los Andes-Colombia)
Camila Andrea Hernandez A. (Universidad de los Andes-Colombia)
Laura Camila Martínez O. (Universidad de América-Colombia)
Maria Jose Marting C. (Universidad de América-Colombia)

Preface

Welcome to all, scientists, researchers, students and colleagues to the 37th ICSC held for the first time in Latin America in Colombia on July 26-29, 2022. We are honored to be able to invite you from Colombia since that is in scientific development in the past years with aims to develop technology and innovation towards the wellbeing of the society. We are happy to contribute and discuss new discoveries in solution chemistry, for this reason we want to invite you all to participate in this conference to meet and share your contributions, discoveries, methods and ideas to spread knowledge and guide the new generations in the field and in its applications to help and improve society.

The past years have been a time of changes and reflection for all. We had a pandemic that no one expected, border closures, lockdowns, and more, but also many scientific advances. Initially we had planned to hold this conference in Cartagena and it is a shame that you all could not get to know this jewel of the Caribbean and that we could not directly share this experience. However, we are very happy to be able to have this conference virtually because we will be able to share our achievements and advances and learn more about different topics and meet even if it is through a computer. We hope all your loved ones are doing well. We hope that we all get out of this pandemic and we can meet again face to face in the 38Th ICSC in Belgrade next year.

37th ICSC will be provide 15 plenary and Key Note lectures given by world renowned professors, 34 oral presentations and 39 flash presentations in 4 days covering the conference themes, We hope that this scientific meeting will be memorable, that it allows you to acquire diverse knowledge in the area and its applications, we are sure that this will allow to strengthen contacts between scientists with a long history and young researchers, we hope that our social activities will be of pleasure for all its participants and their companions at the event. Welcome and we appreciate and value your participation.

Organizing Committee

Table of Contents

Invited Speakers

PROF. MARIJA BEŠTER ROGAČ
SLOVENIA

PROF. LIMEI XU
CHINA

PROF. CLARA MAGALHÃES
AUSTRALIA

PROF. LOUISE J. CRISCENTI
USA

PROF. GABRIEL MERINO
MEXICO

PROF. RICHARD BUCHNER
GERMANY

PROF. INGMAR PERSSON
SWEDEN

PROF. GLENN HEFTER
AUSTRALIA

PROF. DANIEL BOWRON
UK

PROF. TOSHIYUKI TAKAMUKU
JAPAN

PROF. EMIKO OKAMURA
JAPAN

PROF. ROGER M. LEBLANC
USA

PROF. NACER IDRISSI
FRANCE

PROF. WINFIELD EARLE WAGHORNE
IRELAND

PROF. PAL JEDLOVSZKY
HUNGARY

37th ICSC Program

Monday 25th (UTC/GMT -5 hours)

Local Time Americas (UTC/GMT -5 hours)		Name	Abstract Title	Country	Chair	Local Time Europe-Africa	Local Time Asia-Australia
8:00	8:05	Open Ceremony Prof. Dr. Edgar vargas				(UTC/GMT +1 hour)	(UTC/GMT +9 hours)
8:05	8:15	Open Ceremony Prof. Dr. Toshio Yamaguchi					
8:15	9:00	Plenary Lecture (PL1) Prof. Dr. Roger M. Leblanc	Solution State Applications of Carbon Dots	USA	Prof. Dr. Pál Sipos		
9:00	9:45	Plenary Lecture (PL2) Prof. Dr. Gabriel Merino	Microsolvation of Acids	Mexico			
9:45	10:20	Key Note Lecture (KN 1) Prof. Dr. Louise Criscenti	Modeling Ion Adsorption in Aqueous Solutions at Oxide Surfaces	USA			
10:20	10:40	Break					
10:40	11:00	OT 1 Prof. Dr. Cory Pye	Computational chemistry applied to solutions: anions	Canada	Prof. Dr. Luis Branco		
11:00	11:20	OT 2 Prof. Dr. Fleming Martínez	Preferential solvation of baicalein in ethanol + water mixtures at 298.15 K	Colombia			
11:20	11:40	OT 3 Prof. Dr. Jorge. A. Ramírez	Spectral analysis by Functional Enhanced Derivative Spectroscopy (FEDS) method to determine relative values of pH, CECe and OC in agricole soils	Colombia	Prof. Dr. Luis Branco		
11:40	12:00	OT 4 Graduate student. Juan Carlos Sanabria	Influence of tetraalkylammonium salts on the adsorption kinetics of bovine serum albumin in aqueous solutions at the air-liquid interface	Colombia			
12:00	14:00	Lunch					
14:00	14:20	OT 5 Graduate student. Gerson Dirceu	Antioxidant potential of carotenoids-rich extracts from Staphylococcus aureus isolated by pressurized-liquid extraction and conventional extraction	Colombia	Prof. Dr. Cory Pye		
14:20	14:40	OT 6 Prof. Dr. Edgar Vargas	Physicochemical properties of some drugs in solution	Colombia			

Local Time Americas (UTC/GMT -5 hours)		Name	Abstract Title	Country	Chair	Local Time Europe-Africa	Local Time Asia-Australia
14:40	15:00	OT 7 Graduate student. Jhonny Ososrio, Elena Tinoco	Python to determine solubility in cosolvent mixtures	Colombia			
15:00	15:20	OT 8 BASF	To be Confimed	Colombia			
15:20	15:40	OT 9 Graduate student. Alberto Enrique Molina	Preliminary study of photoelectrochemical properties of Cerium Dioxide (CeO2) obtained by electrochemical synthesis	Colombia	Prof. Dr. Gabriel Merino		
15:40	16:00	OT 10 Dr. Martín Emilio González	Cobalt(II) Meso-Tetra-(4-Sulfonatophenyl)-Porphyrinate doped polypyrrole coatings for photoelectrochemical oxygen reduction.	Colombia			
16:00	16:20	Break					
16:20	16:40	OT 11 Prof. Dr. Madelen Galindres	Volumetric properties of two resorcin[4]arenes in solution	Colombia	Prof. Dr. Louise Criscenti		
16:40	17:00	OT 12 Prof. Dr. Jhon Zapata	Solvent Acting as Catalyst: BF3-Mediated Acetylation of Pyrazolo[1,5-a]pyrimidines	Colombia		(UTC/GMT +1 hour)	(UTC/GMT +9 hours)
17:00	18:20	**Posters session (Flash Presentations)**			Prof. Dr. Pál Sipos		
17:00	17:08	P1 Dr. Ruben Caro	Rheological Study f Poly(Styrene-Co-Acrylonitrile)/Carbon Nanotubes Solutions	México			
17:08	17:16	P2 Prof. Dr. Fleming Martínez	Effect of the mixtures composition on acetaminophen mass/volume percentage solubility in (ethanol + propylene glycol + water) mixtures at 25.0 °C	Colombia			
17:16	17:24	P3 Graduate student. Lazaro Ruiz Virgen	Smart polymeric particles sensitive to pH and Temperature and their application in the acid stimulation processes	México			
17:24	17:32	P4 Dr. Mayerly Johana Puchana	Influence of polyols on the activity and thermal stability of Horseradish peroxidase	Colombia			
17:32	17:40	P5 Graduate student. Daniel Carteño	Construction and Automation to improve a Calorimeter	México			

Local Time Americas (UTC/GMT -5 hours)		Name	Abstract Title	Country	Chair	Local Time Europe-Africa	Local Time Asia-Australia
17:40	17:48	P6 Graduate student. Karen segura	Laccase-Catalyzed Reactions in organic media	Colombia	Prof. Dr. Pál Sipos	(UTC/GMT +1 hour)	(UTC/GMT +9 hours)
17:48	17:56	P7 Prof. Dr. Fleming Martínez	Solubility of benzocaine in methanol + water mixtures according to the extended Hildebrand solubility approach	Colombia			
17:56	18:04	Dr. Valeria Eslava	Study of the interaction between resorcin[4}arenes and Insulin in aqueous solution	Colombia			
18:04	18:12	P9 Graduate student. Regina Cuervo Morales	Sodium alginate nanogels synthesis and characterization as potential drug deliverers	México			
18:12	18:20	P10 Graduate Student. Nicolas Espitia	Thermodynamics properties and electronic structure on the complexation of sodium sulfamerazine with an ionic resorcin[4]arene	Colombia			

Tuesday 26th (UTC/GMT +1 hour)

Local Time Europe-Africa (UTC/GMT +1 hour)		Name	Abstract Title	Country	Chair	Local Time Asia-Australia	Local Time Americas
8:00	8:45	Plenary Lecture (PL3) IUPAC Prof. Dr. Winfield Earle Waghorne	Solvent and solute basicities – computational chemistry and experimental parameters	Ireland	Prof Dr. Yongquan Zhou		
8:45	9:30	Plenary Lecture (PL4) Prof. Dr. Richard Buchner	Why does Ethaline not behave like a usual Deep Eutectic Solvent?	Germany	Prof. Dr. Ingmar Persson		
9:30	10:05	Key Note Lecture (KN 3) Prof. Dr. M. Clara F. Magalhães	Dissolution of iron(III) and aluminium minerals with aqueous solutions of siderophores	Portugal			
10:05	10:20	Break					
10:20	10:40	OT 13 Prof. Dr. Luis Branco	Ionic Liquids as functional additives for lubricant applications	Portugal	Prof. Dr. Marija Bešter Rogač		
10:40	11:00	OT 14 Prof. Dr. Slobodan Gadžurić	Interactions in the newly synthesized task specific ionic liquids	Serbia			
11:00	11:20	OT 15 Prof. Dr. Tomaž Urbič	An analytic model of water that gives accurate dynamic properties	Slovenia	Prof. Dr. M. Clara F. Magalhães	**(UTC/GMT +9 hours)**	**(UTC/GMT -5 hours)**
11:20	11:55	Key Note Lecture (KN 4) Prof. Dr. Pal Jedlovszky	Investigation of problems related to the lateral pressure profile	Hungary			
12:00	14:00	Lunch					
14:00	14:35	Key Note Lecture (KN 5) Prof. Dr. Nacer Idrissi	Thermodynamics of mixing of solute solvent mixture as seen from computer simulation and thermodynamic integration	France	Prof. Dr. Jalel Mhall		
14:35	15:05	Key Note Lecture (KN 6) Prof. Dr. Ingmar Persson	Coordination chemistry of Jahn-Teller distorted complexes in solution and solid state	Sweden	Prof. Dr. Jalel Mhall		
15:05	15:40	Key Note Lecture (KN 7) Prof. Dr. Daniel Bowron	Bulk and Local Structure in a 1M Aqueous Solution of Uranyl Chloride via Structure Refinement of Neutron Diffraction and EXAFS spectroscopy Data	UK	Prof. Dr. Pál Sipos		
15:40	16:00	OT 16 Dr. Matjaž Simončič	How co-solutes modulate the complexation between bovine serum albumin and sodium polystyrene sulfonate	Slovenia			

Local Time Europe-Africa (UTC/GMT +1 hour)		Name	Abstract Title	Country	Chair	Local Time Asia-Australia	Local Time Americas
16:00	16:20	OT 17 Prof. Dr. Sondes Boughammoura	New Approach for the Study of the Formation of Tetradecyltrimethylammonium Bromide (TTAB) micelles in (water- dioxane) mixtures.	Tunisia	Prof. Dr. Jhon Zapata	**(UTC/GMT +9 hours)**	**(UTC/GMT -5 hours)**
16:20	16:40	OT 18 Prof. Dr. Anis Ghazouani	Importance of dielectric friction effect in the interpretation of the dependency of the mobility of carboxymethylcellulose polyion chains on the nature of their counterions	Tunisia			
16:40	17:00	OT 19 Prof. Dr. Pál Sipos	Applications of solution chemistry in the industry – selected examples	Hungary	Prof. Dr. Tomaž Urbič		
17:00	17:10	Break					
17:10	17:42	**Posters session (Flash Presentations)**					
17:10	17:18	P11 Prof. Dr. Tomaž Urbič	Anomalous regions in core-softened models	Slovenia	Prof. Dr. Ingmar Person		
17:18	17:26	P12 Prof. Dr. Tomaž Urbič	An electric field changes water's anomalous regions and phase transitions	Slovenia			
17:26	17:34	P13 Prof. Dr. Tomaž Urbič	Phase diagrams of simple models of water	Slovenia			

Wednesday 27th (UTC/GMT +9 hours)

Local Time Asia-Australia (UTC/GMT +9 hours)		Name	Abstract Title	Country	Chair	Local Time Americas	Local Time Europe-Africa
8:00	8:45	Plenary Lecture (PL5) Prof. Dr. Emiko Okamura	Real-time 19F NMR of peptides in solution: Preaggregation of amyloid-a and b-synuclein, and cell entry of membrane-permeable peptides	Japan	Prof. Dr. Glenn Hefter	(UTC/GMT -5 hours)	(UTC/GMT +1 hour)
8:45	9:20	Key Note Lecture (KN 8) Prof. Dr. Toshiyuki Takamuku	Mixing States of Imidazolium-based Ionic Liquids with Molecular Liquids on Meso- and Microscopic Scales	Japan	Prof. Dr. Glenn Hefter		
9:20	9:40	OT 20 Prof. Dr. Xudong Yu	Phase equilibria for system containing the sulfates of lithium, sodium and potassium: effect of temperature	China			
9:40	10:00	Break					
10:00	10:20	OT 21 Prof. Dr. Ke Lin	Hydration shell spectra from ratio spectra and modified excess spectra in aqueous LiCl and aqueous alcohols.	China	Prof. Dr. Toshiyuki Takamuku		
10:20	10:40	OT 22 Dr. Jihae Han	Dielectric Relaxation Study on Li-ion Conduction in Aqueous and Nonaqueous Superconcentrated Electrolyte Solutions	Japan			
10:40	11:00	OT 23 Prof. Dr. Zhiyong Li	Light Switchable Ionic Liquids Systems	China			
11:00	11:20	OT 24 Graduate student. Yui Nagashima	Speciation of aluminum ions in non-aqueous AlCl3 solutions for electrochemical deposition	Japan	Prof. Dr. Xudong Yu		

Local Time Asia-Australia (UTC/GMT +9 hours)		Name	Abstract Title	Country	Chair	Local Time Americas	Local Time Europe-Africa
11:20	11:40	OT 25 Dr. Kaori Fujii	Experimental and Theoretical Studies on the Molecular Dynamics in Ionic Liquids Triggered by Photodissociation of Bis(p-aminophenyl)disulfide	Japan	Prof. Dr. Xudong Yu		
11:40	12:00	OT 26 Prof. Dr. Guanglai Zhu	Studies on the aggregation of N-butylpyridinium tetrafluoroborate confined in carbon nanotubes	China			
12:00	14:00	Lunch					
14:00	14:35	Key Note Lecture (KN 9) Prof. Dr. Glenn Hefter	Volumes of Fun with Electrolyte Solutions	Australia	Prof. Dr. Hajime Torii		
14:40	15:00	OT 27 Graduate student. Masatoshi Ando	Intermolecular Vibrations of 1-Methyl-3-octylimidazolium Tetrafluoroborate Mixtures with Formamide, N-Methylformamide, and N,N-Dimethylformamide	Japan		**(UTC/GMT -5 hours)**	**(UTC/GMT +1 hour)**
15:00	15:20	OT 28 Prof. Dr. Hajime Torii	Hydrogen-bond configurations of hydrogen fluoride in relation to the hidden halogen-bonding ability	Japan	Prof. Dr. Guanglai Zhu		
15:20	15:40	OT 29 Prof. Dr. Toshio Yamaguchi	Structure and properties of a single aqueous electrolyte droplet ultrasonically levitated in the air	Japan			
15:40	16:00	Break					
16:10	17:06	**Posters session (Flash Presentations)**					
Room 1							

Local Time Asia-Australia (UTC/GMT +9 hours)		Name	Abstract Title	Country	Chair	Local Time Americas	Local Time Europe-Africa
16:10	16:18	P14 Graduate Student. Longjie Sun	Theoretical calculation research on ternary system NaCl-CaCl2-H2O based on PSC model	China	Prof. D. Glenn Hefter	**(UTC/GMT -5 hours)**	**(UTC/GMT +1 hour)**
16:18	16:26	P15 Graduate student. Yuki Fujii	Vibrational Dynamics of Thermoresponsive Polymer and Its Monomer Unit in Water Studied by 2D-IR Spectroscopy and MD Simulation	Japan			
16:26	16:34	P16 Graduate student. Li Du	Phase equilibria of the ternary system KCl+MgCl2+H2O at multi-temperature: calculation and comparison	China			
16:34	16:42	P17 Graduate student. Kazuya Takamoto	Solvent Effects on Intramolecular Charge Transfer Dynamics of 9-Aryl Carbazole Studied by Ultrafast Transient Absorption Spectroscopy	Japan	Prof. D. Glenn Hefter		
16:42	16:50	P18 Graduate Student. Fangtong Ma	Solubility phenomena of polyhalite in water at different temperatures	China			
16:50	16:58	P19 Graduate student. Siying Ren	Solid-Liquid Phase Equilibria of Quaternary System Containing the Chlorides of Lithium, Potassium and Calcium at 298.2 K	China			
16:58	17:06	P20 Graduate Student. Ke Chen	Phase equilibria of chlorides containing lithium, magnesium and calcium at 323 K	China			
Room 2							
16:10	16:18	P21 Graduate Student. Zhihao Yao	Phase equilibria for system containing the sulfates of sodium and potassium at 303.2 K	China	Prof. Dr. Ryo Kanzaki		

Local Time Asia-Australia (UTC/GMT +9 hours)		Name	Abstract Title	Country	Chair	Local Time Americas	Local Time Europe-Africa
16:18	16:26	P22 Graduate Student. Zhixing Zhao	Phase equilibria for the ternary system lithium, sodium, and sulfate : effect of the temperature	China	Prof. Dr. Ryo Kanzaki	**(UTC/GMT -5 hours)**	**(UTC/GMT +1 hour)**
16:26	16:34	P23 Graduate Student. Hiroki Sumida	Estimation of conformational entropy of ionic liquids	Japan			
16:34	16:42	P24 Graduate Student. Hongyan Liu	Structure of Aqueous KNO3 Solutions by Wide-Angle X-ray Scattering and Density Functional Theory	China			
16:42	16:50	P25 Prof. Dr. Kazuhiko Ohashi	MD and TD-DFT studies of solvent effects on the spectroscopic properties of aniline: Similarity and dissimilarity between water and methanol	Japan	Prof. Dr. Ryo Kanzaki		
16:50	16:58	P26 Graduate student. Ruirui Liu	The Hydration Structure and Transport Behavior of Li+ and Mg2+ in Confinement Space	China			
16:58	17:06	P27 Graduate Student. Wenzhang Zuo	The Stable Phase Diagram of the Quaternary Water-Salt System	China			

Thursday 28th (UTC/GMT +9 hours)

Local Time Asia-Australia (UTC/GMT +9 hours)		Name	Abstract Title	Country	Chair	Local Time Americas	Local Time Europe-Africa
8:00	8:35	Key Note Lecture (KN 10) Prof. Dr. Limei Xu	Structure and dynamics of water and water-ion hydrates at interfaces	China	Prof. Dr. Koji Yoshida	(UTC/GMT -5 hours)	(UTC/GMT +1 hour)
8:35	9:23	**Poster Session (Flash Presentations)**					
Room 1							
8:35	8:43	P28 Graduate Student. Jun Luo	Phase equilibria of lithium, ammonium and chlorine in aqueous solution at 298.2 K and 323.2 K	China	Prof. Dr. Hajime Torii		
8:43	8:51	P29 Prof. Dr. Yukio Terashima	Non-Arrhenius like behavior in viscosity of 1,2-propanediol solutions with LiBF4	Japan			
8:51	8:59	P30 Graduate Student. Xia Feng	Solid-liquid phase equilibria of the aqueous system containing magnesium chloride and calcium chloride: effect of temperature	China			
8:59	9:07	P31 Graduate student. Mengdan Qiao	Fine Analysis of the component effect on the microstructure of LiCl solution by Synchrotron X-ray Scattering, Raman Spectroscopy and Molecular Dynamics Simulation	China			

Local Time Asia-Australia (UTC/GMT +9 hours)		Name	Abstract Title	Country	Chair	Local Time Americas	Local Time Europe-Africa
9:07	9:15	P32 Graduate student. Wenyu Yang	Phase equilibrium of the aqueous ternary sulfate system containing rubidium and magnesium	China	Prof. Dr. Hajime Torii	(UTC/GMT -5 hours)	(UTC/GMT +1 hour)
9:15	9:23	P33 Graduate student. Feng Zhang	Theoretical calculation of ternary system of NaCl-MgCl2-H2O	China			
Room 2							
8:35	8:43	P34 Graduate student. Guangguo Wang	Significant ionic association and hydrogen bonds instead of hydration shell in nanoconfined aqueous electrolyte solutions	China	Prof. Dr. Emiko Okamura		
8:43	8:51	P35 Prof. Dr.Yoshida Koji	In-situ observation of the decomposing process of biomass samples in high-temperature high-pressure water by neutron imaging	Japan			

Local Time Asia-Australia (UTC/GMT +9 hours)		Name	Abstract Title	Country	Chair	Local Time Americas	Local Time Europe-Africa
8:51	8:59	P36 Graduate student. Keke Chai	Structure of Choline Chloride-Carboxylic Acid Deep Eutectic Solvents from X-Ray Scattering and DFT Calculations	China	Prof. Dr. Emiko Okamura	(UTC/GMT -5 hours)	(UTC/GMT +1 hour)
8:59	9:07	P37 Graduate student. Yunxia Wang	Unveiling the structure of aqueous magnesium nitrate solutions by X-ray diffraction and theoretical calculations	China			
9:07	9:15	P38 Graduate student. Osuka Yuri	Identification of Molybdenum tridecamer by ESI-MS	Japan			
9:15	9:23	P39 Graduate student. Zhuanfang Jing	Hydration and Dynamic Characteristics of Alkali and Halide Ions	China			
9:23 9:40 Break							
9:40	10:00	OT 30 Graduate student. Student Yui Kawana	Ion conductivity and speciation of lithium salt 1,3-propane sultone solution	Japan	Prof. D. Limei Xu		

Local Time Asia-Australia (UTC/GMT +9 hours)		Name	Abstract Title	Country	Chair	Local Time Americas	Local Time Europe-Africa
10:00	10:20	OT 31 Dr. Tetsuro Nagai	Gas transportation in inhomogeneous systems studied using large-scale molecular dynamics simulation and dynamic Monte Carlo method	Japan	Prof. D. Limei Xu	(UTC/GMT -5 hours)	(UTC/GMT +1 hour)
10:20	10:40	OT 32 Prof. Dr. Yongquan Zhou	Alkali Ions Recognition by 18-Crown-6 in Aqueous Solutions: Evidences from Micro-Structure	China			
10:40	11:00	OT 33 Prof. Dr. Kanzaki Ryo	Calorimetric Detection of Aggregation and Redispersion of Polyacrylic acidcoated Maghemite Nanoparticle in Protic Ionic Liquids	Japan			
11:00	11:20	Break					
11:20	11:40	OT 34 Graduate student. Kodai Kikuchi	Effect of temperature at the time of gelation of cellulose dissolved in ionic liquid-DMSO solution on the physical properties of cellulose hydrogels	Japan	Prof. Dr. Toshio Yamagushi		

Local Time Asia-Australia (UTC/GMT +9 hours)		Name	Abstract Title	Country	Chair	Local Time Americas	Local Time Europe-Africa
11:40	12:25	Plenary Lecture (PL6) Prof. Dr. Marija Bešter Rogač	Ionic liquids in solutions: from electrolytes to surfactants	Slovenia	Prof. Dr. Toshio Yamagushi	**(UTC/GMT -5 hours)**	**(UTC/GMT +1 hour)**
12:25	12:40	Presentation 38th ICSC- Belgrade Prof. Dr. Marija Bešter Rogač					
12:40	13:00	Closing Ceremony					

ABSTRACTS PLENARY AND KEY NOTE LECTURES

Solution State Applications of Carbon Dots

Roger M. Leblanc

Department of Chemistry, University of Miami, Coral Gables, FL 33146. United States
rml@miami.edu

Carbon dots (CDs) with a mean diameter less than 10 nm have recently triggered great attention in the research of solution chemistry and biomedical engineering due to their unique properties such as small size, photoluminescence (PL), high water-dispersity, biocompatibility, nontoxicity, and tunable surface functionality. In this presentation, I will firstly introduce preparations of diverse CDs. Extensive structural characterizations have been used to hypothesize comprehensive structural models for 3 distinct CD species that represent both top-down and bottom-up approaches in order to optimize their properties and applications. Then, I will mainly focus on many excellent applications of the CDs in solution work recently developed in our lab: (1), the development of Langmuir-Blodgett film of proteinase K enzyme and its interaction when conjugated with CDs; (2), in vivo experiment suggested that glucose-based CDs could cross the blood-brain barrier (BBB) due to the presence of glucose transporter proteins on the BBB; (3), a drug delivery system of carbon nitride dots conjugated with an anti-cancer therapeutic drug and a targeting molecule was capable of effective treatment against diffuse large B-cell lymphoma both in vitro and in vivo revealing efficient therapeutic capabilities with minimal toxic side effects; (4), our study has shown that CDs prepared with carbon nanopowder bind to calcified bone of zebrafish larvae with high affinity. These observations support a novel and revolutionary use of CDs as highly specific drug delivery carrier; (5), metformin-derived CDs showed a unique mitochondria targeting property, which suggests a huge potential for future mitochondria-targeting drug delivery;

Microsolvation of Acids

Gabriel Merino

Departamento de Física Aplicada, Centro de Investigación y de Estudios Avanzados
Unidad Mérida – México
gmerino@cinvestav.mx

Abstract: Exploration of the potential energy surfaces (PESs) of various microsolvated species associated with the microsolvation of the nitrate anion using density functional theory methods uncovers a rich and complex structural diversity previously unnoticed in the scientific literature for the [NO3(H2O)n]−, n = 1–6 clusters. Two types of interactions are at play in stabilizing the clusters: traditional water to water and charge assisted nitrate to water hydrogen bonds (HBs). The formal negative charge on oxygen atoms in nitrate strengthens hydrogen bonding among water molecules. There is outstanding agreement between available experimental data (sequential hydration enthalpies, IR spectra, and vertical detachment energies) and the corresponding expectation values obtained from our structures.

Solvent and solute basicities – computational chemistry and experimental parameters

Waghorne, W.E.
University College Dublin, Ireland
earle.waghorne@gmail.com

The basicity of a solvent or solute has long been recognized as one of the most important molecular properties determining the solvation of a solute. Thus, a number of experimental parameters have been developed to capture basicity. These include Kamlet and Taft's β_{KT}[1], a measure of the hydrogen bond basicity of a bulk solvent, Gutmann's donor number[2], DN, a measure of the Lewis basicity of an isolated molecule, and Abraham's β_A[3], a measure of hydrogen bond basicity of an isolated, and so solute, molecule.

In a series of papers[4,5] we have successfully correlated a number of solvent and solute parameters, including these basicity parameters, with molecular properties derived from computational chemistry. However, these are complicated by the fact that the partial charges on atoms depend on the model used to assign the electron density to individual atoms.

Here, following work by Schüürmann et al [6,7], parameters were regressed separately for different hydrogen bond acceptor atoms, which overcomes the difficulty in calculating partial charges on different types of atoms.

For oxygen bases, these analyses show that β_{KT}, DN and β_A are all essentially determined by the partial charge on the O atom and the energy of the donor molecular orbital, with the contributions to β_{KT} and β_A being essentially equal while for DN the contribution from the orbital energy is around 50% larger than that from the oxygen atom partial charge. While the analyses indicate that all three parameters reflect similar basicities, they also point to several interesting anomalies.

[1] M.J. Kamlet and W.R. Taft, J. Amer. Chem. Soc. **98**, 377–383 (1976)
[2] V. Gutmann, Electrochim. Acta **21**, 661–670 (1976)
[3] M.H. Abraham, Chem. Soc. Rev. **22**, 73–83 (1993)
[4] W.E. Waghorne, Pure Appl. Chem. **92**, 1539–1551 (2020). doi.org/10.1515/pac-2020-0108 and references therein.
[5] W.E. Waghorne, J. Solution Chem. (2022). https://doi.org/10.1007/s10953-022-01168-w
[6] J. Schwöbel, R-U. Ebert, R. Kühne, G.J. Schüürmann, Chem. Inf. Model. **49**, 956–962 (2009). DOI: 10.1021/ci900040z
[7] J. Schwöbel, R-U. Ebert, K. Kühne, G. Schüürmann, J. Phys. Chem. A **113** 10104–10112 (2009)

Why does Ethaline not behave like a usual Deep Eutectic Solvent?

[1]Agieienko, V., [2]*Buchner, R.

[1] Nanotechnology and Biotechnology Department, Nizhny Novgorod State University, Russian Federation.

[2] Institute of Physical Chemistry, Regensburg University, Germany

* Richard.Buchner@chemie.uni-regensburg.de

Deep Eutectic Solvents (DES), binary mixtures exhibiting exceptional freezing-point depression, are currently in the focus of solution chemistry and related areas as they combine excellent solvent properties with competitive costs and low environmental impact.[1,2] A much studied solvent in this respect is ethaline, the 1:2 molar ratio mixture of choline chloride (ChCl) with ethylene glycol (EG). Surprisingly, we recently found that ethaline lacks the formal criteria of a DES.[3] Neither does its ChCl mole fraction of x_{ChCl} = 0.333 correspond to the eutectic composition, x^*_{ChCl} = 0.171, nor is the freezing-point depression exceptionally large. Actually, for $x_{ChCl} \leq x^*_{ChCl}$ the observed freezing points are those of an ideal binary mixture of two non-electrolytes, although ChCl dissociates almost completely in water.[4]

To shed light on this unexpected behavior we studied solutions of choline chloride, choline iodide and chlorocholine chloride in EG up to saturation at 25 °C using dielectric relaxation spectroscopy. It turned out that the effective solvation numbers of all three salts are negligible. Up to ~2 M solutions are dominated by contact ion pairs before smoothly blending into the behavior of a "solvent-lubricated" molten salt. The implications of these findings for the phase behavior of ethaline and its solvent properties are discussed.

[1] Smith, E.L., et al., Chem. Rev. **2014**, 114, 11060−11082.

[2] Hansen, B.B., et al., Chem. Rev. **2021**, 121, 1232−1285.

[3] Agieienko, V., Buchner, R., Phys. Chem. Chem. Phys. **2022**, 25, 5265-5268.

[4] Shaukat, S., et al., Phys. Chem. Chem. Phys. **2019**, 21, 10970-10980.

Real-time ^{19}F NMR of peptides in solution: Preaggregation of amyloid-b and a-synuclein, and cell entry of membrane-permeable peptides

Okamura, E.

Faculty of Pharmaceutical Sciences, Himeji Dokkyo University, Japan

emiko@gm.himeji-du.ac.jp

The progress of NMR has enabled to analyze peptide reactions such as spontaneous bond cleavage[1] and amino acid isomerization[2] in real time. Recently, we have quantified preaggregation, the initial stage of fibril formation in amyloid-β (Aβ) and its mutants by using ^{1}H NMR.[3] Here we present how the preaggregation proceeds in Aβ and a-synuclein in solution, and how the cell entry of membrane-permeable peptides[4] occurs by real-time ^{19}F NMR.

A□ and a-synuclein finally form □□fibril structure that could be relevant to age-related Alzheimer's disease and Parkinson's disease. The initial stage from monomers to aggregates in solution is still an issue to be solved. ^{19}F NMR labelling at the specific site of each peptide has demonstrated what triggers the aggregate formation and how it is controlled in solution at the molecular level.

Membrane-permeable peptides are cationic or amphiphilic peptides that serve to solve the poor cell membrane permeability of new bioactive molecules such as oligonucleotides, plasmids, peptides and proteins for therapeutic pharmaceuticals. The present ^{19}F NMR has uncovered why and how such cationic peptide shows an ability to go across hydrophobic cell membrane,[4] and how the neutral amino acids modifies the membrane-permeable properties.

References

[1] K Aki, E Okamura, Sci. Rep. **6**, 21594 (2016).
[2] K Aki, E Okamura, J. Soln. Chem. **49**, 1293 (2020).
[3] E Okamura, K Aki, Pure Appl. Chem. **92**, 1575 (2020).
[4] Y Takechi-Haraya et al, Pharmaceuticals **10**, 42 (2017).

Ionic liquids in solutions: from electrolytes to surfactants

Bešter-Rogač, M.
University of Ljubljana, Faculty of Chemistry and Chemical Technology, Ljubljana, Slovenia
marija.bester@fkkt.uni-lj.si

In recent decades, ionic liquids (ILs) have attracted attention due to their suitability as systems for a variety of applications. However, the growing number of studies dealing with the physicochemical properties of ILs in their pure state has been extended to investigations of their mixtures with molecular co-solvents. It turned out that ILs in solutions can serve as excellent (electrolytes) model systems because they exist in a variety of structures and many of them are fully miscible with different solvents, while the solubility of "classical" electrolytes is limited. However, the structures of ions also play a very important role in solutions, since a wide variety of interactions between ions and solvents can occur.[1]

Theories for concentrated electrolyte solutions are still lacking. While for "classical" electrolytes the limited solubility could be the reason for the lower effort in studying concentrated solutions, for ILs the whole concentration range from pure solvent to pure electrolyte can be covered. Despite many studies, the observed maximum in electrical conductivity[2] is still not well described and remains a challenge for the future.

Therefore, ILs can serve as excellent model systems for the study of ionic interactions, hydrophobic effects, and specific ion effects and help us to extend and deepen the knowledge of electrolytes and surfactants in aqueous and non-aqueous solutions.

1. M. Bešter-Rogač, M.V. Fedotova, S.E. Kruchinin, M. Klähn. Phys. Chem. Chem. Phys. 2016, 18, 28594.
2. M. Bešter-Rogač, Acta Chim. Slov. 2020, 67, 1

Modeling Ion Adsorption in Aqueous Solutions at Oxide Surfaces

Louise J. Criscenti
Geochemistry Department, Sandia National Laboratories, Albuquerque, NM 87185, United States
ljcrisc@sandia.gov

Geochemists attempt to bridge field-scale observations of water-rock interactions with a fundamental molecular-scale understanding of the reaction mechanisms that occur at water-rock interfaces. Large-scale computer models that are used to predict contaminant migration, carbon sequestration, or the transport of fluids like water and hydrocarbons through rock, incorporate simplistic geochemical models that may not always capture critical reactive properties of the system under investigation. I will present studies using different types of modeling to investigate the adsorption of cations on single crystal faces, in nanopores, and on nanoparticles. Cation adsorption in nanopores is strongly influenced by interfacial water properties while cation adsorption on nanoparticles provides one example of the importance of surface defects as adsorption sites. Surface complexation models (SCM) are proposed for incorporation into the large-scale computer models that couple chemistry with flow and transport for field-scale applications. These models are typically parameterized by fitting batch experimental data of ion adsorption over a range of ionic strength and ion concentrations. Classical and ab initio molecular dynamics (MD) simulations (along with analytical data like that collected using X-ray absorption spectroscopy) provide insight into the most likely surface complexes to form, narrowing the possibilities for SCM fitting. Classical and ab initio MD simulations provide more mechanistic detail of reactions at oxide-water interfaces, although they eliminate factors of real world (i.e., even laboratory) complexity. The pros and cons of each type of model, potential improvements, and the advantages of using several different modeling approaches will be discussed.

Acknowledgements: This material is based upon work supported by the U.S. Department of Energy, Office of Science, Office of Basic Energy Sciences, Chemical Sciences, Geosciences, and Biosciences Division under Field Work Proposal Number 21-015452 at Sandia National Laboratories. Sandia National Laboratories is a multimission laboratory managed and operated by National Technology & Engineering Solutions of Sandia, LLC, a wholly owned subsidiary of Honeywell International Inc., for the U.S. Department of Energy's National Nuclear Security Administration under contract DE-NA0003525. SAND2022-9470 A.

Dissolution of iron(III) and aluminium minerals with aqueous solutions of siderophores

[1,2*]Magalhães, M.C.F., [2]da Costa, J., [2]Cohen, D.R., [3]Hibbert, D.B., [2]Archer, M., [2]Myers, T.J., & [2]Hand, S.J.

[1] Linking Landscape, Environment, Agriculture and Food Research Centre (LEAF), Associated Laboratory, Laboratory for Sustainable Land Use and Ecosystem Services (TERRA), University of Lisbon; University of Aveiro, Portugal; mclara@ua.pt
[2] School of Biological Earth & Environmental Sciences, UNSW Sydney, NSW 2052, Australia
[3] School of Chemistry, UNSW Sydney, NSW 2052, Australia

The evolution of the Earth has resulted in aluminium and iron being most abundant metallic elements in the crust. In weathered materials on the Earth's surface, these metals are typically present as oxides, hydroxides or aluminosilicates that display extremely low solubilities. Demand for aluminium continues to grow and is mainly extracted from bauxite (a mixture of aluminium hydroxides oxides) at high cost due to the amount of electricity used and high environmental impact. There is potential for the extraction of this metal from sources other than bauxite using new methods of geochemical extraction involving organic complexes.

Palaeontologists are commonly faced with the challenge of separating vertebrate fossils from various iron(III) hydroxides oxides, without damaging bones or teeth that are mainly composed of hydroxidecarbonate-apatite. A study was conducted on the formation of coordination compounds of iron(III) and aluminium with organic compounds (ligands) classified as siderophores and which have exceptionally high formation stability constants that promote the dissolution of the iron(III) minerals without affecting hydroxidecarbonate-apatite. The dissolution of aluminium minerals was also examined due to the presence of kaolinite and Al- substituted iron(III) minerals in the samples and similarity between the chemistry of iron(III) and aluminium ions. As the organic

compounds pyridoxal isonicotinoyl hydrazone (PIH), salicylaldehyde isonicotinoyl hydrazone (SIH) and acetohydroxamic acid (aHA) form coordination compounds with iron(III) and aluminium in moderately alkaline media (pH 9–12), they were used as chelate ligands. As sources of iron(III) were used natural hematite and fossil samples from the Riversleigh World Heritage Area in Australia, which in addition to the iron(III) oxides, hematite, goethite and poorly crystalline solid phases coating the bone fragments, also contained quartz crystals (SiO_2) and clays [mainly kaolinite, $Al_2Si_2O_5(OH)_6$].

The trend of dissolved iron observed for hematite was aHA > SIH > PIH. The ligand with the smallest stability constant, aHA, was able to dissolve the most iron(III) solids. The dissolved iron abundance trends can be explained in terms of ligand structure rather than pH or thermodynamic stability of aqueous coordination entities formed in solution.[1] The trend of dissolved aluminium observed for kaolinite was PIH > SIH > aHA and increased with increasing pH. These trends can be explained in terms of pH associated with thermodynamic stability of aqueous coordination entities formed in solution.

[1] J. da Costa, D.R. Cohen, M.C.F. Magalhães, D.B. Hibbert, M. Archer, T.J. Myers, S.J. Hand (2020) ChemPlusChem **85**, 1747-1753.

Investigation of problems related to the lateral pressure profile

[1,*]Jedlovszky, P., [2]Sega, M., [3]Fábián, B., [4]Hantal, Gy.

*lead presenter
[2]Helmholtz Institute Erlangen-Nürnberg, Nürnberg, Germany
[3]Max Planck Institute of Biophysics, Frankfurt am Main, Germany
[4]University of Natural Resources and Life Sciences (BOKU), Wien, Austria
Eszterházy Károly University, Eger, Hungary
jedlovszky.pal@uni-eszterhazy.hu

The calculation of the lateral pressure profile in computer simulations of anisotropic systems is an important problem in various respects; however, it is not a straightforward

task at all. The difficulty stems from the fact that pressure is an inherently non-local quantity, which has to be localized in the profile calculation. Further, if an Ewald summation-based method is used to account for the long range part of the intermolecular interactions, the reciprocal space term of this correction is not pairwise additive. We have proposed an accurate and computationally very efficient way of calculating the profile of the lateral pressure, which can also take into account the reciprocal space term when using the sPME method. Further, this way the lateral pressure can be distributed among the interacting atoms in the system as if it were a pairwise additive quantity. Since the surface tension is the integral over the imbalance of the lateral and normal pressure components, and the latter of them is constant, this method allows us to calculate the contribution of the individual particles, molecules and moieties t the surface tension. In this talk, I present a couple of our recent results in this respect.

Using an intrinsic surface analyzing method, such as ITIM, the subsequent molecular layers beneath the liquid-vapor interface can be unambiguously identified. This way, the surface tension contribution of the subsequent molecular layers can be calculated. We have performed such a calculation for the liquid-vapor interface of five molecular systems characterized by markedly different intermolecular interactions, namely CCl_4, acetone, acetonitrile, methanol and water. Our results showed that at least 90% of the surface tension comes from the first molecular layer in every case, and in methanol this contribution practically reaches 100%.

We also calculated the contribution of the two liquid phases to the interfacial tension at the interface of five different organic liquids, i.e., hexane, cyclohexane, hexanol, dichloromethane, and carbon tetrachloride, with water. Our results reveal that the organic component contributes 20-30% to the total interfacial tension, and this result is independent from the temperature, pressure, water model used, and also from the type of

the organic molecule as long as it does not interact strongly and, consequently, does not mix in a considerable extent with water. Among the chosen organic liquids, hexanol is the only one that exhibits partial miscibility with water to an extent accessible by computer simulation. We found that this partial miscibility is associated to a negative contribution of the hexanol molecules, and also that of the hexanol-rich mixed phase, to the total interfacial tension, consistent with the tendency of the hexanol molecules to mix with water.

We also considered the liquid-vapor interface of the solutions of five different amphiphilic molecules, representative of anionic, cationic and non-ionic (alcoholic) surfactants in this respect. We found that the headgroups of alcoholic surfactants give a negligible contribution to the surface tension. The opposite is true for ionic surfactants and counterions, whose effect depends on their 'hardness' within the Hofmeister series as well as on the sign of their charge, even though there is a large compensation between ions and counterions.

Thermodynamics of mixing of solute solvent mixture as seen from computer simulation and thermodynamic integration

A. Idrissi

University of Lille, CNRS UMR 8516 -LASIRe - Laboratoire Avancé de Spectroscopie pour les Interactions la Réactivité et l'environnement, 59000 Lille, France.
nacer.idrissi@univ-lille.fr

The desire of understanding of the structure and dynamics of the a solute-solvent mixtures at the molecular level has led to an increasing interest in using computer simulations. In these studies, issues such as the inhomogeneous distribution of the solutes as well as the occurrence and extent of both solvent-solvent or solvent-solute H-bonding interactions have been thoroughly investigated. Probably the most important pre-requisite of performing a reliable computer simulation is the proper development of the force field parameters used. In this regard, a number of force fields have been proposed for many solutes in the recent years. In these force fields, the values of the van der Waals parameters have usually been adapted from widely used, general purpose force fields, such as AMBER, CHARMM, or OPLS-AA, … while the fractional charges carried by the different atoms have been derived from ab initio calculations. These parameters are in general combined with those of the commonly used water models, such as SPC, SPC/E, or TIP4P, …. Although the intermolecular potentilas of solute A and solvent B could be individually "good" (they are parametrized to reproduce teh strutucre and dynamics of the neat solute and the solvent B, respectively), the combination of these two intermolecular potential dosens not necessarly reproduces the structure and dynamics of their mixture. The free energy of mixing then provides one of a rigorous test of the force field accuracy, to the extent that all the system degrees of freedom are adequately sampled. Indeed, the free energy of mixing two components is a key physical–chemical quantity, because its sign determines whether the components mix or demix at a given molar ratio. In cases when the mixing of the two components in computer simulation is accompanied by a slight increase of the free energy, demixing might not visibly occur on the simulation time and length scales. Detection of such demixing is also hindered by the use of periodic boundary conditions. Further, besides the qualitative description of the mixing of the components, good reproduction of the experimental free energy of mixing in computer simulation is a pre-requisite of the accurate description of the microscopic structure (e.g., in terms of self-association) of the mixture.[1–6]

References

1) Effect of the alkyl chain and composition on the thermodynamics of mixing of small alcohols and water, A. Idrissi, P. Jedlovzky J. Mol. Liq. 338, 116777, 2021

2) Calculation of the Free Energy of Mixing as a Tool for Assessing and Improving Potential Models: The Case of the N,N-Dimethylformamide–Water System
B. Honti, A. Idrissi, P. Jedlovszky, J. Phys. Chem. B, 125, 18, 4819-4830, 2021

3)Thermodynamics of mixing methanol with supercritical CO2 as seen from computer simulation and thermodynamic integration R. A. Horváth, G. Horvai, **A. Idrissi** and P. Jedlovszky Phys. Chem. Chem. Phys., 22, 11652-11662 , 202

Coordination chemistry of Jahn-Teller distorted complexes in solution and solid state

Persson, I.
Department of Molecular Sciences, Swedish University of Agricultural Sciences, P.O.Box 7015, SE-750 07 Uppsala, Sweden.
ingmar.persson@slu.se

Metal ions with d^4 and d^9 electron configuration as chromium(II) and manganese(III), and copper(II), respectively, are expected to have Jahn-Teller distorted octahedral coordination. The Jahn–Teller theorem states that any non-linear molecule with a spatially degenerate electronic ground state will undergo a geometrical distortion that removes that degeneracy, as the distortion lowers the overall energy of the species.[1-3] The structure of the hydrated copper(II) ion in aqueous solution has been heavily debated in recent years whether it is five-coordinate or six-coordinate with Jahn-Teller distorted octahedral geometry.[4] The coordination geometry of hydrated and solvated copper(II) ions in solid state will be presented and discussed, and comparisons to aqueous solution will be made. In order to determine accurate structures of especially metal complexes with low symmetry in solid state, it has turned out that crystallographic studies need to be accompanied with a lattice-independent method as EXAFS. This will be discussed in detail with examples from Jahn-Teller distorted metal ion complexes.

References

1. Orgel, L. E. An introduction to transition metal chemistry ligand-field theory, Butler & Tanner Ltd, London, Great Britain, 2nd Edn., 1966, and references therein
2. Figgis, B. N. Hitchman, M. A. Ligand field theory and its application, 2000, and references therein.
3. Bersuker, I. Electronic structure and properties of transition metal compounds, Wiley-Interscience, New York, 1996, and references therein.
4. I. Persson, I.; Lundberg, D.; Bajnoczi, É. G.; Klementiev, K.; Just, J.; Sigfridsson Clauss, K. G. V. EXAFS study on the coordination chemistry of the solvated copper(II) ion in a series of oxygen donor solvents. Inorg. Chem. **2020**, 59, 9538-9550, and references therein.

Bulk and Local Structure in a 1M Aqueous Solution of Uranyl Chloride via Structure Refinement of Neutron Diffraction and EXAFS spectroscopy Data

Daniel T. Bowron[1], Samuel Edwards[2], and Robert J Baker[2]

[1]ISIS Neutron and Muon Source, STFC Rutherford Appleton Laboratory, Harwell-Oxford,
OX11 0QX, United Kingdom
daniel.bowron@stfc.ac.uk

[2]Department of Chemistry, Trinity College Dublin, The University of Dublin, College Green, Dublin 2, Ireland

The aqueous chemistry of the uranyl ion, UO_2^{2+}, is an important aspect of our understanding of geological disposal of nuclear waste, and in particular the complexation of UO_2^{2+} with chloride anions, is thought to be important in processes governing actinide mobility [1]. To investigate the solution structure and ion-pairing of UO_2^{2+}, we have performed a series of neutron diffraction studies on 1M solutions of UO_2Cl_2 in isotopically labelled water: H_2O, D_2O, and HDO, and subsequently refined a comprehensive three-dimensional structural model of the system using the technique of Empirical Potential Structure Refinement [2]. To validate the local structural chemistry of the uranyl ion in this system, a detailed evaluation of the model has been undertaken in which the model predictions are compared with U L_3- edge Extended X-ray Absorption Fine Structure (EXAFS) spectroscopy data taken from the literature [3]. The results of this investigation illustrate that the UO_2^{2+} ion favours a five-fold equatorial coordination by water molecules (Figure 1), and that the information derived from the X-ray spectroscopy data is very important for establishing the details of the chloride ion-pairing that takes place in the system. The model refined from the isotopically enhanced neutron scattering data has furthermore allowed us to confirm the theoretically predicated details [4] of hydrogen bonding capability of the axial uranyl-oxygen sites, and that of the equatorially coordinating water molecules.

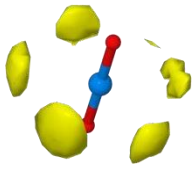

Figure 1: The spatial density function of water molecules (oxygen sites) coordinating the equatorial plane of the UO_2^{2+} ion. This figure illustrates the strong preference for five-fold coordination of the ion by water molecules at a ($U\text{-}O_W$) distance of 2.4±0.1Å, with a mean coordination number of
4.6±0.6 water molecules. A second shell of 20.9±2.3 water molecules can be found in the distance range from 3.5Å $r_{(U\text{-}OW)}$ 5.8Å around the ion.

References

[1] C.Hennig, J.Tutschku, A.Rossberg, G.Bernhard and A.C.Scheinost, Inorg. Chem. (2005) **44**, 6655-6661
[2] A.K.Soper, Phys. Rev. B (2005) **72**, 104204
[3] P.G.Allen, J.J.Bucher, D.J.Shuh, N.M.Edelstein and T.Reich, Inorg. Chem. (1997) **36**, 4676-
4683
[4] J.A.Platts and R.J.Baker, Phys. Chem. Chem. Phys. (2018) **20** 15380

Mixing States of Imidazolium-based Ionic Liquids with Molecular Liquids on Meso- and Microscopic Scales

Toshiyuki Takamuku
Faculty of Science and Engineering, Saga University, Japan
takamut@cc.saga-u.ac.jp

Room temperature ionic liquids (ILs) attract much attention as new solvents from various chemical fields, such as organic syntheses and secondary batteries. This is because, despite the liquid states, ILs have properties of electrolytes, such as thermal stabilities, very low volatilities, and electroconductivities. The physicochemical properties of ILs are also interesting as novel liquids. One of them is that ILs are miscible with not only polar molecular liquids (MLs), such as ethanol, but also nonpolar MLs like benzene.

We have investigated imidazolium-based IL mixtures with various MLs, such as alcohols, benzene and its derivatives, cycloethers, and amides, on both meso- and microscopic scales using small-angle neutron scattering (SANS) and several spectroscopies, respectively. Depending on the characteristics of MLs, the mixing state of IL–ML mixtures varies.

In this talk, I will explain the mixing states of 1-butyl-3-methlyimidazolium bis(trifluoromethanesulfonyl)imide (C_4mimTFSI) mixtures with cycloethers, tetrahydrofuran (THF), 1,4-dioxane (1,4-DIO), and 1,3-dioxane (1,3-DIO).[1] THF and 1,3-DIO are miscible with the IL over the entire ML mole fraction x_{ML} range, while 1,4-DIO cannot be mixed with the IL at high x_{ML}. The interaction of cycloether molecules with $TFSI^-$ is the key to the miscibility. $C_n$mimTFSI–1,4-DIO mixtures with the alkyl chain lengths n = 6 and 8 show the upper critical solution temperature (UCST)-type phase separation.[2] The UCST decreases with the elongation of the alkyl chain length n. On the other hand, the UCST of $C_n$mimTFSI–formamide (FA) mixtures increases against the increase in the length n.[3] According to the SANS results on the mesoscopic scale, the mechanisms of the phase separation of both systems around the UCST composition are assigned to 3D-Ising or mean field. The reasons for the mechanisms are interpreted in terms of the interactions among the IL cation, anion, and ML molecules on the microscopic scale.

References

1. M. Kawano, K. Sadakane, H. Iwase, M. Matsugami, B. A. Marekha, A. Idrissi, T. Takamuku, Phys. Chem. Chem. Phys., **22,** 5332-5346 (2020).
2. M. Kawano, K. Sadakane, H. Iwase, M. Matsugami, B. A. Marekha, A. Idrissi, T. Takamuku, Phys. Chem. Chem. Phys., **23,** 24449-24463 (2021).
3. M. Kawano, A. Tashiro, Y. Imamura, M. Yamada, K. Sadakane, H. Iwase, M. Matsugami, B. A. Marekha, A. Idrissi, T. Takamuku, Phys. Chem. Chem. Phys., **24**, 13698-13712 (2022).

Volumes of Fun with Electrolyte Solutions

Glenn Hefter*, Lubomir Hnedkovsky, Tuomas Vielma
Chemistry Department, Murdoch University, Murdoch, WA 6150, Australia
g.hefter@murdoch.edu.au

The volumetric properties of electrolyte solutions continue to attract interest for many reasons. Scientifically, the volumes of electrolytes (and their component ions) are appealing because, in addition to their importance for quantifying the effects of pressure on chemical equilibria and kinetics, they are far more tangible than most thermodynamic properties. Technologically, density is one of the most important physico-chemical properties of industrial process solutions required, for example, for pump and pipeline sizing. Such properties are often required over very wide ranges of concentration and temperature where the database is often limited or even non-existent. This talk will describe some of our recent investigations on certain aspects of the volumetric behavior of various electrolyte solutions. Topics to be covered will include the following.

- How well do we know the standard molar volumes of simple electrolytes?
- How does chemical speciation affect the volumetric properties of sulfuric acid?
- How do aqueous solutions of nitric acid behave at high temperatures?
- How do the volumetric properties of electrolyte mixtures depend on composition?
- How are the volumetric properties of ions affected by the solvent?

Structure and dynamics of water and water-ion hydrates at interfaces

Limei Xu
School of Physics, Peking University
1106173453@pku.edu.cn

Interfacial water and water-ion hydrates at interfaces are important for understanding many physical, biological and chemical processes, such as dissolution of salts, transport of ions, formation of fog and haze, etc. Interfacial effects are particularly profound in low-dimensions such as nanometre-sized channels where the mechanisms of ion transport in bulk solutions may not apply. Therefore, studying the interactions between water and interface at the atomic scale is necessary to understand interfacial water-related issues. We combining first principles calculation, molecular dynamics simulation, and atomic force microscopy (AFM) techniques to study the structure and dynamics of interfacial water and water-ion hydrates at the atomic scale. A novel growth mechanism of 2D ice and anomalously high diffusion rates for specific hydration numbers of ions were observed, which are usually determined by the interaction between water hydrates and interfaces.

ABSTRACTS ORAL PRESENTATIONS

Computational chemistry applied to solutions: anions

Pye, C.C
Saint Mary's University, Canada
cory.pye@smu.ca

Ab initio computational chemistry has been employed in the past by the author to interpret or predict the vibrational spectra of cations such as Li^{+}[1], Cd^{2+}[2], Mg^{2+}[3], Zn^{2+}[4], Sc^{3+}[5], Al^{3+}[6], Ga^{3+}[7], In^{3+}[8], Bi^{3+}[9], Be^{2+}[10], Hg^{2+}, Tl^{3+}[11], Cu^{+}[12], and Pb^{2+}[13]; anions such as SO_4^{2-}[14], PO_4^{3-}[15], HPO_4^{2-}[16], $H_2PO_4^{-}$[17], ClO_4^{-}, BrO_4^{-}, SeO_4^{2-}, AsO_4^{3-}, VO_4^{3-}[18], the borates[19], HSO_4^{-}[20], and $HSeO_4^{-}$[21]; and ion pairs such as LiX (X = F – I)[22], $ScCl_m^{(3-m)+}$ (m = 1 – 6)[23], $ZnCl_m^{(2-m)+}$ (m = 1 – 6)[24], $ZnBr_m^{(2-m)+}$ (m = 1 – 6)[25], and $CuCl_m^{(m-1)-}$ (m = 0 – 6)[26], in aqueous solution.

In this presentation, the author will discuss the microhydration of selected anions and illustrate the relationships between the vibrational spectra of polyatomic anions in the gas-phase, aqueous-phase, and in ionic liquids.

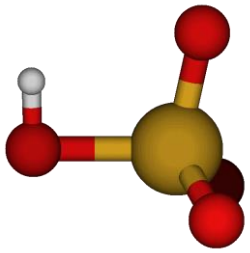

Structure of HVO_4^{2-}

References

[1] J. Phys. Chem., 99 (1995) 3793; J. Phys. Chem., 100 (1996) 601. [2] J. Phys. Chem. B, 102 (1998) 3564; Can. J. Anal. Sci. Spectrosc., 51 (2006) 140. [3] J. Phys. Chem. A, 102 (1998) 9933. [4] Phys. Chem. Chem. Phys., 1 (1999) 4583. [5] J. Phys. Chem. A, 104 (2000) 1627. [6] Phys. Chem. Chem. Phys., 2 (2000) 5030. [7] Phys. Chem. Chem. Phys., 4, (2002) 4319. [8] Phys. Chem. Chem. Phys., 6 (2004) 5145. [9] Can. J. Chem., 85 (2007) 945. [10] Dalton Trans., (2009) 6513; J. Mol. Struct. (Theochem), 913 (2009) 210. [11] J. Sol. Chem., 49 (2020) 1419.
[12] Pure Appl. Chem. 92 (2020) 1643. [13] Liquids, 2 (2022) 39 [14] J. Phys. Chem. A,
105 (2001) 905. [15] J. Phys. Chem. A, 107 (2003) 8746. [16] Can. J. Anal. Sci. Spectrosc., 49 (2004) 175. [17] Can. J. Anal. Sci. Spectrosc., 50 (2005) 70. [18] J. Phys. Chem. A, 115 (2011) 13007. [19] Ind. Eng. Chem. Res., 56 (2017) 13983; Prog. Theor. Chem. Phys., 31 (2018) 107, 143. [20] Comp. Theor. Chem.,

1176 (2020) 112749 [21] J. Mol. Liq., 359 (2022) 119383 [22] Int. J. Quant. Chem., 76 (2000) 62; Can. J. Anal. Sci. Spectrosc., 50 (2005) 254. [23] Can. J. Chem., 80 (2002) 1331. [24] Phys. Chem. Chem. Phys., 8, (2006) 5428. [25] J. Sol. Chem., 40, (2011) 1932. [26] J. Phys. Chem. A, 118 (2014) 204.

Preferential solvation of baicalein in ethanol + water mixtures at 298.15 K

[1] Peña-Fernández, M. A. & [2]* Martínez, F.
[1] Department of Biomedical Sciences, Universidad de Alcalá, Spain.
[2] Department of Pharmacy, Universidad Nacional de Colombia, Sede Bogotá, Colombia.
fmartinezr@unal.edu.co

Baicaelin is a flavonoid component of a traditional Chinese herbal medicine present in the roots of Scutellaria baicalensis with effects antioxidant. In this work is reported equilibrium mole fraction solubility values of baicalein (3) in {ethanol (1) + water (2)} mixtures at T = 298.15 K [1], far along were analyzed for preferential solvation effects based on the "inverse Kirkwood-Buff integrals" (IKBI) [2-4]. Baicaelin is preferentially solvated by water in water-rich mixtures ($\delta x_{1,3} < 0$) but preferentially solvated by ethanol in mixtures of $0.24 < x_1 < 1.00$ ($\delta x_{1,3} > 0$) (Fig. 1). In the former case this result could be due to hydrophobic hydration around the non-polar moieties of this drug. Moreover, in those mixtures where preferentially solvation of baicalein by ethanol is observed, it could be due to the Lewis acidic behavior of this drug in front of ethanol molecules because this cosolvent exhibits higher Lewis basic behavior than water [5].

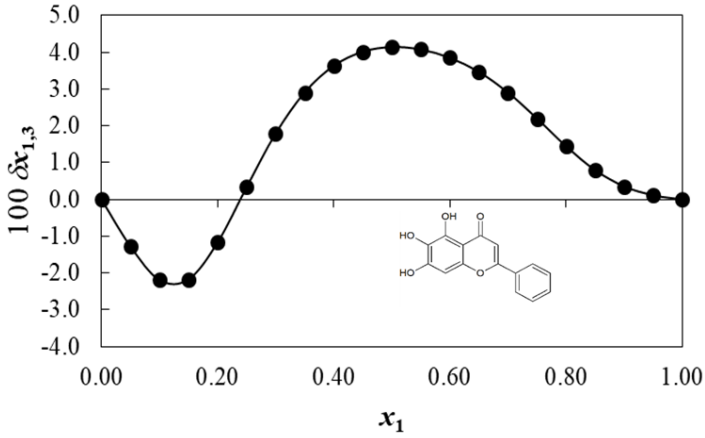

Fig. 1. Preferential solvation parameters ($\delta x_{1,3}$) of Baicalein by ethanol in {ethanol (1) + water (2)} mixtures at T = 298.15 K.

References

[1] A. Martin, P.L. Wu, Solubility and thermodynamic properties of baicalein in water and ethanol mixtures from 283.15 to 328.15 K, Chemical Engineering Communications **208**, 183–196 (2021).

[2] Y. Marcus, Solvent Mixtures: Properties and Selective Solvation, Marcel Dekker, Inc., New York (NY), 2002.

[3] Y. Marcus, On the preferential solvation of drugs and PAHs in binary solvent mixtures, J. Mol. Liq. 140 (2008) 61–67.

[4] Y. Marcus, Preferential solvation of drugs in binary solvent mixtures, Pharm. Anal. Acta 8 (2017) 1000537.

[5] Y. Marcus, The Properties of Solvents, John Wiley & Sons, Chichester (UK), 1998.

Spectral analysis by Functional Enhanced Derivative Spectroscopy (FEDS) method to determine relative values of pH, CECe and OC in agricole soils

J. A. Ramírez-Rincón[12*]& Manuel Palencia[2].

[1]Grupo de Fisicoquímica y Análisis Matemático, Facultad de Ciencias y Humanidades, Fundación Universidad de América, Avda. Circunvalar No. 20-53, Bogotá DC, Colombia.
[2]Departamento de Química, Facultad de Ciencias Naturales y Exactas, Universidad del Valle, Cali – Colombia.
jorge.ramirez@profesores.uamerica.edu.co

Soils are considered as a non-renewable natural resource that provide the nutrients and adequate conditions for plants growth, as well to support several economic activities. Optical spectroscopy has been used during last decades as a reliable technique that allow, by using mathematical and statistical tools, determine simultaneously several physicochemical properties of organic and inorganic species used in agricole industry. The develop of new methodologies for spectral analysis of ease implementation in remote and in-field applications is a current issue, in which stand out those based in operational transformations that highlights hidden information, due to the overlap of individual optical signals generated by its diverse components. This is the case of the Functionally-enhanced derivative spectroscopy (FEDS), lately used for identification of vibrational bands associated to inclusion/presence of chemical compound in solid and liquid matrices, as well for spectral comparison in order to quantify the similarities and differences in multicomponent samples. In this work an algorithm based on FEDS for optical analysis of agricole soil in the spectral region from 1200 to 675 cm^{-1} has been used, to estimate chemical properties related to nutritional and fertility state of 65 soil samples used for planting of corn and cotton in Bolivar and Cordoba departments in Colombia. The results indicate that it is possible to relate the Pearson's correlation coefficient obtained between two FEDS spectra associated to ATR-FTIR signals ($r_F > -0.85$), and their relative values of effective cation exchange capacity, pH and organic carbon content, generating reliable prediction models that present a ratio of performance to deviation higher to 2.0 in all cases (RPD > 2.0). This is possible due to high dependence of optical signal with CECe values, which are in turn conditioned by pH level and OC content in the soil samples considered.

Influence of tetraalkylammonium salts on the adsorption kinetics of bovine serum albumin in aqueous solutions at the air-liquid interface

[1]*Sanabria, J.C., [1]*Romero, C.M.

*Lead presenter: Juan Carlos Sanabria
Corresponding autor: Carmen M. Romero,
[1]Universidad Nacional de Colombia, Colombia
cmromeroi@unal.edu.co

Bovine serum albumin adsorption dynamics in water and in aqueous solutions of tetramethylammonium bromide, hexyltrimethylammonium bromide octyltrimethylammonium bromide, decyltrimethylammonium bromide, and dodecyltrimethylammonium bromide at the air-liquid interface was studied at a temperature of 298.15K.

The kinetics of the adsorption process of the biomolecule in water and in the aqueous alkylammonium solutions was investigated following the changes in surface tension with time. The measurements were performed on a high-precision drop volume tensiometer.
The surface pressure data were adjusted with two of the most used semi-empirical kinetic models that describe the process of adsorption and allow the determination of the equilibrium adsorption parameters.
The results in water and in the aqueous solutions containing tetraalkylammonium salts show that the adsorption kinetics is well described by a model consisting of three steps in which the transport of the protein in the initial stage is diffusion controlled. After some time, the rate is determined by the adsorption and the penetration of the protein at the air-liquid interface and the rearrangement of the protein at the interface; the evolution of both processes is described by steps that follow first-order rate equations.
The results indicate that the overall adsorption process of bovine serum albumin BSA in water and the aqueous alkylammonium salts solutions is controlled by the second step which is the slowest of the three steps; it corresponds to the adsorption and penetration of the biomolecule at the air-liquid interface.

References

1. P. Suttiprasit, V. Krisdhasima, J. McGuire, The surface activity of αlactalbumin, β-lactoglobulin, and bovine serum albumin. J. Colloid Interface Sci. 154(2) (1992), 316–326.
2. S. Magdassi, Surface activity of proteins : chemical and physicochemical modifications. Marcel Dekker Inc., New York, 1996
3. C. M. Romero, J. S. Abella, Y. A. Beltrán, Influence of salts on the surface behavior of α-chymotrypsinogen A in aqueous solutions at 298.15 K, J. Mol. Liq. 344 (2021) 117723.

Antioxidant potential of carotenoids-rich extracts from *Staphylococcus aureus* isolated by pressurized-liquid extraction and conventional extraction

Gerson-Dirceu López[1,2,3,*], Gerardo Álvarez-Rivera[3], Chad Leidy[2], Chiara Carazzone[1], Alejandro Cifuentes[3], Elena Ibáñez[3]

[1]Laboratory of Advanced Analytical Techniques in Natural Products (LATNAP), Chemistry Department, Universidad de los Andes, Bogotá D.C., Colombia.
[2]Laboratory of Biophysics, Physics Department, Universidad de los Andes, Bogotá D.C., Colombia.
[3]Laboratory of Foodomics, Institute of Food Science Research, CIAL, CSIC, Madrid, Spain.

gd.lopez@uniandes.edu.co

Staphylocoocus aureus (*S. aureus*) is a Gram-positive bacterium naturally present in the human body. Bacteria is capable of causing nosocomial and acquired infections. *S. aureus* synthesizes a saccharolipid-linked carotenoid called Staphyloxanthin (STX) [1], characterized by its resistance to oxidative stress [2] and generating lipid domains that produce resistance to antimicrobial peptides [3,4]. STX and its homologs has been obtained for more than 40 years using the same conventional extraction method [1-4]. Therefore, in this research, compressed fluid methods were tested: supercritical fluids extraction (SFE), gas expanded liquid extraction (GXL), and pressurized liquids extraction (PLE), and were compared with conventional method. PLE is the ideal methodology for obtaining bacterial carotenoids and lipids. Carotenoids were quantified by HPLC-MS and lipids were analyzed as fatty acid methyl esters (FAMEs) using GC-MS. Significant statistical differences in antioxidant activity was determined between four carotenoid-producing strains and one strain that does not synthesize pigments using DPPH and ORAC-lipophilic methods. In conclusion, it is possible to obtain carotenoids from *S. aureus* by means of the automated and reproducible PLE method, in addition to bacterial lipids using ethanol as an environmentally friendly solvent compared to the methanol used in the conventional method.

References

[1] G. D. López, E. Suesca, G. Álvarez-Rivera, A. E Rosato, E. Ibáñez, A. Cifuentes, C. Leidy, C. Carazzone. *Biochimica et Biophysica Acta (BBA)-Molecular and Cell Biology of Lipids* **2021**, *1866*, 158941.
[2] N.N. Mishra, G.Y. Liu, M.R. Yeaman, C.C. Nast, R.A. Proctor, J. McKinnell, A. S. Bayer, *Antimicrob. Agents Chemother* **2011**, *55*, 526–531.

[3] A. Clauditz, A. Resch, K.P. Wieland, A. Peschel, F. Götz, *Infect. Immun.* **2006**, *74*, 4950–4953.
[4] E. García-Fern´andez, G. Koch, R.M. Wagner, A. Fekete, S.T. Stengel, J. Schneider, B. Mielich-Süss, S. Geibel, S.M. Markert, C. Stigloher, D. Lopez, *Cell*. **2017**, *171*, 1354–1367.

Physicochemical properties of some drugs in solution

Vivian Torres, Edgar F. Vargas*
Departamento de Química, Universidad de los Andes, Cr. 1 No. 18A 10, Bogotá, Colombia
edvargas@uniandes.edu.co

The apparent molar volumes and isentropic compressibilities of four related drugs compounds, namely benzoic acid, Phenylacetic acid, Cinnamic acid and Ibuprofen in 1-propanol and acetonitrile were determined from density and speed-of-sound measurements. These properties were obtained as a function of molal concentration in the range of $0.005 < m/mol \cdot kg^{-1} < 0.06$ covering temperatures in $278.15 \leq T/K \leq 308.15$. The standard partial molar volumes and the standard isentropic molar compressibilities at infinite dilution were calculated and their dependence with temperature examined. The results found are discussed in terms of solute-solvent interactions.

Python to determine solubility in cosolvent mixtures

[1]*Osorio Gallego, J., [1]*Tinoco Robledo, L. E., [1]Cardenas Torres, R., E.

[1] Grupo de Fisicoquímica y Análisis Matemático (Physchemath), Facultad de Ciencias y Humanidades, Fundación Universidad de América, Bogotá 111321, Colombia
Facultad de Ciencias y Humanidades, Fundación Universidad de América, Bogotá
luz.tinoco@profesores.uamerica.edu.co; jhonny.osorio@profesores.uamerica.edu.co

The determination of the solubility of substances in cosolvent mixtures has potential applications in the pharmaceutical, environmental and industrial areas. The aim of this study was to determine the best-fit parameters of the solubility models using the Python programming language. To perform this, experimental solubility data in co-solvent mixtures at different temperatures were correlated with data calculated through different solubility models between them van't Hoff, Apelblat modified Buchowski-Ksiazaczak λh, van't Hoff-Yaws. The correlation indices obtained from the substances analyzed, including sulfadiazine (SD), sulfamerazine (SMR) and sulfamethazine (SMT), were higher than (R^2 = 0.99). Likewise, the correlation of the solubility data calculated with each of the models vs. the experimental solubility data is shown in Figure 1. In conclusion, Python could be considered as a potential alternative tool to find the best-fit parameters of the solubility models.[1,2]

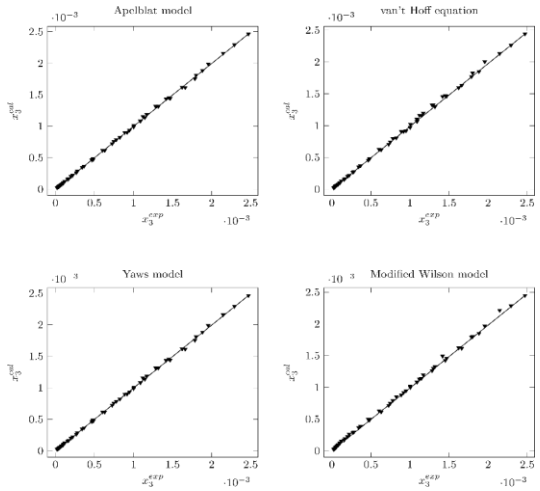

Figure 1. The experimental solubility data versus predicted solubility data of SMT (ethanol + water).

References

1. Tinoco, L. E., Galindres, D. M. ., Osorio, J. ., & E. Cárdenas, R. (2021). Prediction of sulfamerazine and sulfamethazine solubility in some cosolvent mixtures using non-ideal solution models. Revista Colombiana de Ciencias Químico- Farmacéuticas, 50(1). https://doi.org/10.15446/rcciquifa.v50n1.95463.
2. Cárdenas, R. E. ., Tinoco, L. E., Galindres, . D. M. ., Beltrán, A. ., Oviedo, C. D. ., & Osorio, J. . (2020). Prediction of sulfadiazine solubility in some cosolvent mixtures using non-ideal solution models. Revista Colombiana de Ciencias Químico-Farmacéuticas, 49(3). https://doi.org/10.15446/rcciquifa.v49n3.91347.

Innovations in Active Ingredients - Probiotics with live microorganisms

Daniella Cristine Lopes Francischetti
BASF, Brasil
daniella.a.lopes@basf.com,

First probiotic ingredient with living microorganisms that promotes rejuvenating lifting effect and reduces neuromuscular contraction comparable to α-bungarotoxin

Preliminary study of photoelectrochemical properties of Cerium Dioxide (CeO_2) obtained by electrochemical synthesis

Alberto Enrique Molina Lozano*, María T. Cortés*
Chemistry Department, Universidad de los Andes, Cra. 1 #18a-12, Bogotá, Colombia
ae.molina@uniandes.edu.co

Some main factors of the synthesis of cerium dioxide and their influence on the photoelectrochemical properties of the semiconductor were evaluated. Cerium oxide was obtained in a 3-electrode electrochemical cell as a coating on a FTO electrode (Fluor Tin Oxide Coated Glass) from an aqueous solution of $CeCl_3$ and $NaNO_3$ under a potentiostatic signal of 1.2 V (vs. Ag/AgCl) for 300 s. Subsequently, the material was sintered in uncontrolled atmosphere at high temperature. Three concentrations of the Ce^{+3} precursor and seven sintering temperatures were studied. Through Raman and FTIR spectroscopies the structural properties of the oxide coatings were characterized. By means of linear sweep voltammetry (LSV) and chronoamperometry (CA) the photocurrent and photostability of the material were evaluated. These techniques gave indications of phenomena such as exciton production, charge separation and recombination.
The electrochemical measurements show that there is a great influence of sintering temperature and precursor concentration on photocurrent, being favored by the increase in sintering temperature and the low concentration of Ce^{+3}. This could be attributed to changes in particle size favoring the band gap of CeO_2[1]. The photocurrents of the CeO_2 photoelectrode slowly decreased over time, this process could be attributed to electronic saturation in the charge separation or structural changes during the photoelectrocatalytic process due to the application of a potential bias[2].

References

(1) Ma, R.; Zhang, S.; Wen, T.; Gu, P.; Li, L.; Zhao, G.; Niu, F.; Huang, Q.; Tang, Z.; Wang, X. A Critical Review on Visible-Light-Response CeO2-Based Photocatalysts with Enhanced Photooxidation of Organic Pollutants. Catalysis Today 2019, 335, 20–30. https://doi.org/10.1016/j.cattod.2018.11.016.
(2) Liu, Z.; Guo, S.; Hong, C.; Xia, Z. Synthesis and Photocatalytic Properties of CeO2 Nanocubes. Journal of Materials Science: Materials in Electronics 2016, 27 (2), 2146–2150. https://doi.org/10.1007/s10854-015-4004-1.

Cobalt(II) Meso-Tetra-(4-Sulfonatophenyl)-Porphyrinate doped polypyrrole coatings for photoelectrochemical oxygen reduction.

Martín Emilio González*[1], Jhon Puerres[2], Mauro Diaz[1], John Hurtado[1], María T. Cortés[1]

[1]Chemistry Department, Universidad de los Andes, Bogotá, Colombia
[2] Chemical Engineering Program, Universidad de La Salle, Bogotá, Colombia
*m.gonzalezhernandez@uniandes.edu.co

An anionic porphyrin (TPPS: porphyrin meso-tetra-(4-sulfonatophenyl)-porphin) was synthesized[1] and used as a dopant in the electrochemical synthesis of polypyrrole coatings on FTO substrates (glass coated with Fluoride and Tin Oxides). The synthesis of the polymer was performed in a three-electrode cell under galvanostatic signal and in an aqueous solution containing pyrrole and TPPS. The cobalt complex was subsequently obtained by immersion of the polypyrrole coating in aqueous cobalt acetate solution[2]. The new material was chemically characterized and its ability to photoelectrochemically catalyze the oxygen reduction reaction was evaluated.

The incorporation of the porphyrin to the polypyrrole and the generation of the complex was verified by IR spectroscopy and by SEM-EDS, the obtained coatings were homogeneous and with globular topology. The photoelectrochemical response of the material under cathodic conditions (- 0.4 V vs. Ag/AgCl) was evaluated by chopped light chronoamperometry. The material showed cathodic photocurrents in air atmosphere (16 □A/cm^2), corresponding to oxygen reduction. The stability of the material was high since no significant variations in current were observed during the test, and the Raman signals and Soret bands were maintained in position and intensity after the photoelectrochemical test.

Therefore, this new composite material presented photocurrents for oxygen reduction of similar magnitude to other complex-based materials, with the advantage of greater stability during the photoelectrochemical test.

References:

1. Chakraborty, R.; Sahoo, S.; Halder, N.; Rath, H.; Chattopadhyay, K. Conformational- Switch Based Strategy Triggered by [18] Heteroannulenes toward Reduction of Alpha Synuclein Oligomer Toxicity. ACS Chem. Neurosci. 2019, 10, 573–587.
2. Johanson, U.; Marandi, M.; Sammelselg, V.; Tamm, J. Electrochemical properties of porphyrin-doped polypyrrole films. J. Electroanal. Chem. 2005, 575, 267–273.

Volumetric properties of two Resorcin[4]arenes in solution

[1,2]*Diana M. Galindres, [2]Edgar F. Vargas.

[1] Grupo de Fisicoquímica y Análisis Matemático (Physchemath), Facultad de Ciencias y Humanidades,Fundación Universidad de América, Bogotá 111321, Colombia
[2]Universidad de los Andes, Department of Chemistry, Bogotá, Colombia
diana.galindres@profesores.uamerica.edu.co

The resorcin[4]arenes are versatile macrocyclic compounds of great relevance in supramolecular chemistry due to their ability of pre-organization, to form host-guest complexes. The Resorcin[4]arenes have an upper ring and a lower ring, which can be functionalized, the lower ring with hydrocarbon chains, which allow change the hydrophobicity of the macrocycle and the upper ring, with different functional groups, for example, the sulfonate group, which gives it the property of being soluble in water

Apparent partial molar volumes, C-tetra (ethyl) sodium resorcin[4]arene sulfonate (Na_4EtRA) and C-tetra (propyl) sodium resorcin[4]arene sulfonate (Na_4PrRA) (Figure 1) in solution were determinated. Density measurements were made as a function of concentration and temperature. The results were discussed in terms of solute-solute interactions, solvent-solvent interactions and solute-solvent interactions. The results were compared with their homologous compounds reported in the literature such as Na_4MeRA and Na_4BRA. Using Debye Huckel limiting law the values of Bv were found, also the results of the ionic molar volume, finding that the values for this increase with hydrophobicity.

Figure 1. Structure of two ionic resorcinarenes, C-tetra (ethyl) sodium resorcin[4]arene sulfonate (Na_4EtRA) b) C-tetra (propyl) sodium resorcin[4]arene sulfonate (Na_4PrRA)

Solvent Acting as Catalyst: BF3-Mediated Acetylation of Pyrazolo[1,5-a]pyrimidines

Jhon Zapata Rivera
Departamento de Química, Universidad de los Andes – Colombia.
j.zapatar@uniandes.edu.co

Abstract: A plausible mechanism for the BF3-mediated acetylation reaction of pyrazolo[1,5-a]pyrimidines, based on density functional theory (DFT) calculations, is detailed. To the best of our knowledge, this is the first example of the direct acetylation for the functional pyrazolo[1,5-a]pyrimidine. Remarkably, it has been found a notorious lowering in the reaction and activation energy of the reaction by effect of the acetic acid as solvent, which forms a weak ionic pair with the pyrazolo[1,5-a]pyrimidine, namely a catalyst like behavior. That finding explains the kinetic and thermodynamic favorability of the reaction in front of the solvent.

Ionic Liquids as functional additives for lubricant applications

Donato, M. T.[1,2]; Colaço, R. [3], Saramago, B.[2]; Branco, L.C.*[1]
[1]LAQV-REQUIMTE, Departamento de Química, Faculdade de Ciências e Tecnologia, Universidade Nova de Lisboa, Campus da Caparica, 2829-516 Caparica, Portugal
[2]Centro de Química Estrutural, Instituto Superior Técnico, Universidade de Lisboa, Av. Rovisco Pais, 1049-001 Lisbon, Portugal
[3]IDMEC-Instituto de Engenharia Mecânica, Departamento de Engenharia Mecânica, Instituto Superior Técnico, Universidade de Lisboa, Av. Rovisco Pais, 1049-001 Lisbon, Portugal
l.branco@fct.unl.pt

Ionic Liquids (ILs) as low-melting organic salts exhibit interesting physico-chemical properties such as high chemical and thermal stability, almost negligible vapor pressure, high ionic conductivity, non-flammability and ease in dissolving organic, inorganic and polymeric materials. One of the most attractive IL characteristic is related with the selection of cation- anion combinations to modulate their desired properties as well as the final application in several research fields.[1]

One of the potential applications of ILs is focused in the discovery of efficient lubricants for NEMs/MEMs (nano/microelectromechanical) devices, which are a set of new devices that will significantly change our day-to-day lives in the next few decades. In general, ILs as promising lubricants or additives for this type of systems have been recently reported.[2-5] Herein, we report the use of ILs including the protic ones based on different organic cations combined with sulfonate anions as additives to the commonly used base oil PEG 200 and assess the tribological performance, namely friction and wear. All the prepared lubricants were characterized in terms of their water content, viscosity, wettability and tribological properties. The friction coefficients were measured using steel and silicon spheres against Si surfaces. The most promissory ILs showed a good tribological performance, both in terms of friction and wear reduction comparing to commercial lubricant PEG 200 making them very good candidates for future applications in electronic devices.

Acknowledgements: This work was supported by Fundação para a Ciência e Tecnologia (FCT) [projects UID/QUI/50006/2019,UIDB/50006/2020,UID/QUI/00100/2019, UIDB/00100/2020, UIDB/50022/2020 (LAETA) and grant SFRH/BD/140079/2018 from Mariana Donato, respectively].

References

[1] R. L. Vekariya, J. Mol. Liq. **2017**, 227, 44–60.
[2] S.A.S. Amiril, E.A. Rahim, S. Syahrullail, J. Clean. Prod. **2017**, 168, 1571–1589.
[3] M.T. Donato, R. Colaço, L.C. Branco, B. Saramago, J. Mol. Liq. **2021**, 333, 116004.
[4] M. Antunes, M.T. Donato, V. Paz, F. Caetano, L. Santos, R. Colaço, L.C. Branco, B. Saramago, Tribol. Lett. **2020**, 68, 1–14.
[5] M. T. Donato, L. Santos, H. P. Diogo, R. Colaço, L. C. Branco, B. Saramago, J. Mol. Liq. **2022**, 350, 118572.

Interactions in the newly synthesized task specific ionic liquids

[1]Vraneš, M., [2]Bešter-Rogač, M., [1]Panić, J., [1]Papović, S., [1]Borović, T.T., & [1*]Gadžurić, S.

[1]Department of Chemistry, Biochemistry and Environmental Protection, Faculty of Science, University of Novi Sad, Trg Dositeja Obradovića 3, 21000 Novi Sad, Serbia
[2]Faculty of Chemistry and Chemical Technology, University of Ljubljana, Večna pot 113, 1000 Ljubljana, Slovenia
slobodan.gadzuric@dh.uns.ac.rs

Many problems induced by structure properties of conventional active pharmaceutical ingredients such as low solubility, poor bioavailability or the polymorphism of the drugs, can be overcome by their preparing in the liquid ionic form. Recent studies about novel ionic liquids with the potential pharmaceutical application reported that transformation to an ionic liquid form improves lipophilicity/hydrophilicity of drugs, and thus better permeability through a cell membrane compared with solid salts. In addition, these liquids shown better stability, drug release and tunable therapeutic effect in comparison with the compounds they are made from.

In the framework of this work, three agmatine based ionic liquids: agmatinium ibuprofenate, agmatinium salicylate and agmatinium-nicotinate were synthesized and characterized. The successful incorporation of agmatine into the structure of ionic liquids together with biorelevant anions provides a new field of study in the preparation of biologically acceptable double-acting compounds, which could have wide application in agriculture and pharmacy. The correlation found between the binding energy and the aggregate state of the compound can be used for preliminary analysis in the synthesis of ionic liquids as a predictor of whether the salt will crystallize or reward the ionic liquid.

Also, four ionic liquids based on local anesthetics: lidocaine-ibuprofenate, lidocainium salicylate, procainium ibuprofenate and procainium salicylate, were successfully synthesized. Synthesized ionic liquids based on local anesthetics and anti-inflammatory compounds tend to spontaneously associate in aqueous solutions. This property of drug-based ionic liquids can improve their permeability through the skin. The formation of ion pairs enables their transdermal application because it increases the lipophilicity of the drug enough to pass through the skin and exert its pharmacological effect, but reduces their ability to be further absorbed into the bloodstream.

An analytic model of water that gives accurate dynamic properties

Urbic, T.
Faculty of Chemistry and Chemical Technology, University of Ljubljana, Slovenia
Tomaz.urbic@fkkt.uni-lj.si

The structures and properties of biomolecules like proteins, nucleic acids, and membranes depend on water. Water is also very important in industry. Overall, water is an unusual substance with more than 70 anomalous properties. The understanding of water is advancing significantly due to the theoretical and computational modeling. There are different kinds of models, models with fine-scale properties and increasing structural detail with increasing computational expense, and simple models, which focus on global properties of water like thermodynamics, phase diagram and are less computationally expensive. Simplified models give a better understanding of water in ways that complement more complex models. Here, we will present analytical modelling of properties of water on the twodimensional Mercedes–Benz (MB) models of water.

How co-solutes modulate the complexation between bovine serum albumin and sodium polystyrene sulfonate

[1*]Matjaž Simončič[*] and [1]Miha Lukšič

[1] Faculty of Chemistry and Chemical Technology, University of Ljubljana, Večna pot 113, SI-1000 Ljubljana, Slovenia

miha.luksic@fkkt.uni-lj.si

The interaction between an oppositely charged protein and a polyelectrolyte (PE) in aqueous solutions can lead to the formation of protein-PE complexes. This can result in phase separation depending on several parameters, such as the PE charge density, charge anisotropy of the protein surface, pH and ionic strength of the solution, presence of co-solutes, to name a few. Interestingly, complex formation is often initiated on the "wrong side" of the protein's isoionic point, i.e. when both molecules carry the same net charge. Understanding the modulating effect of other components (salt ions, buffer species, sugars, etc.) on the initial formation of protein-PE complexes is crucial considering their importance in number of applications, e.g. biomaterials, drug delivery systems, biosensors, and protein purification.

By using a combination of turbidimetric titrations and isothermal titration calorimetry, complemented by circular dichroism and fluorescence spectroscopy, we were able to elucidate the modulating role of salts (NaCl, NaBr, NaI) and sugars (sucrose, sucralose) on the complexation between a globular protein, bovine serum albumin (BSA), and a synthetic polyelectrolyte, sodium polystyrene sulfonate (NaPSS) at pH values above the isoionic point of the protein ($pH > pI_{BSA}$).[1]

The onset of BSA-NaPSS complex formation is driven by the electrostatic attraction between positively charged patches on the BSA surface and the overall negatively charged NaPSS. Naturally, the presence of salts screens those interactions and prevents the complexation in a concentration dependent manner following the order: NaI > NaBr > NaCl. The effect of sugars is less pronounced as sucrose does not affect the complexation, however its chlorinated analogue, sucralose, prevents the phase separation. The difference can be attributed to their water-structuring capabilities[1,2]. Sucrose does not interact directly with the protein surface (preferential exclusion mechanism), however sucralose adheres to the BSA surface (preferential interaction mechanism) and can hinder the contact between BSA and NaPSS.

References

[1] M. Simončič, M. Lukšič, (2022), Modulating Role of Co-Solutes in Complexation between Bovine Serum Albumin and Sodium Polystyrene Sulfonate. Polymers, 14(6), 1245.

[2] M. Simončič, M. Lukšič, (2021), Mechanistic differences in the effects of sucrose and sucralose on the phase stability of lysozyme solutions. J. Mol. Liq., 326, 115245.

New Approach for the Study of the Formation of Tetradecyltrimethylammonium Bromide (TTAB) micelles in (water-dioxane) mixtures.

[1]* Sondes BOUGHAMMOURA. ,[1]Mariem GABSI., [1]Jalel M'HALLA.
UR Electrolytes and Polyelectrolytes, Laboratory LPQS, Faculty of Sciences of Monastir, University of Monastir, 5000 Monastir, Tunisia
Sondes.mhalla@fsm.rnu.tn

The equivalent conductivity of the cationic surfactant : Tetradecyltrimethylammonium Bromide ($C_{17}H_{38}NBr$) was measured at 25°C and 1atm, in pure water and two water-dioxane mixtures respectively 10% and 20% in percent dioxane weight (P_D%), and in a large range of concentration:1.210^{-3} mol.l^{-1} 2.510^{-2} mol.l^{-1} .

Experimental results was analyzed according to our coherent model[1], in terms of the mass-action model, the generalized Fuoss ionic-association model[2,3], the Onsager–Kim–MSA conductivity theory of mixed electrolytes[4-6] in order to determine electrophoretic and ionic relation effects, and in taking into account the dielectric-friction effect on micelles[3,7] in order to determine their ionic friction coefficient β_{TTAB}^{ir} .

For each P_D%, the degree of condensation (1-α), the degree of micellization (1-β), the apparent charge ($Z_{ap}e = f(\alpha, \beta)$) of the micelle, the *thermodynamic* constant of micellisation $K_{TM}(T,P)$, the conductibilities at infinite dilution $\lambda°_{TTAB}$ and $\lambda°_{TTA+}$ respectively of the micelle and of the free monomers, are obtained by adjusting the theoretical conductivity χ_{th} of the mixture to its corresponding experimental value below and above the CMC concentration.

Results show that all these parameters decrease progressively when P_D% increases, in particular: $\lambda°_{TTA+}$= 19.12 ; 15.36 and 12.79 S.cm.equi^{-1} and $K_{TM}(T,P) \approx 10^{163}$; 10^{147}: 10^{126} respectively for P_D(%) = 0, 10 and 20%.

However, the CMC increases with P_D% : $CMC_{0\%} = 10^{-3}$ mol.l^{-1} < $CMC_{10\%}$ = 5.4510^{-3} mol.l^{-1} < $CMC_{20\%}$ =10^{-3} mol.l^{-1} .

[1] S.Boughammoura, J.M'halla, J.Molecular Liquids ,175 (2012) 148-161.
[2] R. Fuoss, F. Accascina, Electrolytic Conductance, Interscience Publishers, NewYork, 1969.
[3] J. M'halla, Journal of Molecular Liquids 82 (1999) 183–218.
[4] L. Onsager, S.K. Kim, The Journal of Physical Chemistry. B 61 (1957) 215–229.
[5] S. Durand-Vidal, P.Turq, O.Bernard, C. Treiner,The Journal of Physical Chemistry. B101 (1997) 1713–1717
[6] G.M. Roger, S.D. Vidal, O. Bernard, P. Turq, The Journal of Physical Chemistry. B 113(2009) 8670–8674.
[7] R. Zwanzig, Chemical Physics 38 (1963) 1603–1606.

Importance of dielectric friction effect in the interpretation of the dependency of the mobility of carboxymethylcellulose polyion chains on the nature of their counterions

[1*]Anis GHAZOUANI., [1]Sondes BOUGHAMMOURA., [1]Jalel M'HALLA.
UR Electrolytes and Polyelectrolytes, Laboratory LPQS, Faculty of Sciences of Monastir, University of Monastir, 5000 Monastir, Tunisia
jalel.mhalla@fsm.rnu.tn

In general, theoretical interpretation of polyelectrolytes equivalent conductivity is carried out from approaches using modified Manning's equations[2] for ionic condensation and conductivity considering the scaling description for the conformation of a polyion chain[1]. However, none of these approaches takes into account the dielectric friction effect on chain electrically charged groups or blobs.

In this presentation, we propose a new approach in order to interpret the dependency of the equivalent conductivity of some carboxymethylated cellulosic dilute polyelectrolytes XCMCi[3,4,5] on their (X) alkali counterions or ammonium counterions. The CMCi chains are characterized by different degree of substitution (CH_2COO^- groups are randomly linked to the 750 ring-blocks). Moreover, this approach evaluates the degree of ionic condensation in conformity with the Ostwald's principle, and the rate of each of the four frictional contributions (hydrodynamic, electrophoretic, ionic relaxation and dielectric friction) to the equivalent conductivity of the polyion, depending on its conformation, concentration, and the nature of its counterions.[6,7]

This dependency of the equivalent conductivity of CMCi polyion on the nature of its counterions was found to be greatly affected by the dielectric friction effect in the case of stretched polyions or necklace like-chains, and in a lesser extent, by the specific ionic condensation (Hofmeister phenomena), or by the hydrodynamic-electrophoretic friction.

[1] M. Muthukumar, 50th Anniversary Perspective: A Perspective on Polyelectrolyte Solutions, Macromolecules. 50 (24) (2017) 9528–9560.
[2] G. S. Manning, Limiting law for the Conductance of the Rod Model of a Salt-free Polyelectrolyte Solution, J. Phys.Chem.79 (3) (1975) 262-265.
[3] Jan C. T. Kwak, Allan J. Johnston, The Equivalent Conductivity of Aqueous Solutions of Salts of Carboxymethylcellulose: A Test of Manning's Limiting Law, Canadian Journal of Chemistry, March 1975, https://doi.org/10.1139/v75-110.
[4] H. Vink, Studies of Electrical Transport Processes in Polyelectrolyte Solutions, J. Chem. Soc. Faraday Trans.I, 85(3) (1989) 699-709.
[5] Dhiman Ray, Ranjit De, Bijan Das, Thermodynamic, transport and frictional properties in semi

dilute aqueous sodium carboxymethylcellulose solution, J. Chem. Thermodynamics 101 (2016) 227–235
[6] J. M'halla, S. Boughammoura, A. Ghazouani, Translational dielectric friction on a pearl-necklace- like polyelectrolyte chain, J. Mol. Liq. 326 (2021) 115173.
[7] Anis Ghazouani, Jalel M'halla, Sondes Boughammoura, Dependency of the mobility of carboxymethylated cellulosic polyions on the nature of their counterions, J. Mol. Liq. 353 (2022) 118547.

Applications of solution chemistry in the industry – selected examples

Pál Sipos
Department of Inorganic and Analytical Chemistry, University of Szeged, Dóm square 7, 6720, Hungary
sipos@chem.u-szeged.hu

Aqueous solutions are commonly employed in several industrial processes, including various fields of hydrometallurgy (e.g., alumina production via the Bayer process, production of base- and precious metals), selectively extracting the dissolved compounds from salt lakes or handling the high ionic strength formation waters during the enhanced oil recovery (EOR), etc. Traditionally, these operations have been optimized empirically, for a variety of reasons; most importantly, because industrial conditions are most often far outside of the "comfort zone" of the usual laboratory ones (in terms of temperature, pressure, reactant concentrations, pH, just to mention a few.) Over the last couple of decades, due to the development of experimental and theoretical means, considerable fundamental knowledge has been accumulated in this field making it possible to understand and to further polish industrial operations that used to be refined by the "trial and error" method. Our research group has been involved in some industrial endeavors, in which aqueous solutions played pivotal role. Accordingly, the main purpose of the presentation is to demonstrate through selected, largely "home-grown" examples, that the basic principles of solution chemistry are very useful, in some cases may even be vital for the industry.

Phase equilibria for system containing the sulfates of lithium, sodium and potassium: effect of temperature

[1]*Xudong Yu, [1]Fuyu Zhuge, [1]Shan Feng, [1]Qin Huang & [1]Ying Zeng
[1]College of Materials and Chemistry & Chemical Engineering, Chengdu University of Technology, Chengdu, P. R. China.
College of Materials and Chemistry & Chemical Engineering, Chengdu University of Technology, Chengdu, P. R. China.
xwdlyxd@126.com

A huge volume of natural salt lake with high concentrations of lithium, potassium are widely distributed in China. For the comprehensive utilization of salt lake, the concentrating pond and crystallization pond are used for the separation of sodium and potassium, and the content of lithium is also concentrated. However, due to the complex interaction between lithium and co-existing sodium and potassium in the concentrating process, lithium cannot be effectively enriched and precipitated, especially in the sulfate type salt lake, which increases the difficulty of efficient utilization of lithium. Commonly, the dissolution and crystallization behavior of salts in solution can be obtained through the phase equilibria study of the complex salt- water system at multi-temperature. Accordingly, the phase equilibria of the system containing the sulfates of lithium, sodium, potassium at 298 K was investigated, and the comparison of the phase diagrams of the system at 293, 323, and 373 K was done. Results show that (1) the crystallization form of lithium salt are $Li_2SO_4 \cdot H_2O$, $Li_2SO_4 \cdot Na_2SO_4$, $2Li_2SO_4 \cdot Na_2SO_4 \cdot K_2SO_4$, $Li_2SO_4 \cdot 3Na_2SO_4 \cdot 12H_2O$, $Li_2SO_4 \cdot K_2SO_4$ at 298, 323, and 373 K.
(2) the crystallization field of the lithium containing double salt enlarges with the temperature increase, which indicates that lithium can be precipitated in the form of double salt at higher temperature. (3) with the increase of the kinds of coexisting ions in the system, the lithium concentration required for the formation of lithium containing double salt is lower.

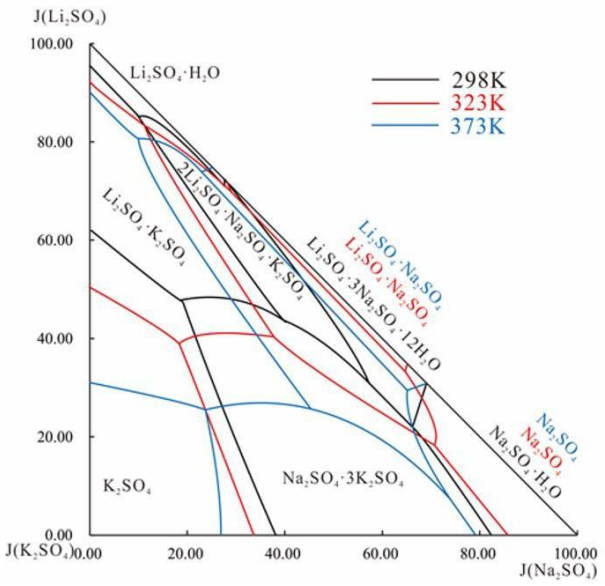

Fig.1 The comparisons of phase diagrams of the system containing the sulfates of lithium, sodium and potassium at 298, 323[1], and 373[1] K.

This work is supported by Sichuan Science and Technology Program(No. 2022YFQ0075).

Reference

1. Sohr, J., Voigt, W., Zeng, D. W. J. Phys. Chem. Ref. Data., 2017, **46**: 023101.

Hydration shell spectra from ratio spectra and modified excess spectra in aqueous LiCl and aqueous alcohols.

Ke Lin*, Zeya Jin, Cheng Peng, Zhiqiang Wang, Lin Ma, Ruiting Zhang
School of Physics, Xidian University, China
klin@xidian.edu.cn

The hydration structure of the solute in aqueous solutions is the basic scientific questions, various technologies are employed to study the hydration structures. IR and Raman spectroscopies are usually used to study aqueous solutions. We used some novel data analysis methods to measure the hydration shell spectra. Ratio spectra were employed to measure the hydration spectra of organic compounds and non-organic compounds in water, and the hydration number were record from the hydration spectra. It was found contacted ion pairs were observed from the hydration shell spectra of aqueous LiCl. Modified excess spectra were employed to measure the hydration shell spectra of alcohols in water. It was found some stable alcohol-water clusters were existed in aqueous solutions. These results demonstrated not only some interesting structure in aqueous solutions, but also the novel data analysis methods could be employed to study the micro-structure in various aqueous solutions.

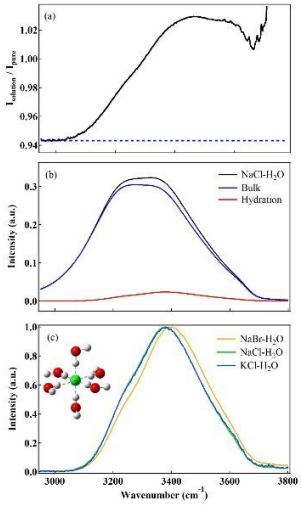

Figure a: IR ratio spectra of aqueous NaCl, b: IR spectra of bulk water, hydration water and total water in aqueous NaCl, c: hydration spectra of aqueous NaCl, NaBr, KCl

References

1. Yuxi Wang, Weiduo Zhu, Ke Lin*, Lanfeng Yuan*, Xiaoguo Zhou, Shilin Liu*, Ratiometric detection of Raman hydration shell spectra, Journal of Raman Spectroscopy, 47 : 1231 (2016)
2. Zhiqiang Wang, Siqi Duan, Bin Fang, Zhenxiang Liu, Ruiting Zhang, Lin Ma, Ke Lin*, Identification of the Molecular Structure of Mandelic Acid in Solid and Aqueous Solutions by Raman Spectra in the C-H/C-D Stretching Region, Vibrational spectroscopy, accepted, 2022

Dielectric Relaxation Study on Li-ion Conduction in Aqueous and Non-aqueous Superconcentrated Electrolyte Solutions

[1]*Jihae Han, [1]Erika Otani, [2]Kouji Shibata, [3]Tsuyoshi Yamaguchi, [4]Hikari Watanabe and [1]Yasuhiro Umebayashi.

[1]yumescc@chem.sc.niigata-u.ac.jp, Niigata University, Japan; [2] Hachinohe Institute of Technology, Japan; [3] Nagoya University, Japan; [4] Tokyo University of Science, Japan.

Superconcentrated electrolyte solutions (SEs) have attracted attention as novel electrolyte materials to exhibit the specific Li^+ conduction. In gylme (CH_3O-$(CH_2CH_2O)_n$-CH_3, Gn) -Li salts equimolar mixtures solutions, i.e., solvate ionic liquids (SILs), the Li^+ moved fast comparable to anion and solvent. [1] Dokko et al. reported that Li^+ hopping conduction occurred in sulfolane (SL)- based SE, which exhibited the faster Li^+ diffusion than that for solvent. [2] However, the details of the specific Li+ conduction mechanism for SEs is unclear. In this works, we investigated the Li- ion conduction in aqueous and non-aqueous SEs by means of dielectric relaxation spectroscopy and speciation of Li ion.

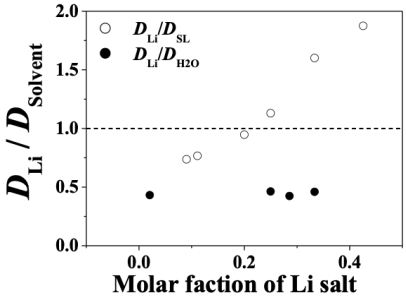

Figure1. A self-diffusion coefficient (D) ratio of D_{Li} to $D_{solvent}$ for LiTFSA- H_2O and $LiBF_4$-SLsolutions at 30 °C.

A self-diffusion coefficient (D) ratio of D_{Li} to $D_{solvent}$ for the LiTFSA-H_2O solutions at 30 °C was estimated and compared that for $LiBF_4$-SL solutions. [2] The results are shown in The value of $D_{Li}/D_{solvent}$ for the LiTFSA- H_2O solutions was ~0.42 with independent concentration of Li salt and its value is lower than that for the $LiBF_4$-SLsolutions. In the $LiBF_4$-SL solutions, the increase in the $D_{Li}/D_{solvent}$ over 1 indicates that the diffusion of Li^+ is faster than that of solvent, resulting a Li^+ hopping conduction. To reveal Li^+ conduction in aqueous and non-aqueous SEs, we carried out a broad band dielectric relaxation spectroscopy (DRS) and speciation of Li ion by Raman spectroscopy and complementary least square analysis (CLSA). We found the formation of contact ion pair (CIP) or aggregate (AGG) in the LiTFSA-H_2O solutions with increasement of concentration by Raman study [4], it was also shown in the the non-aqueous systems, herein, LiTFSA-Gn and $LiBF_4$-SL solutions. In the DRS for the

non-aqueous systems, we found that the specifically slower relaxation under 100 - 200 MHz was observed by shorter length of chain for gylmes[3], and increasing the concentration of Li salt for SL system . We estimated the relation between the relaxation time of slowest dielectric mode and the ionic conductivity as well as viscosity to exhibit a linear line. It suggests that the slowest relaxation time is contributed to the ionic conductivity and viscosity. In the DRS for highest concentration LiTFSA-H_2O solution, the typical lower relaxation strength of H_2O was observed at around 1 GHz, and its position was higher than that for above the non-aqueous systems. We noted that solvent exchange plays an important role in Li^+ conduction in Li-Gn SILs and SL-based SEs which have particularly slower relaxation, whereas the Li^+ diffusion in the LiTFSA-H_2O SEs moved not faster than solvent but anion. It suggests that the Li^+ is not capable to exhibit the specific Li^+ conduction for $LiBF_4$-SL system, and the slowest relaxation is possibly to related to the specific Li^+ conduction.

[1] Zhang et al., J. Phys. Chem. B, **118**, 19, 5144-5153 (2014). [2] Dokko et al., J. Phys. Chem. B, 122, **47**, 10736-10745 (2018). [3] Arai et al., J. Phys. Chem. C, **123**, 30228-30233 (2019). [4] Watanabe et al., J. Phys. Chem. B, **125(27)**, 7477-7484 (2021).

Light Switchable Ionic Liquids Systems

Zhiyong Li, [1]* Liufang Zhao,[1] Yang Zhao[1] & Jianji Wang[1]

[1] Key Laboratory of Green Chemical Media and Reactions, Ministry of Education, School of Chemistry and Chemical Engineering, Henan Normal University, Xinxiang, Henan 453007, China

yli@htu.edu.cn

Light-responsive ionic liquids (ILs) are a class of functional materials that combine the characteristics of light stimuli responsive materials and ILs. Upon UV/vis light irradiation, the structure, property and performance of these "smart" ILs can be significantly changed, which are expected to have important applications in many practical processes. Light trigger is of great importance because of its superiority, such as stable optical signal, accurate stimulation spot, and rapidly switched in a clean and non-invasive manner.

In this abstract, we will show the related work of ionic liquid systems with light switchable property[1-3], the main contents are as follows. 1. light-switched conductivity of ionic liquids aqueous solutions; 2). light-switched reversible emulsification and demulsification of oil-in-water Pickering emulsions; 3). light-triggered switchable ionic liquid aqueous two-phase systems.

References

1. Li, Z.; Yuan, X.; Feng, Y.; Chen, Y.; Zhao, Y.; Wang, H.; Xu, Q.; Wang, J., A reversible conductivity modulation of azobenzene-based ionic liquids in aqueous solutions using UV/vis light. Physical Chemistry Chemical Physics **2018,** 20, (18), 12808-12816.
2. Li, Z.; Feng, Y.; Liu, X.; Wang, H.; Pei, Y.; Gunaratne, H. Q. N.; Wang, J., Light triggered switchable ionic liquid aqueous two-phase systems. ACS Sustainable Chemistry & Engineering **2020,** 8, (40), 15327-15335.
3. Li, Z.; Shi, Y.; Zhu, A.; Zhao, Y.; Wang, H.; Binks, B. P.; Wang, J., Light-Responsive, Reversible Emulsification and Demulsification of Oil-in-Water Pickering Emulsions for Catalysis. Angewandte Chemie International Edition **2021,** 60, (8), 3928-3933.

Speciation of aluminum ions in non-aqueous $AlCl_3$ solutions for electrochemical deposition

[1*]Yui Nagashima, [1]Erika Otani, [2]Atsushi Kitada, [3]Kuniaki Murase, [1]Jihae Han and [1]Yasuhiro Umebayashi

[1] yumescc@chem.sc.niigata-u.ac.jp Niigata University, Japan [2] Tokyo University, Japan [3] Kyoto University, Japan

Non-aqueous Al alloy electroplating baths of low-energy cost are required as a novel bath for Al alloy electroplating at room temperature. Recently, Kitada et al. found that only $AlCl_3$-diglyme ($CH_3O(CH_2CH_2O)_2CH_3$: G2) solution enables good aluminum deposition/dissolution among a other glyme ($CH_3O(CH_2CH_2O)_nCH_3$, Gn).[1] Wen et al. reported that the electrodeposition of aluminum was observed at room temperature in □-butyrolactone (GBL). [2] However, the electrodeposition mechanism is still unclear in non-aqueous solutions such as $AlCl_3$-Gn or $AlCl_3$-

GBL solutions. We found that $AlCl_3$ salts can be dissolved in acetonitrile (AN) and sulfolane (SL) up to $AlCl_3$ mole fraction of 0.15 or more. We investigated the speciation of aluminum ion in non- aqueous solvents such as AN, SL, glymes and the Al^{3+}—Cl□ complex formation reaction by means of ^{27}Al NMR, Raman spectroscopy, and molecular orbital calculations.

In ^{27}Al NMR spectra of the $AlCl_3$-AN system, five signals were independently observed, which should be assigned to kinds of Al^{3+}—Cl□ complexes. Figure1 shows ^{27}Al NMR spectra of the $AlCl_3$-SL solutions. Two sharp signals were observed in the $AlCl_3$-SL solution, which are assigned to the tetrahedral and octahedral Al^{3+}—Cl□ complexes. It has been clarified that the peak of the tetrahedral Al^{3+}—Cl□ complex appears on the low magnetic field side and the peak of the octahedral Al^{3+}— Cl□ complex appears on the high magnetic field side in N,N-dimethylformamide and N,N-Dimethylacetamide.[3] In addition, the signal at around 60 ppm was ascribed to the five-coordinate complex of Al^{3+} in $AlCl_3$-SL solution. The peak position and the full width at half maximum varied as the increase of the $AlCl_3$ salt concentration. It suggests that Al^{3+} chemical exchange between anions and solvents is faster than the NMR time scale, resulting to the time-averaged peaks assigned kinds of Al^{3+} species in $AlCl_3$-SL solutions. Interestingly, such fast exchange reactions were also found in $AlCl_3$-Gn (n=2~4) solutions, though the solvents are multi-dentate ones. According to Raman spectra of $AlCl_3$ solutions, $[AlCl_4]$□ and $[Al_2Cl_7]$□ were found in all systems examined here except SL, in which the formation of $[Al_2Cl_7]$□ were unclear due to the SL Raman bands overlapping. The cyclic voltammetry was carried out for the $AlCl_3$-SL solution (x_{AlCl_3}= 0.2) at various temperature, but good Al electrochemical deposition was hardly found. According to Kaneko et al., the SL oxygen

atoms were eliminated at the interface of a lithium metal to form a lithium oxide surface layer. [4] Al electrochemical deposition may be inhibited owing to the similar oxygen atoms elimination to form aluminum oxide passivation layer at the electrode surface.

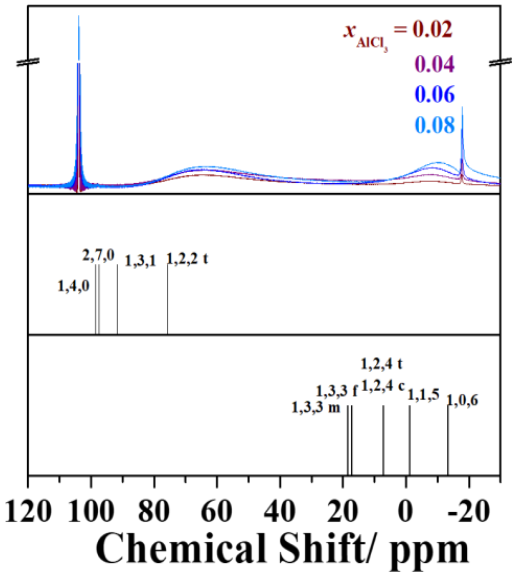

Figure1. ^{27}Al NMR spectra of the $AlCl_3$-SL solution and theoretical NMR spectra of Al^{3+} — Cl^- complexes of $[Al_pCl_q(SL)_r]^{3p-q}$; (p, q, r)

[1] Kitada et al., Electrochimica Acta, 2016, **211**, 561-567. [2] Wen et al., J. Phys. Chem. Lett., 2020, **11**, 1589-1593.[3] Umebayashi et al., Journal of the Chemical Society-Faraday Transactions, 1998, **94**, 5, 647 - 651 [4] Kaneko et al., Chemical Physics Letters, 2021, **762**, 138199

Experimental and Theoretical Studies on the Molecular Dynamics in Ionic Liquids Triggered by Photodissociation of Bis(p-aminophenyl)disulfide

[1]*Kaori Fujii, [2]Tomoaki Yagi, [2]Hiroshi Nakano, [2,3]Hirofumi Sato, [1,4]Yoshifumi Kimura

[1] Faculty of Science and Engineering, Doshisha Univ., Japan.
[2] Graduate School of Engineering, Kyoto Univ., Japan.
[3]FIFC, Kyoto Univ., Japan.
[4] Graduate School of Science and Engineering, Doshisha Univ., Japan
e-mail to K. Fujii: kafujii@mail.doshisha.ac.jp

Ionic liquids (ILs) have been revealed to show unique behaviour as a reaction solvent due to their heterogeneous solvation environment derived from alkyl chains of cation. In this study, we focused on the photodissociation reaction in ILs. Bis(p-aminophenyl)disulfide undergoes bond dissociation when irradiating UV pulse, and generates geminate pair of p-aminophenylthyil (PAPT) radical. Since dipole moment and molecular volume of photo-dissociated product are different from the parent molecule, surrounding solvent ILs reorient to stabilize geminate radicals. These solvation dynamics competes with the recombination process of geminate radical. Since both solvation and recombination dynamics are affected by the solvent properties such as polarity and viscosity, we selected various tetraalkylphosphonium and tetraalkylammonium ILs with different alkyl chain length. To monitor these molecular dynamics triggered by the photodissociation, we conducted ultrafast transient absorption spectrum measurement after the photodissociation and discuss how the physicochemical properties of ILs alter the solvation and geminate recombination dynamics by non-equilibrium molecular dynamics simulation and theoretical model.

Transient absorption spectrum of PAPT radicals in ILs shifted to lower energy with time, which means the solvent reorganization occurred after the photodissociation. However, time constant for the solvation dynamics occurred in the time range of picosecond to several hundred picoseconds was unexpectedly independent of the viscosity of ILs.1

We also found interesting behaviour for the geminate recombination of PAPT radicals.2 Both recombination yield and dynamics were independent of the

cation species of ILs. To discuss those experimental results, time-profiles of recombination yield calculated by the band integral of transient absorption was theoretically analysed based on diffusion limited reaction model (Smoluchowski-Collins-Kimball equation). To consider solvent cage effect of ILs that constructs an activation barrier for the recombination, the original model was modified to include square well potential (SWP). The experimentally obtained time-profiles of recombination yield was simulated with long-time asymptotic form of the SWP model, and validity of the parameters, diffusion coefficient, radius and depth of solvent cage was discussed.

1) Phys. Chem. Phys. Chem., 2021, 23, 4569-4579. 2) J. Chem. Phys., 2021, 154, 15404(1-11).

Studies on the aggregation of N-butylpyridinium tetrafluoroborate confined in carbon nanotubes

[1]*Guanglai Zhu, [1]Zhicong Liu, [1]Chenchen Wang & [1]Zhaopeng Ma

[1] School of Physics and Electronic Information, Anhui Normal University, P. R. China
zhglai@mail.ahnu.edu.cn

The one-dimensional confined space inside carbon nanotubes (CNTs) has a complex effect on the liquid, which leads to the aggregation state of the liquid in it is different from that of the bulk phase.[1,2] In a series of molecular dynamics simulations, we found interesting changes in the aggregation state of the ionic liquid N-butylpyridinium tetrafluoroborate ([BPy][BF_4]) in CNTs.

As shown in Fig. 1, we could found that anions and cations show an asymmetric distribution in (12,12) CNT which is very difference with that in (16,16) CNT. As the diameter increases, the aggregation behavior in the center of CNTs changes alternately, and it almost disappears in CNTs which has enough large diameter. The angular probability distribution shows that pyridine ring tends to lie flat on the inner wall of carbon nanotubes by the π-π interaction. Our results could improve the understanding of the [BPy][BF_4] microstructure in different carbon nanotubes.

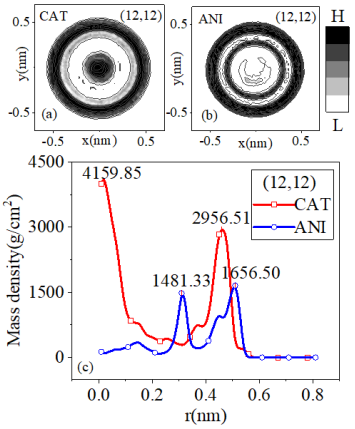

Fig. 1. Density distributions of [BPy][BF_4] in CNT (12, 12): the density projection along the axial of $[BPy]^+$ cations (a) and $[BF_4]^-$ anions (b), the radial mass density of $[BPy]^+$ cations and $[BF_4]^-$ anions (c).

This work was supported by the Natural Science Foundation of Anhui Province of China (No. 2108085MA21).

1. Hummer G, Rasaiah J C, Noworyta J P. Water conduction through the hydrophobic channel of a carbon nanotube. Nature. 414 (2001) 188–190.
2. Wang X, Fu F, Peng K, Huang Q, Li W, Chen X, Yang Z. Understanding of Competitive Hydrogen Bond Behavior of Imidazolium-Based Ionic Liquid Mixture around Single-Walled Carbon Nanotubes. J. Phys. Chem. C. 124 (2020) 6634–6645.

Intermolecular Vibrations of 1-Methyl-3-octylimidazolium Tetrafluoroborate Mixtures with Formamide, N-Methylformamide, and N,N-Dimethylformamide

[1]*Masatoshi Ando, [1]Yue Peng, [2]Atsuya Tashiro, [2]Masahiro Kawano, [3]Toshiyuki Takamuku, [1]Hideaki Shirota

[1]Department of Chemistry, Chiba University, Japan, [2]Graduate School of Science and Engineering, Saga University, Japan, [3]Faculty of Science and Engineering, Saga University, Japan

anmasatoshi1@chiba-u.jp, Department of Chemistry, Chiba University, Japan

In this study, we measured the low-frequency spectra of 1-methyl-3-octylimidazolium tetrafluoroborate ([MOIm][BF_4]) mixtures with formamide (FA), N-methylformamide (NMF), and N,N-dimethylformamide (DMF) by femtosecond Raman-induced Kerr effect spectroscopy[1] to elucidate the effects of hydrogen bonds of molecular liquids (MLs) on intermolecular vibrations of ionic liquids.

The low-frequency spectra of the [MOIm][BF_4] mixtures are shown in Figure 1. As increasing ML mole fraction X_{ML}, the spectral intensity of the mixtures gradually increased. In the neat MLs, FA had a peak at 100 cm^{-1} and a shoulder at 200 cm^{-1} and NMF also had a shoulder at 130 cm^{-1}. We assigned the band at 100 cm^{-1} in FA and that at 130 cm^{-1} in NMF to the linear hydrogen-bonding (HB) band and the band at 200 cm^{-1} in FA to the two-dimensional HB band based on the quantum chemistry calculations by Torii and Tasumi.[2]

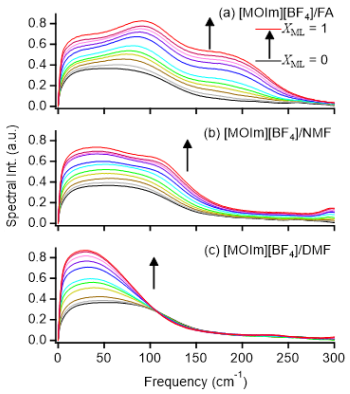

Figure 1. Low-frequency spectra of the [MOIm][BF_4] mixtures with (a) FA, (b) NMF, and (c) DMF.

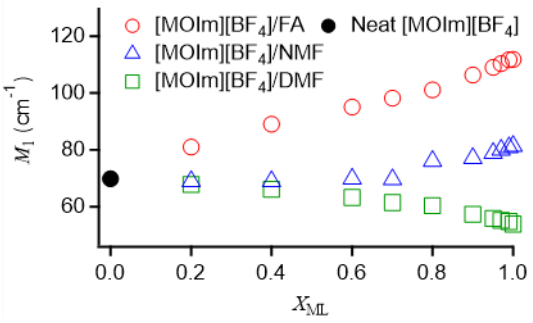

Figure 2. Plots of M_1 vs. X_{ML} for the [MOIm][BF_4] mixtures with FA, NMF, and DMF.

To characterize the X_{ML} dependence of the entire intermolecular vibrations including the HB vibrations in detail, we plotted the first moment M_1 of the low-frequency band vs. X_{ML} for the [MOIm][BF_4] mixtures in Figure 2. As increasing X_{ML}, the M_1 for the [MOIm][BF_4]/FA shifted to the higher-frequency side, and that for the [MOIm][BF_4]/DMF shifted to the lower-frequency side. The M_1 for the [MOIm][BF_4]/NMF showed almost constant in $X_{ML} \leq 0.7$ and shifted to higher-frequency side in $X_{ML} \geq 0.7$. The difference in the X_{ML} dependence of the M_1 for the mixture systems should be attributed to the HB abilities of the MLs.

References

1) H. Shirota, J. Phys. Chem. A **2012**, 115, 14262.
2) H. Torii and M. Tasumi, Int. J. Quant. Chem. **1998**, 70, 241.

Hydrogen-bond configurations of hydrogen fluoride in relation to the hidden halogen-bonding ability

[1]Saito, K. & [1]*Torii, H.
[1] Shizuoka University, Japan
torii.hajime@shizuoka.ac.jp

Hydrogen fluoride (HF) is known as a molecule of high electrically quadrupolar nature to the extent that the hydrogen-bond chains are significantly bent. In fact, molecules containing other halogen atoms (Cl, Br, I) are also known as involved in intermolecular interactions of electrically quadrupolar nature, which is called halogen bonding. In the latter cases, a practical and widely adopted way to represent this electrostatic situation is to place a partial positive charge on an additional site called "extra point" located on the line extended from the d–X covalent bond (where d is the atom that is covalently bonded to halogen X). Then, is this way of placing partial charges practical also for HF? In the present study, this problem is tackled by conducting electron density analysis on the HF molecule (Fig. 1), by examining the polarization properties based on the calculations on the HF dimer, and by doing MD simulations on liquid HF.[1]

[1] K. Saito and H. Torii, J. Phys. Chem. B **125**, 11742–11750 (2021).

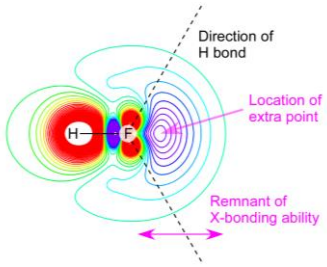

Fig. 1. Two-dimensional contour plot of the electron density difference taken between the HF molecule and the F^- ion calculated at the MP2/6-31+G(2df,p) level, and its relation to the location of the extra point and the hydrogen-bond direction.[1]

Structure and properties of a single aqueous electrolyte droplet ultrasonically levitated in the air

Toshio Yamaguchi,[1,2,*] Shun-ichiro Matsuo,[2] Koji Yoshida,[2] Shoji Ishizaka,[3] Koji Ohara[4]

[1]Xinghai Institute of Salt Lakes, CAS, Xining 81008 China
[2]Department of Chemistry, Fukuoka University, Fukuoka 814-0180 Japan
[3]Department of Chemistry, Hiroshima University, Hiroshima, 739-8526 Japan
[4]Diffraction & Scattering Division, Japan Synchrotron Radiation Research Institute, Hyogo 679-5198 Japan

e-mail: yamaguch@fukuoka-u.ac.jp

Atmospheric aerosols are critical in global climate change and the atmospheric environment. They are fully involved in the formation of clouds and global warming. To understand the physicochemical properties of aerosols and the underlying mechanism of cloud formation and reaction in aerosols, the compositions, properties, and structure of aerosol droplets in the air are highly needed at the molecular level.

In the present study, the composition, properties, and structure of single aqueous electrolyte droplets in the air are investigated under the ambient condition at the molecular level by Raman spectroscopy and in situ synchrotron X-ray diffraction. Aqueous electrolytes measured are aqueous solutions of ammonium sulfate, magnesium nitrate, and magnesium sulfate. A single aqueous electrolyte droplet of about 1 mm is levitated in the air ultrasonically. The compositions of the droplets are determined by measuring the sulfate S-O, nitrate N-O, and the water O-H bands on Raman spectra using a 532-nm laser. The structure of the droplets is determined by using synchrotron X-rays of the wavelength 0.108 Å. The experimental interference functions are subjected to empirical potential structure refinement to reveal the ion solvation and association, water structure in terms of the pair correlation function, coordination number distribution, and spatial density function (3D structure).

Analysis of the Raman spectra shows that the concentration of electrolytes in the droplets is several times higher than that of the corresponding bulk solutions, particularly the supersaturation of aqueous magnesium sulfate droplets. The octahedral coordination geometry of a magnesium ion, hydration of a sulfate ion, ion association, and water structure are revealed. Furthermore, in-situ X-ray scattering measurements observe crystallization from a magnesium sulfate droplet. The present methods apply to the investigation of supercooling phenomena and chemical reactions of aerosol droplets at the molecular level.

Ion conductivity and speciation of lithium salt 1,3-propane sultone solution

[1]*Yui Kawana, [1]Jihae Han, [2]Hikari Watanabe & [1]Yasuhiro Umebayashi

[1] yumescc@chem.sc.niigata-u.ac.jp , Niigata University, Japan
[2] Tokyo University of Science, Japan

Higher energy density is required for next-generation lithium-ion batteries, so that a highly ionic conductive electrolyte is crucial peticulaly for the battery capasitance. It was suggested that the specfic ionic conduction occurs in the super-concentrated lithium salt solutions, which are the solution whose lithium salt concentration is so high that the ions are not sufficiently solvated[1]. Yamada et al. reported that acetonitrile-based super-concentrated solutions shows the fast charging/dischargeing. Super-concentrated solutions of tetrahydrothiophene 1,1-dioxide (SL) were also proposed as electrolytic solutions for lithium-ion batteries, in which the self-diffusion coefficient for Li^+ is greater than those for the anion and the solvent[2]. 1,3-propane sultone (PS) is an analog of SL, which contains an oxygen atom in the 5 membered ring. DFT calculations suggest that as the number of oxygen atoms introduced into the 5 membered ring increases, the solvation power to Li^+ is weakened without the Li^+ solvation structure change from that in SL. In order to clarify the effect of the electron-pair donating ability on the lithium ion conduction, the electrochemical properties of some lithium salts in 13PS solutions were investigated.

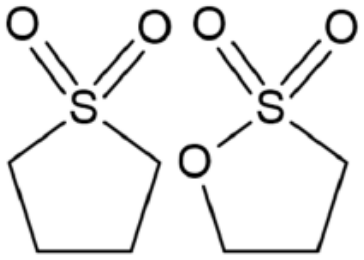

SL **PS**

The neat PS is a solid at a room temperature. Mixing LiTFSA ($Li(CF_3SO_2)_2N$) with PS lowered both the freezing and the melting points to expand the liquid temperature range. In the Walden plots, the higher the LiTFSA concentration is, the closer the plots approaches to the ideal line. Interestingly, the Walden plot of the LiTFSA:PS = 1:2 (Fig. 1) almost on the ideal line, suggesting that Li^+ moves fastest in PS, similarly to that in SL. The slope for the temperature dependence in the Walden plots was significantly smaller than unity of 0.75 in the temperature range of 25 to 85 °C, which suggests that the relaxation of the ionic conduction is smaller than that of the viscosity. The temperature dependences of the ionic conductivity and the viscosity were approximated by the Arrhenius equation to yield Arrhenius activation energy for the ionic

conductivity and the viscosity. In fact, the Arrhenius activation energy for the ionic conduction was smaller than that for the viscosity.

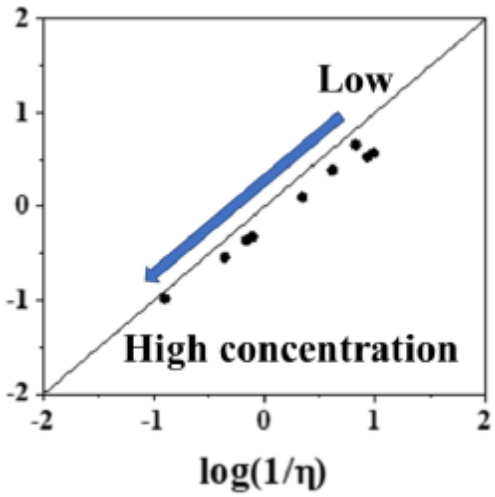

Fig 1. The Walden plots for LiTFSA-PS solutions with varying composition ratio at 25 ° C.

References

[1] Yamada, Y. *et. al. J. Am. Chem. Soc*. **2014**, 136, 13, 5039–5046
[2] Dokko, K. *et. al. J. Phys. Chem. B.* **2018**, 122, 10736−10745

Gas transportation in inhomogeneous systems studied using large-scale molecular dynamics simulation and dynamic Monte Carlo method

[1,2*]Tetsuro Nagai and [2]Susumu Okazaki

[1]Department of Chemistry, Faculty of Science, Fukuoka University, Fukuoka 814–0180, Japan
[2]Department of Advanced Materials Science, Graduate School of Frontier Sciences, The University of Tokyo, Kashiwa 277-8561, Japan
okazaki@edu.k.u-tokyo.ac.jp , The University of Tokyo, Japan

Nafion membranes, which are representative polymer electrolyte membranes, exhibit microphase separation forming heterogeneous structures. The membranes play a role in separating reactant gas molecules, and gas permeation deteriorates performance of the fuel cells. An understanding of gas permeation mechanism should help to rationally design molecules in the membranes to prevent the gas permeation, but it is not clear yet. There are conflicting reports as to the microscopic mechanism of the permeation and the paths of gas permeation are also unclear.

The molecular dynamics (MD) simulation is a powerful method to investigate a microscopic mechanism, but it is not straightforward to directly trace trajectories of the gas permeation in the heterogeneous system. Because of the heterogeneity, we need to study relatively large displacements of the gas molecules, but the diffusion constant of the gas molecules is estimated to be so low at the order of 10^{-7} cm^2/s. Therefore, it is required to track tens-of-microsecond long trajectories. It is too time-consuming to perform all-atom MD simulations for such time scales.

We develop and apply a new methodology and thereby we investigate the gas permeation in the Nafion membranes. In particular, we obtain free energy landscape and position-dependent diffusion constant from all-atom MD simulations. Using these obtained physical quantities input of dynamic Monte Carlo method, we build and evaluate a coarse-grained dynamics. We can clarify the details of the permeation mechanism by analyzing the coarse-grained dynamics. In the presentation, we would like to discuss not only our new methodology but also our recent results on the gas permeation in the Nafion membranes.

Alkali Ions Recognition by 18-Crown-6 in Aqueous Solutions: Evidences from Micro-Structure

[1,2]Zhuanfang Jing, [1*]Yongquan Zhou, [1]Toshio Yamaguchi, [4]Koji Ohara, [3]Jianming Pan, [1,2]Guangguo Wang, [1]Fayan Zhu, [1]Hongyan Liu

[1] Qinghai Institute of Salt Lakes, Chinese Academy of Sciences, Xining, Qinghai 810008, China.

[2] University of Chinese Academy of Sciences, Beijing 100049, China.

[3] School of chemistry & chemical engineering, Jiangsu University, Zhenjiang, Jiangsu 212013, China.

[4] Research and Utilization Division, Japan Synchrotron Radiation Research Institute, 1-1-1 Kouto, Sayo, Hyogo 679-5198, Japan.

Corresponding author: Prof. Yongquan Zhou

yongqzhou@163.com

X-ray scattering and density functional theory were employed to systematically investigate the structure and alkali metal ions recognition by 18-crown-6 in aqueous solutions. Li^+, Na^+ and K^+ locate inside the 18-crown-6 cavity to form the complexes. Among them, Li^+ and Na^+ deviate from the centroid of 18-crown-6 by 0.95 Å and 0.35 Å, respectively. Rb^+ and Cs^+ lie outside the 18-crown-6 ring plane with 0.05 Å and 1.35 Å away from the centroid of 18-crown-6. The formation of all 18-crown-6/alkali ions complexes is dominated by electrostatic attraction. Li^+, Na^+, K^+ and Rb^+ form the $H_2O\cdots$18 crown-6/$M\cdots H_2O$ "sandwich" hydrates, while the water molecules only hydrate with Cs^+ in 18-crown-6/Cs^+ from the same side of Cs^+. The recognition sequence of alkali metal ions by 18-crown-6 follows $Li^+ < Na^+ < K^+ > Rb^+$ in the aqueous solutions, which is totally different from that in the gas phase. The cations recognition by crown ethers is affected by the properties of cations and the solvation effect, etc.

Keywords: Complexation; Hydration; Ion recognition; X-ray scattering; Density functional theory

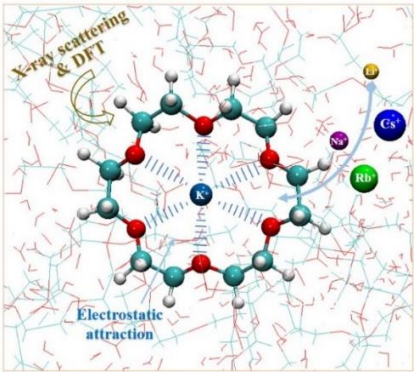

Figure 1. Alkali metal ions recognition by 18-crown-6 in aqueous solutions.

Acknowledgements: This work was financially supported by the National Natural Science Foundation of China (No.201973106) and the Innovation Platform Construction Project of Qinghai Province (2019-ZJ-T03).

Calorimetric Detection of Aggregation and Redispersion of Polyacrylic acid-coated Maghemite Nanoparticle in Protic Ionic Liquids

***KANZAKI Ryo, SAKO Mika, KODAMATANI Hitoshi, TOMIYASU Takashi**
Graduate School of Science and Engineering, Kagoshima University, 1-21-35, Korimoto, Kagoshima, 890-0065, Japan
kanzaki@sci.kagoshima-u.ac.jp , Kagoshima University, Japan

Ionic liquids, regarded as an extremely condensed electrolyte solvent, are interesting colloidal dispersion media. According to DLVO theory, the addition of electrolytes is generally the primary cause for reduced colloidal stability for charged nanoparticles in water. Therefore, ionic liquids could not to be "good" dispersing media of colloids. Even those predictions, techniques to yield stable dispersions of nanoparticles have already been obtained in various ionic liquids. We have investigated the pH response of the colloidal stability of maghemite magnetic nanoparticles, whose surface is functionalized with polyacrylic acid (pAA), coated nanoparticle (CNp). In aqueous solution, CNps aggregate to precipitate in an acidic condition, showing a single threshold pH, however, the same CNp shows two switching pH in some protic ionic liquids (PILs), ethylammonium nitrate (EAN) and *N*,*N*-diethylethanolammonium trifluoro-methanesulfonate. That is, CNps dispersed in basic PILs flocculate in mildly acidic condition, then redisperse in stronger acidic condition. It is interesting that this flocculation-redispersion is reversible; implying that different types of CNp-solvent interaction contribute the colloidal stability. With the aid of calorimetric investigation, it has been concluded that CNps attract solvent cations before aggregation, which remain among CNps in the flocculation phase, as if CNps are well swollen. These inter-particle cations allow the CNp surface carboxylic group to ionize in response to the bulk pH even in the aggregation state. Then, once the appropriate pH is reached, the charge repulsion of CNps causes redispersion. From these results, we propose a dual role of ionic liquids as colloidal dispersing media, i.e., the solvent ions in ionic liquids work as counterions surrounding charged nano-particles, at the same time, behave as a solvent to transmit the chemical environment of the bulk liquid phase.

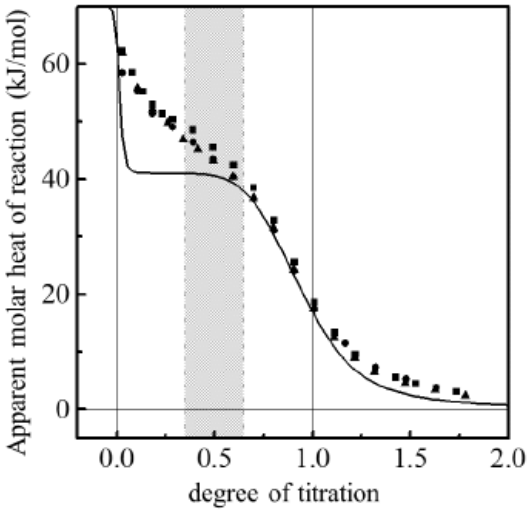

Calorimetric titration curve of CNp in *N*,*N*-diethylethanolammonium trifluoromethane-sulfonate. Shadowed are means the flocculation region. The solid line is the theoretical curve assuming ionization of carboxylic acid of pAA on CNp surface, showing an obvious deviation from the experimental points (filed symbols).

Effect of temperature at the time of gelation of cellulose dissolved in ionic liquid-DMSO solution on the physical properties of cellulose hydrogels

[1]*Kikuchi, K., [1]Seonju, J., [1]Ichihashi, S., [2]Kazuyoshi, K., [3]Yamada, M.,
[3]Ishii, H., [3]Inoue, T., [1,2]Shimizu, A.
[1]Graduate school of Science and Engineering, Soka University, Japan
[2]Faculty of Science and Engineering, Soka University, Japan
[3]Corporate science research, Nichirei Corporation, Japan
Corresponding author: Shimizu, A., shimizu@soka.ac.jp

Cellulose hydrogels (CHGs) have various advantages such as non-toxicity, biocompatibility, biodegradability, etc. Therefore, CHGs are expected to be used in various applications1,2,3, and gel properties are recommended to be tunable depending on the application. In general, it is known that the preparation conditions of CHGs affect the gel properties. The objective of this study is to clarify the relationship between the temperature during the gelation and gel properties such as mechanical strength, water content, shrinkage, and crystallinity.

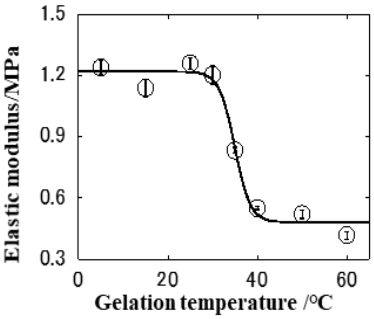

Fig 2. The relation of gelation temperature and elastic modules (n=3)

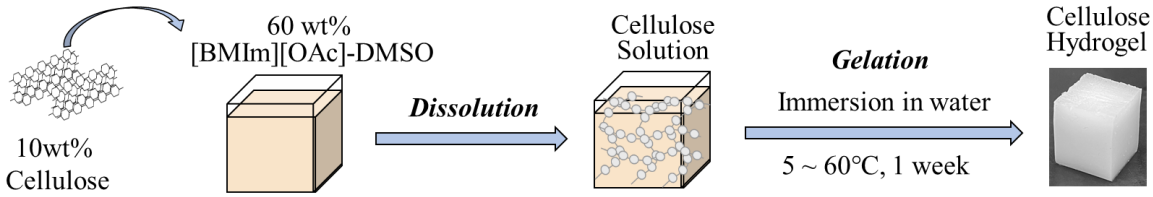

Fig 1. Manufacturing process diagram of CHGs

Microcrystalline cellulose (Avicel PH-101, DP=170) was used in this study. Ionic liquid 1-butyl-3-methylimidazolium acetate ([BMIm][OAc]) and Dimethyl sulfoxide （DMSO） were used as a cellulose solvent and cosolvent, respectively.

The relationship between elastic modulus and temperature during gelation is shown in the Fig 1. The elastic modulus showed a sharp sigmoidal transition with gelation temperature around 36°C. Moreover, the water content, shrinkage, crystallinity, and Congo red adsorption

were also showed the same trend. We will discuss the reason why these changes occur around 36°C from a point of view of the properties of cellulose solution.

1. Li J, Mooney DJ. Nat. Rev. Mater, 1, 16071 (2016). 2. Karlgard CC, Wong NS, Jones LW, Moresoli C. Int. J. Pharm. 257,141-51 (2003). 3. Basak S, Nanda J, Banerjee A. J. Mater. Chem, 22,11658 (2012).

ABSTRACTS POSTERS (FLASH PRESENTATIONS)

Rheological study of poly(styrene-co acrylonitrile)/carbon nanotubes solutions

[1]Caro, R., [1]Rocha, A., [1]Ruíz, L., [1]Martínez, G. & [1]Corea, M.
[1]Laboratorio de Nanomateriales y Polímeros. Escuela Superior de Ingeniería Química e Industrias Extractivas, Instituto Politécnico Nacional, Mexico.
Corresponding author: mcoreat@yahoo.com.mx, Instituto Politécnico Nacional, Mexico.

Rheological studies play a fundamental role in polymer processing, including fiber electrospinning. In this work, the rheological behavior of poly(styrene-co-acrylonitrile)/carbon nanotubes P(S:AN)/CNT solutions was studied. A sweep of monomeric concentrations: 0:100, 20:80, 40:60, 50:50 wt.%:wt.% and dispersions of 1.0 and 0.5 wt.% content of CNTs in dimethylformamide (DMF) were used. The presence of CNTs increased the shear-thinning behavior of polymeric solutions at room temperature 11 Pa·s (±2 Pa·s). The viscosity (η) of the solutions as a function of temperature (T) (rising ramp) shows typical shear-thinning from 30 °C until 70 °C, and then there is an abrupt increase from 11 to 2000 Pa·s over a temperature range of $74.93<T/°C<111.04$, for the dope with CNTs content of 0.5 wt.%, while for the content of 1.0 wt.% CNTs the viscosity increase occurs in the range of $81.82<T/°C<102.24$. The glass transition temperature (Tg) range of the polymeric solutions is dependent on the CNTs concentration, shifting the Tg range to higher temperatures as higher is the CNTs content, because of CNTs restrict the alignment and movement of the polymeric chains. Polymeric solutions can be electrospinnable in a viscosity range of $1\leq \eta/$ Pa·s≤ 15; below this range, the solution is electrosprayed forming micro- or nano-droplets; above this range, there is entanglement between polymeric chains and CNTs, and therefore the fibers are not electrospun.[1]

[1] Tiwari, S. K.; Venkatraman, S. S. Importance of viscosity in electrospinning: Of monolithic and core-shell fibers. Mat. Sci. Eng, C. 2012, 32, 1037-1042.

Effect of the mixtures composition on acetaminophen mass/volume percentage solubility in (ethanol + propylene glycol + water) mixtures at 25.0 °C

1 Romdhani, A., 2 Peña-Fernández, M. A. & 1* Martínez, F.

[1] Department of Pharmacy, Universidad Nacional de Colombia, Sede Bogotá, Colombia.

[2] Department of Biomedical Sciences, Universidad de Alcalá, Spain.

fmartinezr@unal.edu.co

The available values of solubility of pharmaceutical products in aqueous ternary mixtures are increasing in recent times [1]. In this work, the grammar solubility (g/100 mL) at saturation of acetaminophen in (ethanol + propylene glycol + water) mixtures at 25.0 °C was reported [2]. Solubility of drug increases when the ethanol and/or propylene glycol proportions increase in the mixtures.

Figure 1 shows the solubility profiles of acetaminophen in ternary solvent mixture as function of the ethanol mass fraction for different fixed mass fractions of propylene glycol. These solubility profiles could be used to define compositions of mixtures during the design of homogeneous liquid drugs based on this drug, particularly for injectable administration, where high drug concentrations are required to deliver a high dose in a small volume of product.

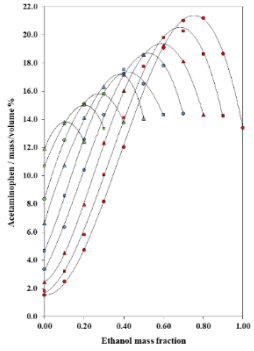

Figure 1: Experimental solubility of acetaminophen expressed in mass/volume % as function of the ethanol mass fraction in ethanol + propylene glycol + water mixtures for different mass fractions of propylene glycol (w_2) at 25.0 °C. Red circle: w_2 = 0.00; red square: w_2 = 0.10; red triangle: w_2 = 0.20; blue circle: w_2 = 0.30; blue square: w_2 = 0.40; blue triangle: w_2 = 0.50; green circle: w_2 = 0.60; green square: w_2 = 0.70; green triangle: w_2 = 0.80.

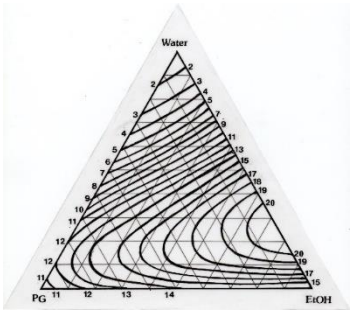

Figure 2: Experimental solubility of acetaminophen expressed in mass/volume percentage in ethanol + propylene glycol + water mixtures at 25.0 °C.

The three pure solvents, 27 (3×9) binary and 36 ternary solvent systems as seen in the Cartesian were considered. From this graph by interpolation, the triangle with fixed values of grammar solubility was constructed [3]. Isometric lines indicate solubility values as shown numerically in the triangle sides (**Figure 2**). This figure could find composition zones when some specific solubility values are imposed as required during design of pharmaceutical dissolutions.

References

[1] A. Jouyban, Handbook of Solubility Data for Pharmaceuticals, CRC Press, Boca Raton (FL), 2010.

[2] A. Romdhani, F. Martínez, O.A. Almanza, A. Jouyban, W.E. Acree Jr., Solubility of acetaminophen in (ethanol + propylene glycol + water) mixtures: Measurement, correlation, thermodynamics, and volumetric contribution at saturation, J. Mol. Liq., **318**, 114065 (2020).

[3] L.S. Palatnik, A.I. Landau, Phase Equilibria in Multicomponent Systems, Holt, Rinehart and Wilson, Inc., New York (NY), 1965.

Smart polymeric particles sensitive to pH and Temperature and their application in the acid stimulation processes

[1] Ruiz Lazaro, [1] Hernández Miguel*, [1] Martínez Gabriela, [1] Caro Rubén, [1] Corea Mónica & [1] Del Rio José Manuel.

[1] Escuela Superior de Ingeniería Química e Industrias Extractivas, Instituto Politécnico Nacional, Av. Luis Enrique Erro S/N, Unidad Profesional Adolfo López Mateos, Zacatenco, Alcaldía Gustavo A. Madero, C.P. 07738, Ciudad de México, México.
mcoreat@yahoo.com.mx, mcorea@ipn.mx, Instituto Politécnico Nacional, México.

Two series of latex with different proportions of monomers were obtained by means of emulsion polymerization technique. The first one (Serie 1) is a core – shell morphology, while the second one (Serie 2) is a core - gradient concentration morphology. The monomer ratio composition of both series were acrylic acid (AA) and acrylamide (AAm). Latex were formulated to have a total of functional of 40 wt.% and a solids content of 3 wt.%. These materials sensitive to pH and temperature can be used as possible dosing agents in the acid stimulation process for oil extraction.

The preliminary results are: the total solids content for each serie was determined using the gravimetric technique. The results of the amount of solid in the samples of Series 1 and Serie 2 is close to 2 wt%; except the polymeric material with 100 % AA that had a value of 1.01 wt.%. The polymeric materials with different morphologies were measured by dynamic light scattering (DLS) to determine the particle size distribution. In general, the average particle size (Dz) of polymeric particles in both series had values 100 < Dz/nm z 250. The polymer with a 100 wt.% content of AA reached Dz close to 600 nm.
The materials were analyzed in a density and sound velocity meter. From the density (ρ) and speed of sound (U) data, the volumetric thermodynamic properties were determined: Specific volume (v), and specific compressibility (k). The results of both series, a linear behavior is observed for each latex indicating that the material is in a high dilution region, allowing study the interaction only between the particles and water molecules. The linear behavior occurs for all latex at different temperatures (30, 40 and 60 °C).
The specific partial volume ($VP;1O$) and specific partial compressibility ($kP;1O$) at infinite dilution was calculated for the Serie 1 and Serie 2. The results of Serie 1 show at low concentration of AA, there is an increment in the values of $VP;1O$. This means that in this range of concentration there is a generation of free volume caused by electrostatic repulsions of the functional groups into the polymeric particle. At high concentrations of AA, there is a decrease in the values of $VP;1O$ due to the increase in the entry of water molecules into the interior of the particle. For Serie 2, there are no changes with respect to the different proportions of acrylic acid.

Influence of polyols on the activity and thermal stability of Horseradish peroxidase

Mayerly Johana Puchana-Rosero[1,2*], Julio Alberto Clavijo-Penagos[2*], Carmen Maria Romero-Isaza[2], Pablo Danilo Humpola [1,3]

1- Health and Life Science Faculty, Environmental Analysis Laboratory, Health and Life Science Research Centre, Universidad Autónoma de Entre Ríos, Argentina

2- Department of Chemistry, Basic Research Laboratory. Universidad Nacional de Colombia, Colombia.

3- Biological Sciences and Biochemistry Faculty. Research Laboratory, General and Inorganic Chemistry, Universidad Nacional del Litoral, Argentina.

*Corresponding authors: puchana.johana@.uader.edu.ar; jaclavijop@unal.edu.co

Horseradish Peroxidase (HPR) has been widely used in diverse biotechnological processes. In the field of environmental chemistry, particularly, in the wastewater treatment, it's native or modified form (as precursor of other materials) have been employed in the bio-transformation of phenolic compounds to reduce its negative impact on the environment. Furthermore, the literature has reported diverse stabilization methods that involved modification on the enzymatic structure or in the environment in which it act (solvent).

The aim of this work was analyse the effect of the presence of polyols as EG (ethylene glycol, purity 90%) and SB (D-sorbitol, purity 99%) in the action of HPR, throughout UV-Vis spectroscopic, enzymatic activity and thermal stability assays.

Studies of UV-Vis, showed an increase in the intensity of its Soret band at λ=403 nm. The remaining activity determined throughout the colorimetric method of 4-aminoantypirine, using hydrogen peroxide as co-sustrate, showed a high retention of the catalytic activity on the presence of these additives, being more pronounced this trend when increased the concentration. On the thermal stability studies, EG and SB showed a lightly stabilizing effect of the HPR, increasing in consequence its denaturation temperature (T_m). Other state functions as ΔH_m and ΔS_m decreased, which suggest an enthalpic-enthropic compensation process.

According to this, HPR might suffer exposition of its heme group and hydrophobic groups, which was induced by the solvent in the presence of EG and SB, when interact with the enzyme, affecting its activity and consequently its application in the bio-transformation or treatment of pollutants.

Construction and Automation to Improve a Calorimeter

Pedro Daniel Carteño Ventura[a], Mónica Corea [a], Jorge Isaac Chairez Oria[b], José Manuel del Rio[a], Cristopher Ordaz González[a], Takasuke Matsuo[c]
Lead Presenter Pedro Daniel Carteño Ventura
[a] Laboratorio de Investigación en Polímeros y Nanomateriales, ESIQIE-IPN, C.P. 07738, CDMX, México.
[b] Laboratorio de Ingeniería Biomédica, UPIBI-IPN, C.P. 07340 CDMX, México.
[c]Research Center for Structural Thermal Science, Graduate School of Science, Osaka University, Toyonaka, Osaka, Japan
mcoreat@yahoo.com.mx; mcorea@ipn.mx, Instituto Politécnico Nacional

The mechano-calorific effect is defined as the caloric phenomenon that is reflected in a thermodynamic system through mechanical action. Investigations include those of Profesor Takasuke Matsuo, who designed a device (calorimeter) that through the elongation of coatings of various rubber materials can indirectly obtain the entropic values of polymer materials. Due to the boom in calorimetry as a frequent tool in investigation, the importance of the technique suggests an economic, efficient way to obtain mechanical thermodynamic properties.

The construction was based on two parts: automation of the mechano-calorimeter designed in previous works and validation of the instrument with obtaining

Various characteristics were improved over the original instrument: an acrylic hood was placed to facilitate the operation of the device, given that it allows viewing the experiment and reduces the dissipation of heat, data readings directly offer the temperature values in °C required to obtain dissipative graphics, the heating and ventilation systems operate automatically when the DHT22 sensors of the aluminum box take environmental temperature readings above or below the desired temperature, if and when it is above room temperature, the temperature sensor of the DS18B20 coating records direct measurements of temperature changes of the sample, with data similar to those of Prof. Matsuo.

The instrument was validated with: λPDMS=5.3 and λE-P=5.9, using PDMS and E-P coatings. The results demonstrate that PDMS is a dissipative polymer whose deformation is an irreversible process that consumes mechanical energy. In addition, that E-P is a polymer without dissipation whose deformation is a reversible process that conserves energy. The equipment constructed was able to reproduce the tendencies of both rubbers.

Laccase-Catalyzed reactions in organic media

Karen Segura*, Edgar F. Vargas
Departamento de Química, Universidad de los Andes, Cr. 1 No. 18A 10, Bogotá, Colombia
k.segura@uniandes.edu.co

Laccase belongs to the copper oxidases and is used in environmental applications such as a ring cleavage of aromatic compounds. Resorcinarenes are macrocyclic molecules that can interact with macromolecules like proteins and enzymes[2]. In this work, the activity of laccase was measured using guaiacol in aqueous and water-1-propanol solutions at 298 K and pH 7. In addition, the effect of two resorcinarenes on the laccase activity, in organic media, was also studied.

References

[1] Xu Han, Chuan Tian, Ingrid Gandra, Valeria Eslava, Diana Galindres, Edgar Vargas, Roger Leblanc. (2017) The Investigation on Resorcinarenes towards either Inhibiting or Promoting Insulin Fibrillation. Chemistry – A European Journal. 23, 17903-17907.
[2] Nicole Collazos, Germán García, Malagon E, Obradith Caicedo, Vargas E. (2019) Binding interactions of a series of sulfonated water-soluble resorcinarenes with bovine liver catalase. International journal of biological macromolecules. 139 (1), 75-84.

Solubility of benzocaine in methanol + water mixtures according to the extended Hildebrand solubility approach

[1] Cárdenas, Z. J., [2] Peña-Fernández, M. A. & [1]* Martínez, F.
[1] Department of Pharmacy, Universidad Nacional de Colombia, Sede Bogotá, Colombia.
[2] Department of Biomedical Sciences, Universidad de Alcalá, Spain.
fmartinezr@unal.edu.co

Knowledge of the forces of interaction between solutes and solvents is of great interest in fields such as Pharmacy or Physical Chemistry, among others. The Hildebrand-Scatchard

Regular Solution Theory was applied to estimate the solubility of nonpolar drugs in nonpolar solvents [1], however, it is the polar system of irregular solutions that are commonly found in Pharmacy. For this reason, a modification of the Hildebrand-Scatchard equation (Eq. 1) was made, Martin et al. [2] developed the Extended Hildebrand Solubility Approach (EHSA) (Eq. 2), which allows the calculation of the solubility of polar and non-polar solutes in solvents ranging from non-polar hydrocarbons to very polar solvents.

$$-\ln X_2 = -\ln X_2^i + \frac{V_2\phi_1^2}{RT}(\delta_1 - \delta_2)^2 \qquad \text{(Eq. 1)}$$

$$-\ln X_2 = -\ln X_2^i + \frac{V_2\phi_1^2}{RT}(\delta_1^2 + \delta_2^2 - 2W) \qquad \text{(Eq. 2)}$$

where $\frac{V_2.\phi_2^1}{RT}$ is A term and V_2 is the partial molar volume, ϕ_1 is the volume fraction, and δ_1 and δ_2 are the solubility parameters of solvent and solute, respectively and W term is equal to $2K\delta_1\delta_2$ (K is the Walker parameter).

The experimental values of the W parameter can be correlated by means of regression analysis by using regular polynomials as a function of δ_1, as follows

$$W = C_0 + C_1\delta_1 + C_2\delta_1^2 + C_3\delta_1^3 + ... + C_n\delta_1^n \qquad \text{(Eq. 3)}$$

EHSA was applied in the present work to evaluate the solubility of benzocaine in (methanol + water) mixtures at 298.15 K [3]. EHSA method get a good prediction using W as a function of the solubility parameter of solvent mixtures free of solute and containing a regular polynomial in order 4 (**Figure 1**).

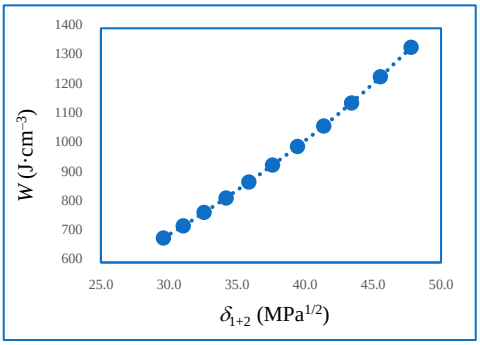

Figure 1. *W parameter as a function of the solubility parameter*

References

[1] A. Martin, P.L. Wu, Extended Hildebrand Solubility Approach: Hydroxybenzoic acid in mixtures of dioxane and water, J. Pharm. Sci. **72**, 587–592 (1983).

[2] A. Martin, J. Newburger, A. Adjei, Extended Hildebrand Solubility Approach: Solubility of theophylline in polar binary solvents, J. Pharm. Sci. **69**, 487–491 (1980).

[3] Z.J. Cárdenas, D.M. Jiménez, O.A. Almanza, A. Jouyban, F. Martínez, W.E. Acree Jr., Solubility and preferential solvation of benzocaine in {methanol (1) + water (2)} mixtures at 298.15 K, Phys. Chem. Liq., **56**, 465–481 (2018).

Thermodynamic properties and electronic structure on the complexation of sodium sulfamerazine with an ionic resorcin[4]arene

Nicolás Espitia*, David J. Hernández, Jhon E. Zapata, Edgar F. Vargas.
Departamento de Química, Universidad de los Andes, Cr. 1 No. 18A 10, Bogotá, Colombia
n.espitia@uniandes.edu.co

The formation of host-guest complexes with macrocycles and sulfonamides is of great interest in pharmaceutical chemistry. Herein, we report an experimental and computational study on the complexation of sodium sulfamerazine (SMR) with C-methylresorcin[4]arene tetraminomethylated hydrochloride (TAM). According to the Job´s plot, isothermal titration calorimetry (ITC), and mass spectrometry analysis the complex formation is given in a 1:1 ratio. The spectroscopic and computational experiments indicates that SMR is stabilized in a lateral posture on the upper amino rim of TAM. Further, the ITC experiments and frequency calculations confirms the presence of electrostatic interactions and favorable solvent reorganization that allows the complexation process. Finally, the TAM-SMR complex presented a greater association constant than those reported for β-CD presumably due to the anion-cation electrostatic interactions, being TAM more selective towards SMR in the complex formation.

Sodium alginate nanogels synthesis and characterization as potential drug deliverers

[1]Cuervo R.*, [1]Quiñones D.L.*, [1]Salazar J.L., [1]Martínez G.*, [1]Del Rio J.M*. & [1]Corea M.L*.

[1]Laboratory of polymers and nanomaterials, Higher School of Chemical Engineering and Extractive Industries, National Polytechnic Institute, Gustavo A. Madero, Mexico City, 07730, Mexico.
mcoreat@yahoo.com.mx, Higher School of Chemical Engineering and Extractive Industries, National Polytechnic Institute, Gustavo A. Madero, Mexico City, 07730, Mexico.

Nanogels are hydrogels with a size between 100-800 nm formed by cross-linked polymers. They present properties such as high water content, three-dimensional structure, biocompatibility, and the degree of swelling that allows the release of drugs through variations of conditions external to the nanogel, such as; temperature and pH. On the other hand, alginate is an anionic polymer widely used in pharmaceutical and biomedical applications, due to its properties such as the absence of toxicity, biodegradability, bioavailability, biocompatibility, and mucoadhesive properties among others, therefore, in this work the development of drug delivery through a system that maintains the structure of the drug to its target cell and delivers the indicated dose over a

prolonged period[1].

In this study, the synthesis and characterization of sodium alginate nanogels as potential drug deliverers are reported. The materials were synthesized with alginate and calcium chloride and characterized by their reaction order and calcium chloride conversion (CC), infrared spectroscopy (FT-IR), scanning electron microscopy (SEM), degree of swelling, and desorption and drug absorption.

The synthesis of sodium alginate nanogels was carried out as follows: a solution of sodium alginate with deionized water was prepared in a beaker. In a ball flask equipped with magnetic stirring, a hexane solution with surfactant was prepared. The surfactant solution was then added to the alginate solution with constant stirring. The drug was extracted and added to the alginate solution and stirred by means of a syndicator for 20 min.

The size obtained from the nanogels of sodium alginate and calcium chloride was 80 to 100 nm with a monodispersion which is optimal for loading the nanoparticles with Tamoxifen and Levofloxacin.

References

1. Matai, I., & Gopinath, P. (2016). Chemically Cross-Linked Hybrid Nanogels of

Alginate and PAMAM Dendrimers as Efficient Anticancer Drug Delivery Vehicles. ACS Biomaterials Science & Engineering, 2(2), 213–223. doi:10.1021/acsbiomaterials.5b00392.

Study of the interaction between resorcin[4]arenes and Insulin in aqueous solution

Valeria Eslava[a], Edgar F. Vargas[a] and Roger Leblanc[b]
[a]Universidad de los Andes, Chemistry Department, [b]University of Miami
v.eslava29@uniandes.edu.co

Two resorcin[4]arenes with sulfonate groups in opposite positions of the macrocycle rings, one with the sulfonate group in the upper ring Na4BRA and the other with the sulfonate group in the lower ring Na4SfRA (R' and R respectively, in Figure 1), were synthesized and their interaction with Recombinant Human Insulin were studied in aqueous solution.

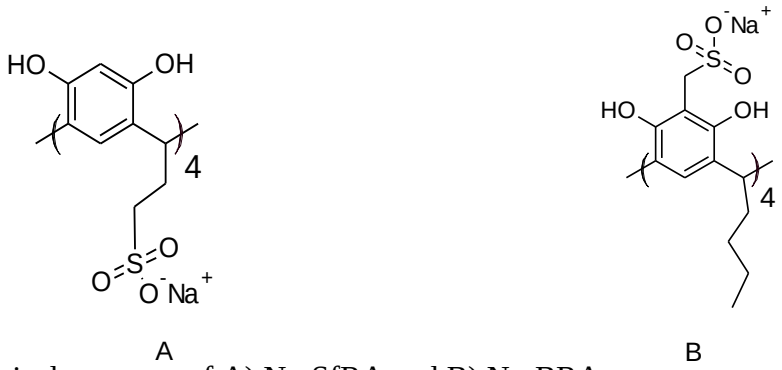

A B

Figure 1. Chemical structure of A) Na_4SfRA and B) Na_4BRA.

The interaction of Na4BRA and Na4SfRA with human recombinant insulin (IRH) was studied by fluorescence, UV-vis, circular dichroism and AFM. It was found that both solutes are inhibitors of the fibrillation process, and a complex formation was proposed.
It was determined that the position of the sulfonate group in the macrocycle and the change in the hydrophobic character of the resorcin[4]arenes have an important effect on the intermolecular interactions present, which is reflected in the interaction with the IRH.

Anomalous regions in core-softened models

[1]Medos, G., Turk, M., [1]*Urbic, T.

[1] Faculty of Chemistry and Chemical Technology, University of Ljubljana, Slovenia
Tomaz.urbic@fkkt.uni-lj.si

We determined hierarchy of anomalous regions in the core-softened system. Core-softened disks have two length scales of interaction, a hard core with one diameter and a soft corona with a larger diameter. One model has pure repulsion other has small attraction. The study was done by molecular dynamics, Monte Carlo simulation and integral equation theory. We determined regions of density, diffusivity and structural anomalies and their hierarchy.
We also checked the possibility that fluids with core-softened potential has the critical points and we could not determine them. Regarding integral equation theory, some versions failed to get the correct structure and thermodynamics of the system depending on the position in phase space while others are working rather well like modified Verlet closure for example.

An electric field changes water's anomalous regions and phase transitions

[1]*Urbic, T.
[1] Faculty of Chemistry and Chemical Technology, University of Ljubljana, Slovenia
Tomaz.urbic@fkkt.uni-lj.si

We have modelled influence of the electric field on water properties. We use the MB model of water, a simple two-dimensional statistical mechanical model in which waters are represented as Lennard-Jones disks having Gaussian
hydrogen-bonding arms, modified to interact with electric field. We perform Monte Carlo simulations to explore how water molecules are organized in the electric field of different strengths. The small strength of the electric field does not affect properties of water and position of phase transitions, while the strong strengths shift boiling and melting points as well as position of the density anomaly. From certain strength on the density anomaly disappears.

Phase diagrams of simple models of water

[1]Ogrin, P., [1]*Urbic, T.
[1] Faculty of Chemistry and Chemical Technology, University of Ljubljana, Slovenia
Tomaz.urbic@fkkt.uni-lj.si

When it comes to understanding of properties of a material, it is useful to know in which phases this material exists at different conditions. By constructing phase diagram of the material, knowledge about positions of phase transitions and structure of different phases can be obtained. Here, we used Nested Sampling (NS) algorithm to predict phase transitions and construct phase diagrams of Mercedes-Benz (MB) and rose water model. Nested Sampling is an algorithm that enables direct calculation of partition function, from which other thermodynamic quantities can be calculated. Using nested sampling no a priori knowledge about phases is needed in order to determine phase transitions, moreover all phase transitions regardless their type can be determined. Mercedes-Benz and rose water model are simple two-dimensional water models, in both models water molecules are modelled as Lennar-Jones disks, however orientationally dependent hydrogen bonding potential of the models is different. Using nested sampling we located multiple phase transitions and determined complete phase diagrams of both models.

Theoretical calculation research on ternary system NaCl-$CaCl_2$- H_2O based on PSC model

[1]*Longjie Sun, [1]Li Du, [1]Ying Zeng & [1]Xudong Yu
[1]College of Materials and Chemistry & Chemical Engineering, Chengdu University of Technology, Chengdu, P. R. China.
Chengdu University of Technology, Chengdu, P. R.
zengyster@163.com

The Sichuan Basin is rich in underground brine resources, containing a large amount of sodium and calcium resources, which have great development and utilization value. Most of the underground brine is of chloride type. Therefore, the ternary system NaCl-

$CaCl_2$-H_2O thermodynamic data was calculated by PSC model[1], so as to provide basic thermodynamic data for the phase equilibrium study of sodium and calcium coexistence high-element system[2]. It has important guiding significance for the industrial extraction of sodium and calcium resources in brine resources. Result shows that (1) the system is a simple co-saturation system, no double salts and solid solutions are formed, and it has one co-saturation point, two solubility univariate curves and two crystallization regions.
(2) The crystallization form of calcium chloride is $CaCl_2 \cdot 6H_2O$ at 303.2 K, while the crystallization form of calcium chloride is $CaCl_2 \cdot 2H_2O$ at 333.2 K and 373.2 K. (3) In the temperature range studied in this work, the crystallization area of NaCl is larger than $CaCl_2$. With the increase of temperature, the crystallization area of NaCl increase, $CaCl_2 \cdot 6H_2O$ is converted into $CaCl_2 \cdot 2H_2O$, and the crystallization area of $CaCl_2 \cdot 2H_2O$ increases.

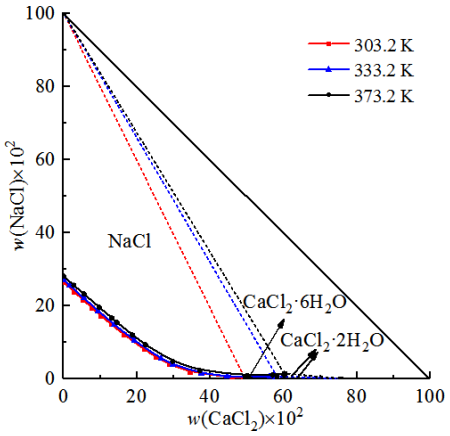

Fig.1 Phase diagram of the ternary system NaCl-$CaCl_2$-H_2O at 303.2 K, 333.2 K, 373.2 K

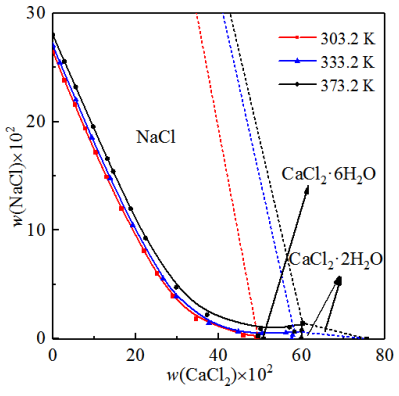

Fig.2 Partial enlarged view of Figure 1

This work is supported by the National Natural Science Foundation of China (No. U21A2017).

References

1. Clegg, L., Pitzer, K. S., Brimblecombe, P. J. Phys. Chem., 1992, **96**: 9470-9479.
2. Li, D. D., Zeng, D. W., Yin, X., Gao, D. D., Fan Y. F. Calphad, 2020, **71**: 101806.

Vibrational Dynamics of Thermoresponsive Polymer and Its Monomer Unit in Water Studied by 2D-IR Spectroscopy and MD Simulation

[1]*Yuki Fujii, [1]Hikaru Ioka, [2]Chihiro Hashimoto, [3]Ikuo Kurisaki, [3]Shigenori Tanaka, [4]Kaoru Ohta and [1,4]Keisuke Tominaga

[1] Graduate School of Science, Kobe University, Japan
[2] Department of Applied Chemistry and Biotechnology, Niihama National College of Technology, Japan
[3] Graduate School of System Informatics, Kobe University, Japan
[4] Molecular Photoscience Research Center, Kobe University, Japan
Molecular Photoscience Research Center, Kobe University, Japan
tominaga@kobe-u.ac.jp

Poly(N,N-diethylacrylamide) (PdEA, Figure 1) is one of the thermoresponsive polymers that shows a drastic conformational change, known as the coil-to-globule transition, in aqueous solutions at certain temperature. In this study, we studied the vibrational dynamics of the CO stretching modes of PdEA and its monomer unit; N,N-diethylpropylacrylamide (dEP) in D_2O by two-dimensional infrared (2D-IR) spectroscopy and molecular dynamics (MD) simulations to obtain the transiton mechanism at a molecular level. 2D-IR spectroscopy provides the time correlation functions (TCFs) of the transition frequencies of the vibrational modes, which are sensitive to structural changes of the local hydration.

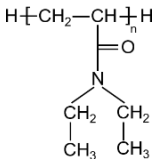

Figure 1. Molecular structure of PdEA.

The initial value of TCF of PdEA significantly increased upon the heating, whereas that of dEP did not. This is because the number of the immobilized water molecules inside the carbon backbone increases. Furthermore, we estimated the instantaneous frequencies of the CO stretching mode to reproduce linear IR spectra by MD simulations. The calculated TCFs suggested that the environment around the immobilized water molecules is inhomogeneous, where reorientational dynamics of hydrogen bonds around the CO group is significanlty slow.

Phase equilibria of the ternary system KCl+$MgCl_2$+H_2O at multi-temperature: calculation and comparison

[1]*Li Du, [1]Ying Zeng & [1]Xudong Yu
[1]College of Material and Chemistry & Chemical Engineering, Chengdu University of Technology, Chengdu, 610059, P. R. China
Chengdu University of Technology, Chengdu, P. R. China.
zengyster@163.com

Electrolyte solution theory is often used to explain the principle of phase equilibria, and thus a phase equilibria calculation model based on electrolyte solution theory is produced. Pitzer-Simonson-Clegg (PSC) model is often used to calculate the activity coefficient of solution[1]， while the model's three ion-interaction terms with parameters Ucc'a and Uaa'c are sequence-dependen, which is easy to cause confusion. Li improved the model and regressed a new set of parameters for describe
the non-ideality of the aqueous phase[2]. In his work, the solubilities in the ternary system KCl+$MgCl_2$+H_2O have been calculated by using revised PSC model at various temperatures. By comparing the solubility experimental values of the system KCl+$MgCl_2$+H_2O at 273.15 K[3], 298.15 K[4] and 323.15 K[5], results show that the experimental values are in good agreement with the calculated values, indicating the model and multi-temperature parameters is correct.

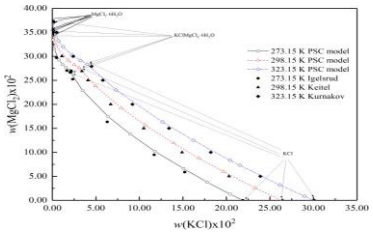

Fig.1 Comparison of multi-temperature phase diagrams of the ternary system KCl+$MgCl_2$+H_2O

This work is supported by National Natural Science Foundation of China (No. U21A2017).

References

1. Clegg, L., Pitzer, K. S., Brimblecombe, P. J. Phys. Chem., 1992, **96**: 9470-9479.
2. Li, D. D., Zeng, D. W., Yin, X., Gao, D. D., Fan Y. F. Calphad, 2020, **71**: 101806.
3. Igelsrud, I., Thompson, T. J. Am. Chem. Soc., 1936, **58**: 318-322.
4. Keitel, H., Gerlach. Kali, 1923, **17**: 248-265.
5. Kurnakov, N., Osokoreva, N. Kali, 1932, **2**: 26-27

Solvent Effects on Intramolecular Charge Transfer Dynamics of 9-Aryl Carbazole Studied by Ultrafast Transient Absorption Spectroscopy

[1]*Takamoto, K., [1]Ueno, Y., [1,2]Ohta, K., [3]Hayashi, M., [1]Akimoto, S., [1]Matsubara, R. & [1,2]Tominaga, K.

[1] Graduate School of Science, Kobe University, Japan
[2] Molecular Photoscience Research Center, Kobe University, Japan
[3] Center for Condensed Matter Sciences, National Taiwan University, Taiwan
Molecular Photoscience Research Center, Kobe University, Japan
tominaga@kobe-u.ac.jp

Solution phases are the most common reaction fields for many chemical reactions and biological processes. In particular, charge transfer (CT) is included in most of them as a fundamental step and depends on static and dynamic properties of solvents. In this work we studied the intramolecular CT (ICT) dynamics of 3,6- bis(dimethylamino)-9-(4-cyanophenyl)carbazole (BANCC, Fig. 1 [1]) in various solvents with different polarity using femtosecond transient absorption (TA) spectroscopy.

The fluorescence spectrum of BANCC shifts to the longer wavelengths more greatly than that of BAC (Fig. 2), a donor part of BANCC (Fig. 1), as the solvent polarity increases. On the other hand, both of the molecules show two bands at 340 and 390 nm in the absorption spectra, which are independent of the solvent. These results show that BANCC undergoes charge separation upon photoexcitation. Figure 3 displays TA spectra of BANCC in THF after photoexcitation at 400 nm. A band emerges at 680 nm immediately after the excitation, and another band rises at 540 nm with a decay of the initial band. Comparing the band at 680 nm with TA spectra of BAC, BANCC is considered to be locally excited (LE) at the BAC moiety. The band at 540 nm temporally evolves with a blue shift, whose time constant is similar to the solvation time of THF. Because the similar behavior is observed in the other solvents, ICT dynamics of BANCC is influenced by both the static and dynamic properties of solvents.

[1] Matsubara, R., et al., J. Org. Chem., **84**, 5535 (2019).

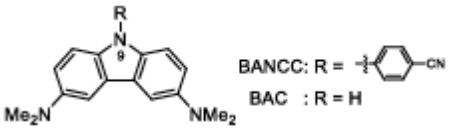

Fig. 1. Molecular structures of BANCC and BAC.

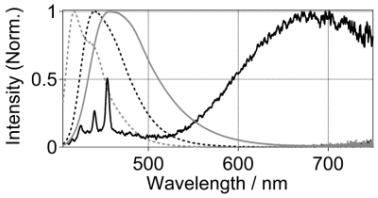

Fig. 2. Fluorescence spectra of BANCC (solid lines) and BAC (dashed lines) in cyclohexane (gray) and acetonitrile (black).

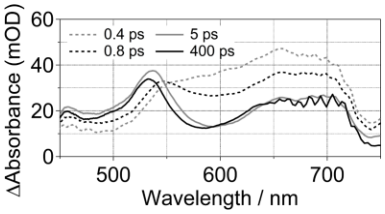

Fig. 3. TA spectra of BANCC in THF at each of delay times.

Solubility phenomena of polyhalite in water at different temperatures

[1]* Fangtong Ma, [1]Ying Zeng & [1]Xudong Yu

[1]College of Materials and Chemistry & Chemical Engineering, Chengdu University of Technology, Chengdu, P. R. China.

College of Materials and Chemistry & Chemical Engineering, Chengdu University of Technology, Chengdu, P. R. China.

zengyster@163.com

Polyhalite ($K_2SO_4·MgSO_4·2CaSO_4·2H_2O$) is an important potassium resource[1]. The investigation of solubility of polyhalite is the key to utilize polyhalite. Then, the solubility experiment of polyhalite in water was carried out at 50 ℃, 60 ℃, 75 ℃ and 90 ℃. And the variation of concentrations of potassium and calcium with time in water at different temperatures were explored. As shown in Fig. 1, in the initial stage of the dissolution, the concentration of potassium in water increases rapidly over 0-15 minutes at 90 ℃. The concentration of calcium in water increases first and then decreases with the increase of the dissolution time. It shows that the Ca^{2+} and SO_4^{2-} released by the dissolution of polyhalite are re-adsorbed on the surface of polyhalite to form "calcium sulfate inclusions"($CaSO_4·nH_2O$), which is not conducive to the further dissolution of polyhalite. As a result, the concentration of potassium ion is far from saturated when the solution is in equilibrium. After 15 minutes, the concentration of potassium at 75 ℃, 60 ℃ and 50 ℃ gradually exceeds the concentration of 90 ℃. This fact may be controlled by the difference of "inclusions" composition and structure caused by the difference of solution temperature.

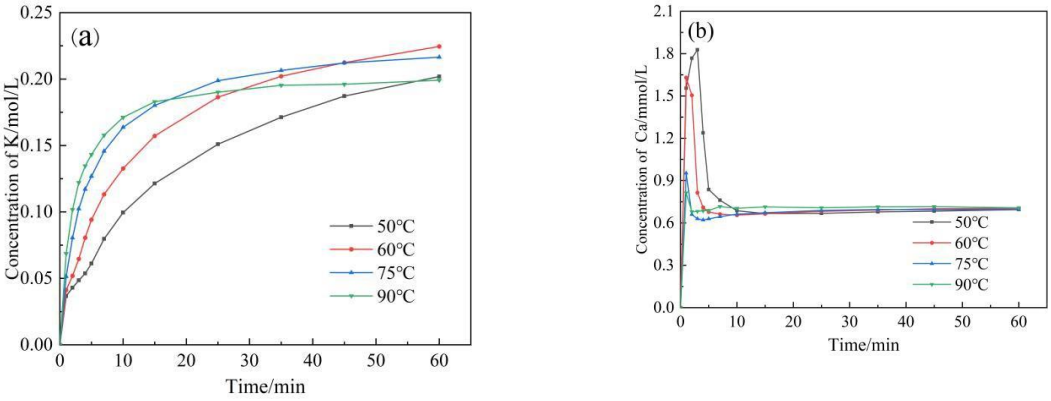

Fig 1. Relationship between potassium(a) ion and calcium(b) ion concentration in water with dissolution time and temperature

This work is supported by National Natural Science Foundation of China (No. U21A2017)

Reference

1. Zheng, M. P., Zhang, Y. S., Shang, W. J., et al. Geol China., 2018, **45** 1074-1075.

Solid-Liquid Phase Equilibria of Quaternary System Containing the Chlorides of Lithium, Potassium and Calcium at 298.2 K

[1]*Siying Ren, [1]Jun Luo & [1]Xudong Yu

[1]College of Materials and Chemistry & Chemical Engineering, Chengdu University of Technology, Chengdu, P. R. China.

College of Materials and Chemistry & Chemical Engineering, Chengdu University of Technology, Chengdu, P. R. China.

xwdlyxd@126.com

The underground brine in the Sichuan Basin is one of the main distribution areas of underground brine resources in China[1]. It belongs to chloride-type and potassium-rich brine, and the concentration of lithium also has reached the comprehensive utilization grade[2]. It is worth noting that due to the high concentration of Ca^{+} in the brine, the interaction between salts becomes very complicated, and complex salts such as double salts are formed. In order to obtain the dissolution and precipitation rules of the salts in the underground brine, it is necessary to carry out the study of phase equilibria according to the composition characteristics of the brine, so as to provide data support for the subsequent brine mining.

Therefore, the phase equilibria of the quaternary system LiCl-KCl-$CaCl_2$-H_2O at 298.2 K was investigated by using the isothermal dissolution method. The stable phase diagram of the quaternary system was plotted in Fig 1. Result shows that the system is a complex type with the double salt LiCl·$CaCl_2$·5H_2O formed, indicating that the crystalline form of lithium in the system becomes complicated with the existence of Ca^{+}. The crystallization area of KCl is the largest in the phase diagram, accounting for about 85% of the total crystallization area, which indicating that the solubility of KCl in this system is the smallest. In addition, the size of the crystallization areas of this system decrease in the order of KCl, LiCl·H_2O, $CaCl_2$·4H_2O, LiCl·$CaCl_2$·5H_2O and $CaCl_2$·6H_2O, and the components in the system can be separated out according to this crystallization rule.

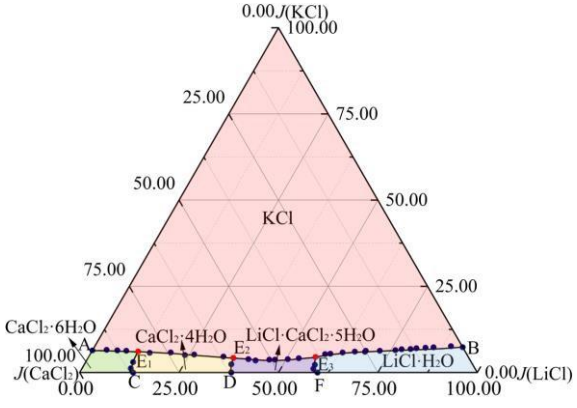

Fig 1. Stable phase diagram of the quaternary system LiCl-KCl-$CaCl_2$-H_2O at 298.2 K

This work is supported by Sichuan Science and Technology Program(No. 2022YFQ0075).

References

1. Han, J. H., Nie Z., Fang, C. H., Wu, Q., Cao, Q., Wang, Y. S., Bu L. Z., Yu, J. J. Inorg. Chem. Ind., 2021, **53**: 61-66.
2. Zhou, X., Cao, Q., Yin, F., Guo, J., Wang, X. C., Zhang, Y. S., Wang, L. D., Shen, Y. Acta Geol. Sin., 2015, **89**: 1908-1920.

Phase equilibria of chlorides containing lithium, magnesium and calcium at 323 K

[1]*Ke Chen, [1]Ying Zeng, [1]Xudong Yu, [1]Ke Wang & [1]Siying Ren
[1]College of Materials and Chemistry & Chemical Engineering, Chengdu University of Technology, Chengdu, P. R. China
Chengdu University of Technology, Chengdu, P. R. China
zengyster@163.com

Lithium, which is one of important materials of green energy in the 21st century, has attracted worldwide attention as a vital strategic reserve resource. There is a high concentration of lithium in underground brine in Sichuan Basin, an important liquid mineral resource in China. However, due to the complex interaction of Li^+, Mg^{2+} and Ca^{2+} in aqueous solution, it's easy to form double salts $LiCl{\cdot}MgCl_2{\cdot}7H_2O$, $LiCl{\cdot}CaCl_2{\cdot}5H_2O$ and $2MgCl_2{\cdot}CaCl_2{\cdot}12H_2O$, resulting in the difficulty of separating Mg^{2+} & Ca^{2+} from Li^+ and the decrease of recovery rate of Li^+. In order to better understand the dissolution of Li^+, Mg^{2+} and Ca^{2+}, the phase equilibria of quaternary system $LiCl+MgCl_2+CaCl_2+H_2O$ at 323 K was studied by the isothermal dissolution method and compare the phase diagrams at 323 K and 298 K.[1] As shown in Fig. 1, results show that (1) the quaternary system at 323 K and 298 K belongs to a complex system with double salts $LiCl{\cdot}MgCl_2{\cdot}7H_2O$ & $2MgCl_2{\cdot}CaCl_2{\cdot}12H_2O$ and $LiCl{\cdot}CaCl_2{\cdot}5H_2O$ formed. (2) calcium chloride hydrate exists in the form of $CaCl_2{\cdot}4H_2O$ and $CaCl_2{\cdot}6H_2O$ at 298 K and $CaCl_2{\cdot}2H_2O$ at 323 K, but $LiCl{\cdot}CaCl_2{\cdot}5H_2O$ only exists at 298 K. (3) with the increase of temperature, the crystallization region of $LiCl{\cdot}H_2O$ increases, and the crystallization regions of $MgCl_2{\cdot}6H_2O$ and$\cdot CaCl_2{\cdot}2H_2O$ decrease, while $CaCl_2{\cdot}4H_2O$ and $CaCl_2{\cdot}6H_2O$ transform into $CaCl_2{\cdot}2H_2O$. (4) the crystallization regions of $CaCl_2{\cdot}2H_2O$, $CaCl_2{\cdot}4H_2O$, $CaCl_2{\cdot}6H_2O$ and $LiCl{\cdot}H_2O$ are small, and the crystallization region of $MgCl_2{\cdot}6H_2O$ is maximum.

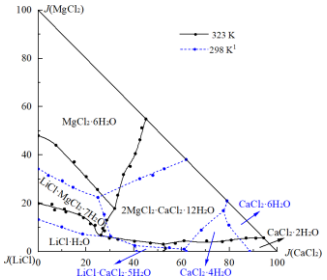

Fig 1. Comparison diagram of the quaternary systems $LiCl+MgCl_2+CaCl_2+H_2O$ at 323 K and 298 K

This work is supported by National Natural Science Foundation of China (No. U21A2017)

References

1. Cui R. Z., Li W., Dong Y. P., Sang S. H., CIESC J. 2018, **69**: 4148-4155.

Phase equilibria for system containing the sulfates of sodium and potassium at 303.2 K

[1]*Zhihao Yao, [1]Xudong Yu, [1]Zhixing Zhao, [1]Xia Feng & [1]Ying Zeng
[1]College of Materials and Chemistry & Chemical Engineering, Chengdu University of Technology, Chengdu, P. R. China.
College of Materials and Chemistry & Chemical Engineering, Chengdu University of Technology, Chengdu, P. R. China.
xwdlyxd@126.com

Potassium resources in China are mainly distributed in the salt lake brine in the form of liquid mineral resources[1], due to the complex interaction between salt lake ions, the separation and extraction of potassium are more difficult, especially in sulfate-type salt lakes. The stage of drying salt in the salt field, the sodium and potassium are continuously concentrated to form sodium potassium mixed salt, which increases the difficulty of extracting and separating potassium. Generally, phase equilibrium research is theoretical basis for the development of brine resources. Therefore, the phase equilibria study of Na^+, K^+ // SO_4^{2-} - H_2O 303.2 K was carried out and compared the phase diagrams of the system at different temperatures. Fig.1 shows that the system is a complex system with double salt $Na_2SO_4 \cdot 3K_2SO_4$, and the crystallization field of $Na_2SO_4 \cdot 3K_2SO_4$ is the largest. A comparison of phase diagrams at different temperatures is shown in Fig.2, there is no double salt $Na_2SO_4 \cdot 3K_2SO_4$ produced at 273.2 K, and with the increase of temperature, the double salt $Na_2SO_4 \cdot 3K_2SO_4$ formed at 303.2 K, and the crystallization field of the $Na_2SO_4 \cdot 3K_2SO_4$ decreases, which indicates that the temperature conditions can be controlled to avoid the loss of potassium due to the formation of double salt.

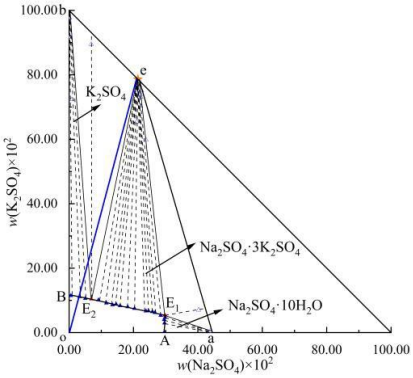

Fig 1. The phase diagram of system containing the sulfates of sodium and potassium at 303.2 K

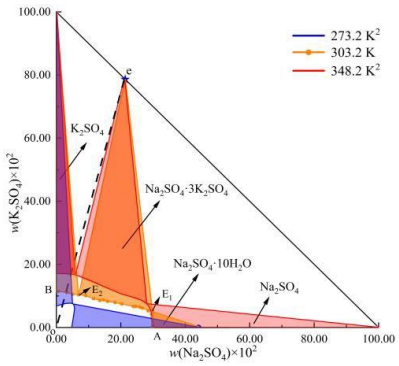

Fig 2. The multi-temperature phase diagram of the system containing sulfates of sodium and potassium

This work is supported by Sichuan Science and Technology Program(No. 2022YFQ0075).

References

1. Hou, X. H., Fan, F., Zheng, M. P., Song, P. S. Sci. Technol. Rev., 2017, **35**: 67-71.
2. Howard, D., Silcock, L. Nature, 1979, **2**: 339-348.

Phase equilibria for the ternary system lithium, sodium, and sulfate：effect of the temperatura

[1]*Zhixing Zhao, [1]Xudong Yu, [1]Shuai Chen & [1]Ying Zeng.
[1]College of Materials and Chemistry & Chemical Engineering, Chengdu University of Technology, Chengdu, P. R. China.
College of Materials and Chemistry & Chemical Engineering, Chengdu University of Technology, Chengdu, P. R. China
xwdlyxd@126.com

The advantages of many co-existence ions (Li^+, Na^+, K^+, Mg^{2+}, SO_4^{2-}, et al) and high lithium content in the sulfate - type salt lake brine resources of the Qinghai-Tibet Plateau have broad prospects for development and utilization. Due to the complexity of the interaction between lithium and coexisting ions in salt lake, double salts containing lithium are easily formed, and the types of double salts are greatly affected by temperature, both of which will lead to the difficulty of development and utilization of lithium resources in salt lake. Therefore, the phase equilibrium of the ternary system Li^+, Na^+ // SO_4^{2-} - H_2O at 303.2 K was determined in this work. Combined with experimental and literature data[1-3], the phase diagram of the ternary system Li^+, Na^+ // SO_4^{2-} - H_2O at 288.2, 298.2, 303.2, and 308.2 K was plotted (Fig. 1). Results show that (1) salts $Li_2SO_4{\cdot}3Na_2SO_4{\cdot}12H_2O$ and $Li_2SO_4{\cdot}H_2O$ are formed at all temperatures, salt $Na_2SO_4{\cdot}10H_2O$ is formed at 288.2, 298.2, and 303.2 K, and salts $Li_2SO_4{\cdot}Na_2SO_4$ and Na_2SO_4 are formed at 308.2 K. (2) With the temperature increasing from 288.2 to 303.2 K, the crystallization areas of $Li_2SO_4{\cdot}3Na_2SO_4{\cdot}12H_2O$ and $Li_2SO_4{\cdot}H_2O$ increase, while the crystallization area of $Na_2SO_4{\cdot}10H_2O$ decreases. Because of the formation of the double salt $Li_2SO_4{\cdot}Na_2SO_4$ at 308.2 K, the crystallization areas of $Li_2SO_4{\cdot}3Na_2SO_4{\cdot}12H_2O$ and $Li_2SO_4{\cdot}H_2O$ decrease.

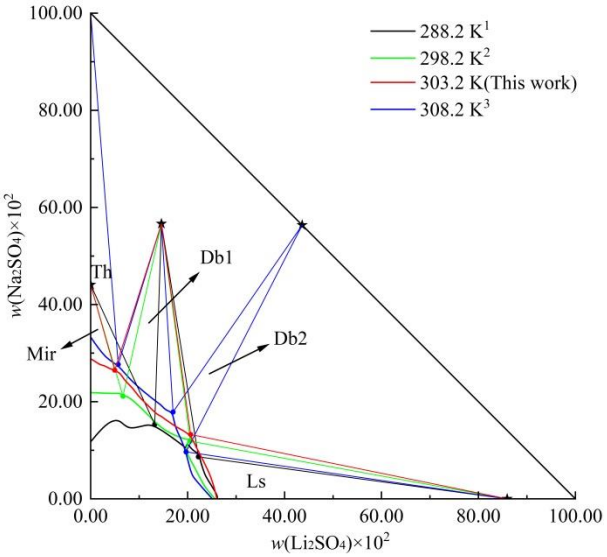

Fig. 1 Phase diagram of the ternary system Li^+, Na^+ // SO_4^{2-} - H_2O at 288.2, 298.2, 303.2, and 308.2 K (Th, Na_2SO_4; Mir, $Na_2SO_4{\cdot}10H_2O$; Ls, $Li_2SO_4{\cdot}H_2O$ Db1, $Li_2SO_4{\cdot}3Na_2SO_4{\cdot}12H_2O$; Db2, $Li_2SO_4{\cdot}Na_2SO_4$;).

This work is supported by Sichuan Science and Technology Program (No. 2022YFQ0075).

References

1 Guo, Y. F., Liu, Y. H., Wang, Q., et al. J. Chem. Eng. Data, 2013, **58**: 2763 - 2767.
2 Sohr, J., Voigt, W., Zeng, D. W. J. Phys. Chem. Ref. Data, 2017, **46**: 69 - 72.
3 Ji, Z. Y., Peng, J. L., Yuan, J. S., et al. Fluid Phase Equilib., 2015, **397**: 81 - 86.

Estimation of conformational entropy of ionic liquids

[1]*Hiroki Sumida, [1,2]Yoshifumi Kimura, [2]Takatsugu Endo
[1] Department of Applied Chemistry, Graduate School of Science and Engineering, Doshisha University, Japan
[2] Department of Molecular Chemistry and Biochemistry, Faculty of Science and Engineering, Doshisha University, Japan
Department of Applied Chemistry, Graduate School of Science and Engineering, Doshisha University, Japan
cyjg1703@mail4.doshisha.ac.jp

Ionic liquids (ILs) are defined as salts with melting points below 100 °C. Since the melting point is the crucial physical property for ILs, numerous investigations have been made to answer why ionic liquids have such a low melting point as salts. Thermodynamically, melting point (T_m) is expressed by $T_m = \Delta_{fus}H/\Delta_{fus}S$ where $\Delta_{fus}H$ is the fusion enthalpy and $\Delta_{fus}S$ is the fusion entropy. Contrary to the conventional discussion[1)], we have found that $\Delta_{fus}S$ plays a more important role than $\Delta_{fus}H$ in lowering the melting point of ILs[2)], i.e., large $\Delta_{fus}S$ of ILs drastically lowers their T_m. Since most ILs have flexible alkyl chains, the conformational entropy (S_{conf}) in the liquid state may contribute to the large $\Delta_{fus}S$ of ILs. In this research, conformations of the alkyl chain, e.g., trans, gauche, gauche′, were analyzed by molecular dynamics (MD) simulations and NMR spectroscopy to estimate S_{conf} of ILs in the liquid state. 1-Alkyl-3-methylimidazolium bis(trifluoromethylsulfonyl)imide ([$C_n$mim][NTf_2]) were used for both simulations and experiments.

First, S_{conf} of [$C_n$mim][NTf_2] (n = 1~12) in the liquid states were estimated from NPT MD trajectories (Fig. 1. (a)). The black line in the figure represents maximum S_{conf} where the population of all conformations of the alkyl chain exists equally. The estimated S_{conf} by MD (red circles) was always lower than the maximum S_{conf} and the gap increased with increasing the alkyl chain length. It was found that the small S_{conf} originated from the large population of the trans conformation (e.g., Fig. 1. (b)). A similar result was also obtained from J-coupling constants that reflect the conformations of the alkyl chain by NMR experiments. The MD simulations and NMR measurements suggested that strong interactions among the alkyl chains led the formation of the trans conformation.

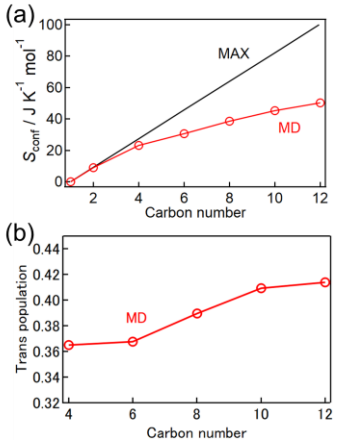

Fig. 1. (a) S_{conf} versus the number of carbon in the alkyl chain of $C_n$mim+. (b) Population of the trans conformation of N-C-C-C versus carbon in the alkyl chain of $C_n$mim+.

1) P. M. Dean et al. Phys. Chem. Chem. Phys. **2010**, 12, 9144.
2) T. Endo et al. Chem. Sci., in press.

Structure of Aqueous KNO_3 Solutions by Wide-Angle X-ray Scattering and Density Functional Theory

Hongyan Liu[1], Yongquan Zhou[1], Fayan Zhu[1], Toshio Yamaguchi[1,2*]

[1] Key Laboratory of Comprehensive and Highly Efficient Utilization of Salt Lake Resources; Key Laboratory of Salt Lake Resources Chemistry of Qinghai Province; Qinghai Institute of Salt Lakes, Chinese Academy of Sciences, Xining, Qinghai 810008, China.

[2] Department of Chemistry, Faculty of Science, Fukuoka University, 8-19-1 Nanakuma, Jonan, Fukuoka 814-0180, Japan.

*Corresponding author: Toshio Yamaguchi, yamaguch@fukuoka-u.ac.jp.

The structure of aqueous KNO_3 solutions was studied by wide-angle X-ray scattering (WAXS) and density functional theory (DFT). The interference functions were subjected to empirical potential structure refinement modelling to extract the detailed hydration structure information. In aqueous KNO_3 solutions at a concentration from 0.50 to 2.72 mol·dm^{-3}, K^+ is coordinated by water molecules with a mean coordination number (CN) from 6.6±0.9 to 5.8±1.2, respectively, at a K-O_W(H_2O) distance of 2.82 Å. To further describe the hydration properties of K^+, a hydration factor (f_h) was defined on the basis of the orientational angle between the water O-H vector and the ion-oxygen vector. The f_h value obtained for K^+ is 0.792, 0. 787, 0.766, and 0.765; the corresponding average hydration numbers (HN) are 5.2, 5.1, 4.8, and 4.5, respectively. The reduced HN is compensated by direct binding of oxygen atoms of NO_3^- with the average CN from 0.3±0.7 to 2.6±1.7, respectively, and the K-O_N(NO_3^-) distance of 2.82 Å. The average number of water molecules around NO_3^- slightly reduces from 10.5±1.5 to 9.6±1.7 with $r_{N\text{-}OW}$=3.63 Å. K^+-NO_3^- ion association is characterized by K-O_N and K-N pair correlation functions. A K-N peak is observed at 3.81 Å as a main peak with a shoulder at 3.42 Å in $g_{K\text{-}N}(r)$. This finding indicates two occupancy sites available for K^+, i.e. one is bidentate and the other is monodentate contact ion pairs. The structure and stability of $KNO_3(H_2O)_{10}$ cluster were investigated by a DFT method and cross-checked with the results from WAXS.

Keywords: Potassium nitrate; Wide angle X-ray scattering; Empirical potential structure refinement; Density functional theory; Hydration factor

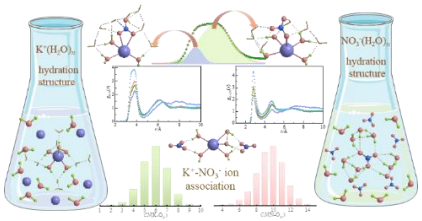

Fig. 1. Microhydration structures of aqueous KNO_3 solutions including the hydration of K^+, NO_3, and K^+-NO_3^- ions association.

MD and TD-DFT studies of solvent effects on the spectroscopic properties of aniline: Similarity and dissimilarity between water and methanol

[1]Watanabe, T. & [1]*Ohashi, K.
[1] Department of Chemistry, Kyushu University, Japan
kazu@chem.kyushu-univ.jp

Solvent effects on the $S_1 \leftarrow S_0$ absorption spectra are investigated for aniline ($C_6H_5NH_2$) dissolved in cyclohexane, methanol, and water. Density functional theory (DFT) calculations for 1:1 aniline–solvent complexes in the S_0 state predict that an N-bound isomer with an intermolecular OH···N hydrogen bond is the global minimum for the water and methanol complexes. In the S_1 state, on the other hand, the OH···N bond gets weakened while an H-bound isomer with an NH···O hydrogen bond becomes lowest, as predicted from time-dependent DFT (TD-DFT) calculations. The N-bound solvent causes a blue shift, while the H-bond solvent and a solvent binding to the □ electrons cause red shifts of the $S_1 \leftarrow S_0$ transition. Molecular dynamics simulations are used to allocate water or methanol molecules around aniline for constructing model structures with a complete solvation shell. TD-DFT calculations for 50 model structures are successful in reproducing the experimental observation that the absorption band is broadened inhomogeneously and that the band maximum in methanol is less-blue shifted than that in water. Inspection of the local solvation environment of aniline suggests that at least one water molecule is almost incessantly bound to the nitrogen atom and causes the significant blue shift. In contrast, methanol molecules are less frequently bound to the nitrogen atom and therefore the blue-shifting effect is less significant.

The Hydration Structure and Transport Behavior of Li^+ and Mg^{2+} in Confinement Space

Ruirui Liu, Yongquan Zhou*, Fayan Zhu, Hongyan Liu, Yifan Shao
Key Laboratory of Comprehensive and Highly Efficient Utilization of Salt Lake Resources; Key Laboratory of Salt Lake Resources Chemistry of Qinghai Province; Qinghai Institute of Salt Lakes, Chinese Academy of Sciences, Xining, Qinghai 810008, China
yongqzhou@163.com

The behaviors of the ionic hydration in nanopore are both biological and chemical interests. Using carbon nanotube (CNT) as the 1-D nanopore model, we investigated the hydration and transfer of Li^+ and Mg^{2+} with molecular dynamics simulation. The simulation results indicate that the hydration structure of these two cations is different from the bulk solution and causes a diameter-dependent variation for the interaction energy between the cation and water molecules. In the five researched CNTs of this work, it is energetically favorable for confining a hydrated Li^+ and Mg^{2+} inside the narrow CNTs with diameters of 0.60 nm, whereas the situation is reverse inside the wide CNTs with diameters of 1.0, and 1.28 nm. Moreover, the diffusion constant D of Li^+ in each CNT is always greater than that of Mg^{2+}, which provides a theoretical reference for Li^+ and Mg^{2+} separation. These results help to understand the chemical processes under confined conditions and may shed some light for the separation in salt lake brine.

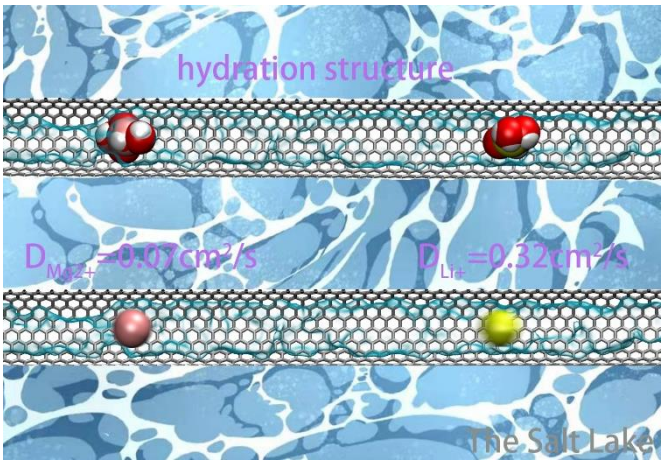

The Stable Phase Diagram of the Quaternary Water-Salt System Li^+, K^+, Mg^{2+} // SO_4^{2-} - H_2O at T = 323.2 K

[1]*Wenzhang Zuo, [1]Shuang Liao, [1]Ying Zeng, [1]Xudong Yu

[1]College of Materials and Chemistry & Chemical Engineering, Chengdu University of Technology, Chengdu, P. R. China.

Chengdu University of Technology, Chengdu, P. R. China.

zengyster@163.com

The salt lakes, localed in the Qaidam Basina, Qinghai-Tibet Plateau, are abundant with The salt lakes, localed in the Qaidam Basina, Qinghai-Tibet Plateau, are abundant with mineral resources such as Li, K and Mg, and exhibit great potential. The higher the magnesium-lithium ratio and a large number of associated elements in local salt lake brines, the more difficult extraction and separation of high-value elements from brine.1 In order to efficiently separate lithium, potassium and magnesium resources in sulfate-type brines and realize comprehensive utilization of the saline lake, the phase diagram of the quaternary system Li^+, K^+, Mg^{2+} // SO4^{2-} - H2O at 323.2 K were carried out.

The phase diagram contains two double salts (Li2SO4·K2SO4, K2SO4·MgSO4·4H2O) in Figure 1. The MgSO4·6H2O occupies the smallest phase area and has the largest solubility. Compared to the stable phase diagram of the system at different temperatures (273.22, 323.2, and 348.2 K2), it is found that the crystal forms is MgSO4·7H2O, MgSO4·6H2O, and MgSO4·H2O correspond-ing to temperatures of 298.2, 323.2, and 348.2 K, respectively. The K2SO4·MgSO4·6H2O and K2SO4·MgSO4·4H2O have been formed at 273.2 K and 323.2 K, respectively. At 348.2 K, K2SO4·MgSO4·4H2O and K2SO4·2MgSO4 were formed simultaneously.

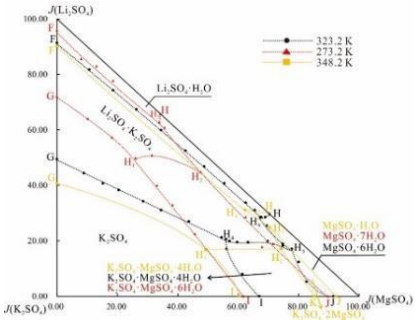

Fig. 1 Phase diagram of the quaternary system Li^+, K^+, Mg^{2+} // SO_4^{2-} - H_2O 273.2 K、323.2 K、348.2 K

References:

1 Zheng M P, Li X F. 2007. Lithium resources in China [J]. New material industry, **9(08)**: 13-16.

2 Sohr, J, Voigt, W, Zeng, D. W. 2017. IUPAC-NIST solubility data series. 104. Lithium sulfate and its double salts in aqueous solutions [J]. Journal of Physical and Chemical Reference Data, **46,** 23101.

Phase equilibria of lithium, ammonium and chlorine in aqueous solution at 298.2 K and 323.2 K

[1]*Jun Luo, [1]Xudong Yu, [1]Siying Ren, & [1]Ying Zeng

[1]College of Materials and Chemistry & Chemical Engineering, Chengdu University of Technology, Chengdu, P. R. China.

College of Materials and Chemistry & Chemical Engineering, Chengdu University of Technology, Chengdu, P. R. China.

xwdlyxd@126.com

There is a large amount underground brine with high lithium content widely distributed in the Sichuan Basin. Compared with the salt lake and seawater, the ammonium ion was found in the underground brine[1], which brings a new salt relationship. To understand the crystallization rule of lithium and ammonium coexist in the chloride type underground brine, the phase equilibria of the system Li^+, NH_4^+ // Cl^- - H_2O at 298.2 K and 323.2 K were investigated by using isothermal equilibrium dissolution method, meanwhile the comparison of the phase diagrams of the system at 298.2 and 323.2 K was done in Fig.1[2]. Results show that (1) lithium is crystallized and precipitated with the form of LiCl and solid solution $(NH_4Cl)_x(LiCl{\cdot}H_2O)_{1-x}$ at 298.2 K and 323.2 K. (2) the solid solution $(NH_4Cl)_x(LiCl{\cdot}H_2O)_{1-x}$ occupies almost all the phase regions of lithium crystallization at 298.2 K and 323.2 K. (3) the crystalline phase regions of NH_4Cl, $LiCl{\cdot}H_2O$ and $(NH_4Cl)_x(LiCl{\cdot}H_2O)_{1-x}$ decrease with the increase of temperature.

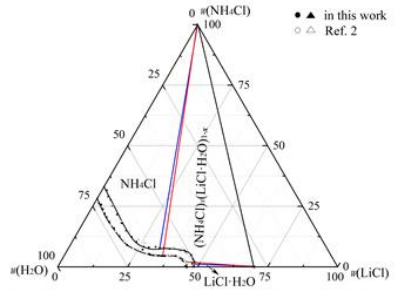

Fig.1 The comparison of phase diagrams of Li^+, NH_4^+ // Cl^- - H_2O system at 298.2 K (▲, △) and 323.2 K(●, ○)[2]

This work is supported by Sichuan Science and Technology Program (No. 2022YFQ0075).

References

1. Zhou, X., Cao, Q., Yin, F., Guo, J., Wang, X. C., Zhang, Y. S., Wang, L. D., Shen, Y. Acta Geol. Sin., 2015, **89**: 1908 - 1920.
2. Ouyang, H. T., Zeng, D. W., Zhou, H. Y., Han, H. J., Yao, Y. J. Chem. Eng. Data, 2011, **56**: 1096 - 1104.

Non-Arrhenius like behavior in viscosity of 1,2-propanediol solutions with $LiBF_4$

Terashima, Y.
Naruto University of Education, Japan
yterashima@naruto-u.ac.jp

1,2-Propanediol is one of the simple alcoholic solvents with a high solubility for $LiBF_4$ and a wide temperature range for liquids. The physical properties of good solvents for lithium ions and its solutions are important not only for pure solution chemistry but also for industrial applications such as the development of electrolytes for lithium ion batteries. In this study, we measured the viscosity of 1,2-propanediol solutions mixed with $LiBF_4$ at the temperature range of 280–340 K using a sine-wave vibro-viscometer. The temperature dependence of the viscosity of the mixtures was found to be fitted by the Vogel-Fulcher-Tamman (VFT) equation, which has been used for describing non-Arrhenius like behavior of liquids. The VFT fitting parameter, D, which is an indicator of non-Arrhenius like behavior (fragility), was found to be consistent with the results from a thermal analysis with differential scanning calorimetry. A smaller D corresponds to a more pronounced non-Arrhenius like behavior, i.e., a more fragile liquid. With increasing $LiBF_4$ mole fraction, x, the value of D decreased rapidly for $x < 0.20$, whereas it remained approximately unchanged for $x > 0.20$. The concentration dependence of D indicates that the intrinsic hydrogen-bonding networks between solvent molecules are rapidly destroyed by the intervention of added ions at lower salt concentrations, while such a structural breaking effect of ions weakens at higher salt concentration. The other VFT parameter, T_0, which gives the temperature at which the viscosity diverges infinitely, corresponds to the ideal glass transition temperature. The concentration dependence of T_0 also differed at around $x = 0.20$ as well as that of D. These results suggest that the solvation structure and ion association in the alcoholic solution of $LiBF_4$ strongly depend on the salt concentration.

Solid-liquid phase equilibria of the aqueous system containing magnesium chloride and calcium chloride: effect of temperature

[1]*Xia Feng, [1]Jun Luo, [1]Xudong Yu & [1]Ying Zeng
[1]College of Materials and Chemistry & Chemical Engineering, Chengdu University of Technology, Chengdu, P. R. China.
College of Materials and Chemistry & Chemical Engineering, Chengdu University of Technology, Chengdu, P. R. China.
xwdlyxd@126.com

Magnesium and calcium are the major elements of the chloride brine, it is of great significance to study the solubility and crystallization behavior of $MgCl_2$ and $CaCl_2$ for development and utilization of the brine resource. The ternary system Mg^{2+}, Ca^{2+}//Cl^- - H_2O, as a basic system of the brine, has been studied by many scholars[1-4], which finds that the system is a simple system at 273.2 K, while a complex system with the double salt tachyhydrite ($2MgCl_2 \cdot CaCl_2 \cdot 12H_2O$) formed at 308.2 - 383.2 K. The annual temperature of the Qarhan salt lake is close to 278.2 K. Accordingly, the solid-liquid phase equilibria of the system Mg^{2+}, Ca^{2+}//Cl^- - H_2O at 278.2 K was studied, and the comparison of phase diagrams of the system at 278.2, 308.2 and 348.2 K was drawn in Fig 1. Results show that the system Mg^{2+}, Ca^{2+}//Cl^- - H_2O is a complex system with the double salt tachyhydrite formed at 278.2 K, the crystallization regions decrease in the sequence of $MgCl_2 \cdot 6H_2O$, $CaCl_2 \cdot 6H_2O$ and $2MgCl_2 \cdot CaCl_2 \cdot 12H_2O$. As seen in Fig.1, with the increase of temperature, the crystallization zone of tachyhydrite increases obviously, while that of $MgCl_2$ and $CaCl_2$ decreases, which indicates that low temperature is favorable for the separation of $MgCl_2$ from the solution co-existing magnesium and calcium, and high temperature is conducive to the co-precipitation of calcium and magnesium in the form of double salt.

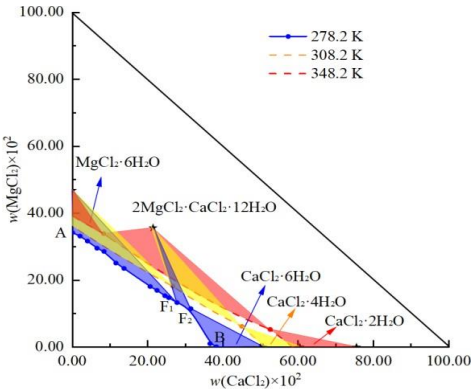

Fig 1. Comparison of phase diagrams of the system Mg^{2+}, Ca^{2+}//Cl^- - H_2O at 278.2, 308.2[2] and 348.2[3] K

This work is supported by NSFC (No. U21A2017) and State Key Laboratory of Oil and

Gas Reservoir Geology and Exploitation (No. PLC20210502).

References

1. Iver, I., Thomas, G. Thompsom. J. Am. Chem. Soc., 1936, **58**: 318-322.
2. William, J. L., Carl, F. P. J. Am. Chem. Soc., 1946, **68**: 1001-1002.
3. William, J. L., Carl, F. P. J. Am. Chem. Soc., 1947, **69**: 2098-2100.
4. Assarsson, G. O. J. Am. Chem. Soc., 1950, **72**: 1442-1444.

Fine Analysis of the component effect on the microstructure of LiCl solution by Synchrotron X-ray Scattering, Raman Spectroscopy and Molecular Dynamics Simulation

[1]Meiling Wang, [1,2,3,4*]Fei Li, [1]Mengdan Qiao, [1]Hanyu Zhu, [1]Yu Zhang, [1,2,3,4*]Junsheng Yuan

[1] Engineering Research Center of Seawater Utilization of Ministry of Education, School of Chemical Engineering and Technology, Hebei University of Technology,China

[2] Hebei Collaborative Innovation Center of Modern Marine Chemical Technology, China

[3] National-Local Joint Engineering Laboratory of Chemical Energy Saving Process Integration and Resource Utilization, School of Chemical Engineering and Technology, Hebei University of Technology, China

[4] Tianjin Key Laboratory of Chemical Process Safety, China
Hebei University of Technology, China

lifei2008_ok@126.com,

Lithium resources are abundant in Chinese salt lakes, while the high magnesium-lithium ratio has brought difficulties to the development of lithium resources. Synchrotron X-ray scattering and molecular dynamics (MD) simulation method were used to study the microstructure of LiCl aqueous solutions with different concentration. The results of the two methods show that with the increase of the LiCl mass fraction in the aqueous solution, the original tetrahedral hydrogen bond network structure is destroyed. When the mass fraction is 25%, more and more new contact ion pairs appear. The effect of $MgCl_2$ on the solution structure of LiCl aqueous solutions were also investigated and discussed in this study. Through the X-ray scattering results, it was found that the peak at r=3.2 Å in the G(r) shifted to right of the abscissa with the increase of $MgCl_2$ concentration. This phenomenon indicated the probability of Cl^--O contact ion pairs decreased with more $MgCl_2$ contained in the solution. The molecular dynamics results showed that with the decrease of Mg/Li ratio in aqueous solution, the coordination number of Li^+-Cl^- and Mg^{2+}-Cl^- gradually increased. When the amount of Cl- was the same, compared with Li^+, Mg^{2+} was more easily to form contact ion pairs with Cl^-. It was speculated that this was the micro reason why it was difficult to separate pure LiCl crystal from the LiCl and $MgCl_2$ mixed aqueous solution.

[1] Are Yllö, Chao Zhang. Experimental and molecular dynamics study of the ionic conductivity in aqueous LiCl electrolytes[J]. Chemical Physics Letters, 2019, 729: 6-10.

[2] Yuan R, Yan C, Fayer Michael. Ion-Molecule complex dissociation and formation dynamics in LiCl aqueous solutions from 2D IR spectroscopy[J]. The Journal of Physical Chemistry B, 2018, 122(46): 10582-10592.

Phase equilibrium of the aqueous ternary sulfate system containing rubidium and magnesium

[1]*Wenyu Yang, [1]Xinxin Lv, [1]Ying Zeng & [1]Xudong Yu
[1]College of Materials and Chemistry& Chemical Engineering, Chengdu University of Technology, Chengdu, P. R. China
Chengdu University of Technology, Chengdu, P. R. China
zengyster@163.com

Qaidam Basin is an important sulfate salt lake mining area in China, which is rich in beneficial elements such as lithium, magnesium, rubidium and cesium. Due to the complex interaction between magnesium and alkali metal ions, it is easy to form complex hydrate complex salts, which makes the comprehensive utilization of salt lake brine resources in Qaidam Basin difficult. According to the composition characteristics of rubidium and magnesium brine in Qaidam Basin, the study on phase equilibrium of related systems can provide theoretical guidance for the development and utilization of salt lake resources.

The phase diagram of the ternary system Rb_2SO_4+$MgSO_4$+H_2O with Rb_2SO_4·$MgSO_4$·$6H_2O$ at 273.2K, 298.2K and 323.2K, consists of three crystallization zones, three univariate curves and two invariant points. Comparing the stable phase diagrams of this ternary system at three temperatures, it was found that the crystalline region of Rb_2SO_4·$MgSO_4$·$6H_2O$ increased with increasing temperature. The temperature change also affects the crystalline from of magnesium sulfate. At 273.2K and 298.2K, $MgSO_4$ is precipitated in the form of MgSO ·7H O, and at 323.2 K, it is $MgSO_4$·$6H_2O$.

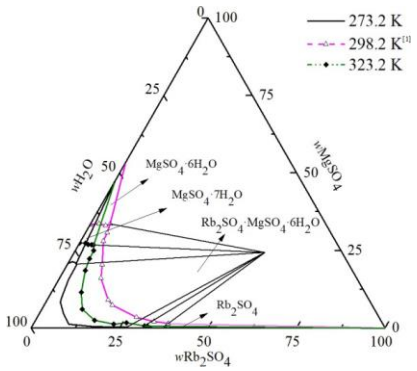

Fig.1 Multi-temperature comparison phase diagrams of the Rb_2SO_4+Mg_2SO_4+H_2O system

This work is supported by National Natural Science Foundation of China (No. U1607121).

References

1. Chen, Y., Sun, H. B., Zeng, Y., et al. Conserv. Util. Min. Resour., 2019, **39**: 73-7

Theoretical calculation of ternary system of NaCl-$MgCl_2$-H_2O based on PSC model

[1]*Feng Zhang, [1]Li Du, [1]Ying Zeng, &[1]Xudong Yu.

[1]College of Materials and Chemistry & Chemical Engineering, Chengdu University of Technology, Chengdu, P. R. China.

Chengdu University of Technology, Chengdu, P. R.

zengyster@163.com

In order to predict the crystallization forms of salts in the stable phase equilibrium of the ternary systems NaCl-$MgCl_2$-H_2O at 273.2 K, 303.2 K and 333.2 K, the phase diagrams were described and predicted from the perspective of thermodynamics.Based on the theory of electrolyte solution, free energy and average solubility product were generated by Gibbs respectively, and the phase diagram was calculated by PSC (Pitzer- Simonson-Clegg) model[1], and the calculated parameters of the system NaCl-$MgCl_2$- H_2O come from reference[2]. It can be seen from the Fig 1. that the phase diagram of the system consists of a invariant point, two dissolution curves and two crystallization regions (NaCl, $MgCl_2 \cdot 6H_2O$). Comparing multi-temperature phase diagrams of the system, it can be seen that with the increase of temperature, the crystallization region of NaCl increased and that of $MgCl_2 \cdot 6H_2O$ decreased.

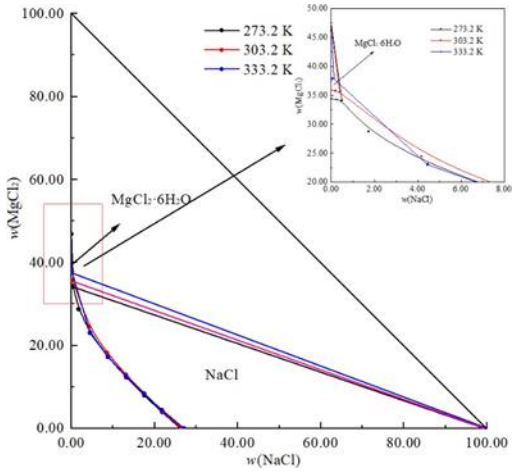

Fig 1. Calculated phase diagram of NaCl-$MgCl_2$-H_2O system at 273.2 K, 303.2 K and 333.2 K

This work is supported by National Natural Science Foundation of China (No. U21A2017).

References

1. Clegg, L., Pitzer, K. S., Brimblecombe, P. J. Phys. Chem., 1992, **96**: 9470-9479.
2. Li, D. D., Zeng, D. W., Yin, X., Gao, D. D., Fan Y. F. Calphad, 2020, **71**: 101806.

Significant ionic association and hydrogen bonds instead of hydration shell in nanoconfined aqueous electrolyte solutions

Guangguo Wang[1,3], Yongquan Zhou*[1], Yunxia Wang[1,3], Toshio Yamaguchi[2], Kazutaka Ikeda[4], Zhuanfang Jing[1,2], Hongyan Liu[1], Fayan Zhu[1]

[1]Qinghai Institute of Salt Lakes, Chinese Academy of Sciences, Xining, Qinghai 810008, China;
[2]Department of Chemistry, Faculty of Science, Fukuoka University, 8-19-1 Nanakuma, Jonan, Fukuoka 814-0180, Japan;

[3]University of Chinese Academy of Sciences, Beijing 100049, China;

[4]High Energy Accelerator Research Organization (KEK), Tsukuba, Ibaraki 305-0801, Japan
*Corresponding author: Prof. Yongquan Zhou

yongqzhou@163.com

The neutron scattering and the inverse Monte Carlo simulation technique were organically combined to study the structure of calcium chloride solution in confined space. The solution is unevenly distributed along the direction perpendicular to the pore wall in the confined space, and it can be divided into a core region, a transition region, and an interface region. In the confined space, the distance between water molecules of nanowater becomes shorter, which means that the hydrogen bond is enhanced to form a nanoscale assembly structure. From the core region to the interface area, the coordination number increases from ~4 to ~7. In the core region far away from the interface, the structure of nanoelectrolyte is similar to that of nanowater, while in the transition region, the ion association is enhanced. The density disturbance distances of the interface to the nanowater and nanoelectrolyte are 7 Å and 6 Å, respectively. The solution in the interface region is affected by the interface effect, exhibiting similar structure and properties to the bulk solution under high pressure, i.e the distance between water molecules in nanoelectrolyte is stretched, and the hydrogen bond is weakened.

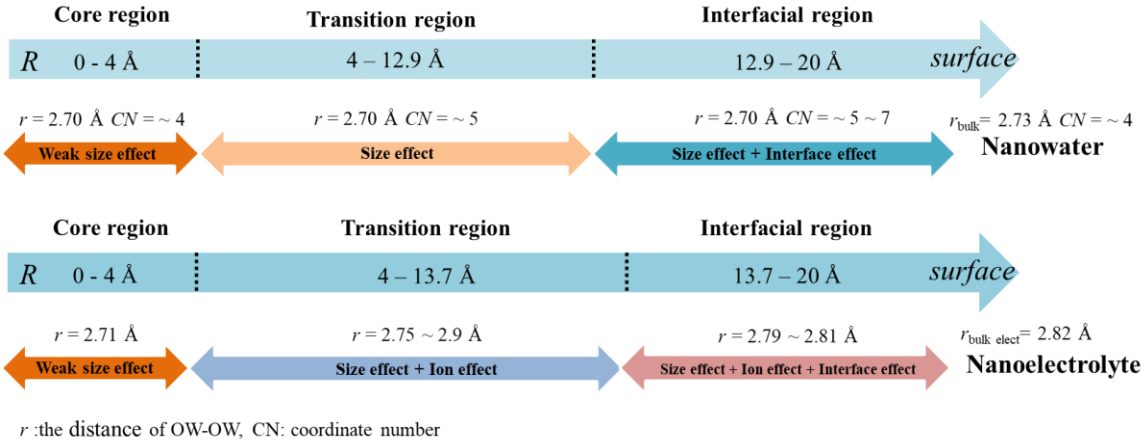

Keywords: Confined space; Electrolyte solution; Ion association; Neutron scattering; Interface effect
Acknowledgments: This work was financially supported by the National Natural Science Foundation (21973106).

In-situ observation of the decomposing process of biomass samples in high-temperature high-pressure water by neutron imaging

[1]*Yoshida K., [2]Mishima K., [3]Abe J. & [3]Matsumoto Y.
[1]Faculty of Science, Fukuoka University, Japan
[2]Faculty of Technology, Fukuoka University, Japan
[3]Comprehensive Research Organization for Science and Society (CROSS), Fukuoka University, Japan
kyoshida@fukuoka-u.ac.jp

High-temperature and high-pressure (HTHP) water has excellent properties for directly utilizing biomass. For example, HTHP water converts biomass wastes into biochar and gasifies them without drying. The development of biomass processing technology needs to reveal how the biomass sample changes in HTHP water. The reaction of the biomass waste with HTHP water progress in a stainless vessel. Since neutrons can penetrate stainless steel well, the neutron imaging technique makes the in-situ observation of the sample in stainless vessel.

In the present study, neutron transmission images of biomass samples (ceader and quercus acutissima) in HTHP water (D_2O) were observed in the temperature range from 25 °C to 450 °C at BL22 RADEN [1] in J-PARC MLF. The biomass samples were inserted into a stainless tube with D_2O. Using D_2O enhances the contrast of the biomass sample which contains many hydrogen atoms. The tubes were installed in a heating box specially designed for neutron imaging. The neutron transmission images were recorded every 6 seconds during heating. It is clarified that the images of the biomass sample in HTHP water became obscure in a range of 400 - 450 °C (17 – 20 MPa), indicating the decomposition of the biomass sample. The result would be helpful for the development of biomass processing technology using HTHP water.

[1] T. Shinohara et al., The energy-resolved neutron imaging system, RADEN, Review of Scientific Instruments 91 043302 (2020). DOI: 10.1063/1.5136034.

Structure of Choline Chloride-Carboxylic Acid Deep Eutectic Solvents from X-Ray Scattering and DFT Calculations

[1,2]Keke Chai, [1]Hongyan Liu, [1*]Yongquan Zhou, [1]Toshio Yamaguchi, [3]Koji Ohara

1. Qinghai Institute of Salt Lakes, Chinese Academy of Sciences, Xining, Qinghai 810008, China.
2. University of Chinese Academy of Sciences, Beijing 100049, China.
3. Research and Utilization Division, Japan Synchrotron Radiation Research Institute, 1-1-1 Kouto, Sayo, Hyogo 679-5198, Japan

*Corresponding author: yongqzhou@163.com

Choline chloride-carboxylic acid deep eutectic solvents (DESs) are promising green solvents for the biomass pretreatment. The micro-interaction way determines the DESs physical properties such as melting point, viscosity. In this work, interactions, coordination number and 3-dimensional spatial density function of a molar ratio 1:2 choline chloride (ChCl)/formic acid (FA), ChCl/acetic acid (AA) DESs are investigated by combining the High-Energy X-ray scattering, empirical potential structure refinement (EPSR) and density functional theory (DFT) calculations. Atom-atom radial distribution functions (PDFs) reveal that DESs are stabilized by both classic hydrogen bonds and C-H···O interactions between the components. Atoms in molecules (AIM) analysis of DESs further demonstrated hydrogen bonds and C-H···O interactions exist in DESs. The present work provides an important basis for the further applications of choline chloride-carboxylic acid DESs.

Keywords: Choline chloride; Carboxylic Acid; Deep eutectic solvent; Density functional theory; X-ray scattering; Empirical potential structure refinement

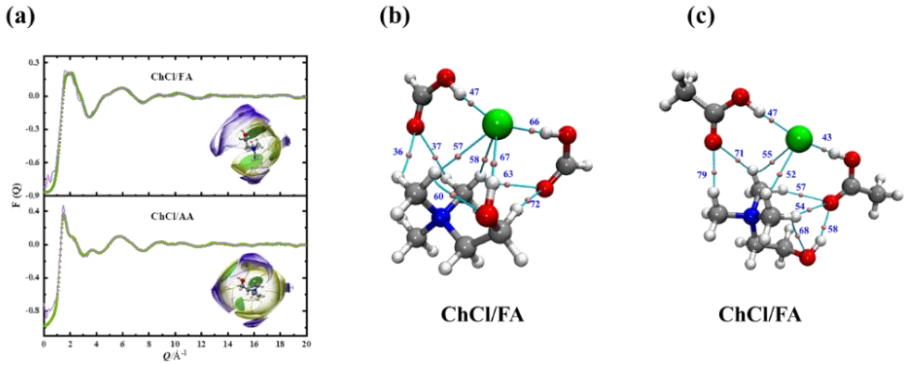

Fig. 1. Experimental (points, green) and EPSR simulated (solid lines, purple) F(Q) for ChCl/FA and ChCl/AA (a), AIM analysis of of ChCl/FA (b) and ChCl/AA (c).

Acknowledgments

The Innovation Academy for Green Manufacture (NO. ISGM2020C12), Science and Technology Department of Qinghai province (No 2019-ZJ-7001), the Instrument Function Development and Technology innovation Project of CAS (2023g104).

Unveiling the structure of aqueous magnesium nitrate solutions by X-ray diffraction and theoretical calculations

[1, 2]Yunxia Wang, [1, 2]Guangguo Wang, [3]Daniel T. Bowron, [1,3*]Fayan Zhu, [3*]Alex C. Hannon, [1]Yongquan Zhou, [1]Hongyan Liu

[1] Qinghai Institute of Salt Lakes, Chinese Academy of Sciences, Xining 81008, China
[2] University of Chinese Academy of Sciences, Beijing 100049, China
[3] ISIS Facility, STFC, Rutherford Appleton Laboratory, Chilton, Didcot, Oxon OX11 0QX, UK.
[*]Corresponding authors: Fayan Zhu, Email: zhufayan@126.com
Alex C. Hannon, Email: alex.hannon@stfc.ac.uk

The structure of aqueous magnesium nitrate solution is gaining significant interest among researchers, especially whether contact ion pairs exist in concentrated solutions. Here, combining X-ray diffraction experiments, quantum chemical calculations and ab initio molecular dynamics simulations, we found that the $[Mg(NO_3)_2]$ molecular structure in solution from the coexistence of an free $[Mg(H_2O)_6]^{2+}$ octahedral supramolecular structure with an free $[NO_3(H_2O)_n]^-$(n = 11~13) supramolecular structure to an $[Mg^{2+}(H_2O)_n(NO_3^-)_m]$ (n=3, 4, 5; m=3, 2, 1) associated structure with the increasing concentration. Interestingly, two hydration layers of NO_3^-—the first hydration layer with hydration distance less than 3.9 Å and the second hydration layer with hydration distance ranged from 3.9 to 4.3 Å—were distinguished. With the solution concentration increasing, the hydrated NO_3^- ions lost its outer layer water molecules, and the hexagonal octahedral hydration structure of $[Mg(H_2O)_6^{2+}]$ was destroyed, resulting in direct contact between Mg^{2+} and NO_3^- ions in a monodentate way. As the concentration of the solution further increased, NO_3^- ions replaced water molecules in the hydration layer of Mg^{2+} to form three-ion clusters and even more complex chains or linear ion clusters.

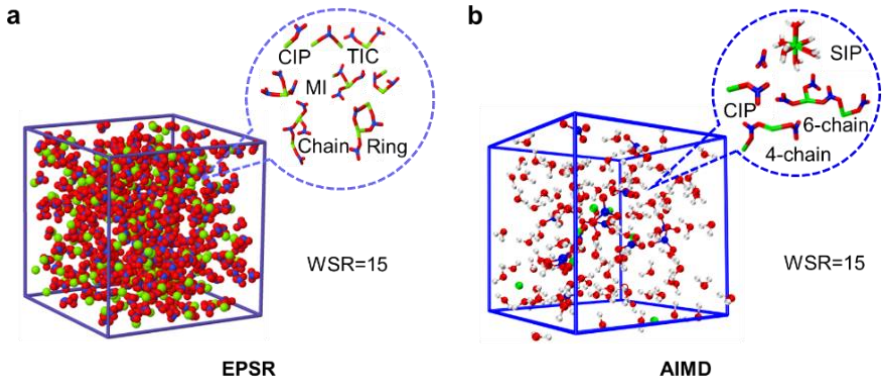

Fig. 1. EPSR (a) and AIMD (b) simulation boxes of magnesium nitrate solutions at WSR=15 and main microscopic species in each box.

[1] A. K. Soper, Physical Review B, 2005, 72, 104204.
[2] T. Laino, F. Mohamed, A. Laio, et al, J. Chem. Theory Comput, 2006, 2, 5, 1370–1378.

Identification of Molybdenum tridecamer by ESI-MS

[1]* Osuka, Y. and [1]Tanaka. M.

[1] Graduate School of Marine Science and Technology, Tokyo University of Marine Science and Technology, Japan

Graduate School of Marine Science and Technology, Tokyo University of Marine Science and Technology, Japan

mihotnk@kaiyodai.ac.jp

When ammonium molybdate is dissolved in pure water and measured by ~~the~~ electrospray ionization mass spectrometry (ESI-MS), the Mo tridecamer $[Mo_{13}O_{40}]^{2-}$ (m/z 948) is observed. To investigate the position of molybdenum (Mo) in the molecular ~~and~~ structure of $[Mo_{13}O_{40}]^{2-}$, ammonium molybdate solutions were reacted with silicic acid and phosphoric acid, respectively, and the molecular ions were identified.

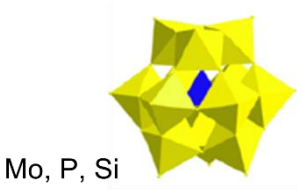

Fig.1 Keggin structure

Silicic acid: The peak intensity of $[Mo_{13}O_{40}]^{2-}$ decreased with increasing concentration of silicic acid, and the peak intensity of $[SiMo_{12}O_{40}]^{2-}$ increased.

Phosphoric acid: $[Mo_{13}O_{40}]^{2-}$ reduced to $[Mo_{13}O_{40} \cdot H_2O]^{6-}$ (m/z 319 with increasing concentration of phosphoric acid, whereas the peak intensity of $[PMo_{12}O_{40}]^{3-}$ increased.

No peaks of chemical species with Si and P bound to $[Mo_{13}O_{40}]^{2-}$ were observed. From this result, we concluded that the Mo tridecamer is preserved in the Keggin structure and Mo exists at the center of $[Mo_{13}O_{40}]^{2-}$. Further, $[SiMo_{12}O_{40}]^{2-}$ and $[PMo_{12}O_{40}]^{3-}$ are more stable than $[Mo_{13}O_{40}]^{2-}$. Also, the central Mo is easily replaced with Si or P when the concentration of the silicic acid or phosphoric acid is high.

Hydration and Dynamic Characteristics of Alkali and Halide Ions

[1,2]Zhuanfang Jing, [1*]Yongquan Zhou, [1,2]Guangguo Wang, [1,2]Keke Chai, [1]Hongyan Liu, [1]Fayan Zhu

[1] Qinghai Institute of Salt Lakes, Chinese Academy of Sciences, Xining 810008, China.
[2] University of Chinese Academy of Sciences, Beijing 100049, China.
Corresponding author: Prof. Yongquan Zhou

yongqzhou@163.com

The hydration characteristics of alkali and halides ions were systematically studied by neutron scattering, X-ray scattering and molecular dynamics simulation. When defining the ionic solvation layer based on the pair distribution functions, the larger the ion radius, the more water molecules can be contained around the ions, and the thicker the ionic solvation layer. However, when considering the orientation of water molecules (where the hydration factor is defined) in the ion hydration layer, the hydration factor of ions decreases with the ionic charge radius ratio, meaning the hydration ability of ions is weakened, and the cage effect of water molecules on ions is weaker, which makes the ion hydration radius, hydration number, hydration energy, the viscosity of the solution and the average residence time of water molecules in the first hydration layer of the ion decrease, while the self-diffusion coefficient of the ion increases, and the time the velocity autocorrelation function takes to reach the lowest point is longer. The dynamic hydration number obtained from the average residence time of water molecules has the same trend as the static hydration number obtained from the hydration factor. Li^+, Na^+ and F^- have obvious second hydration layer, while other ions have unobvious or no second hydration layer.

Keywords: Alkali halides; Hydration; Neutron scattering; X-ray scattering; Molecular dynamics

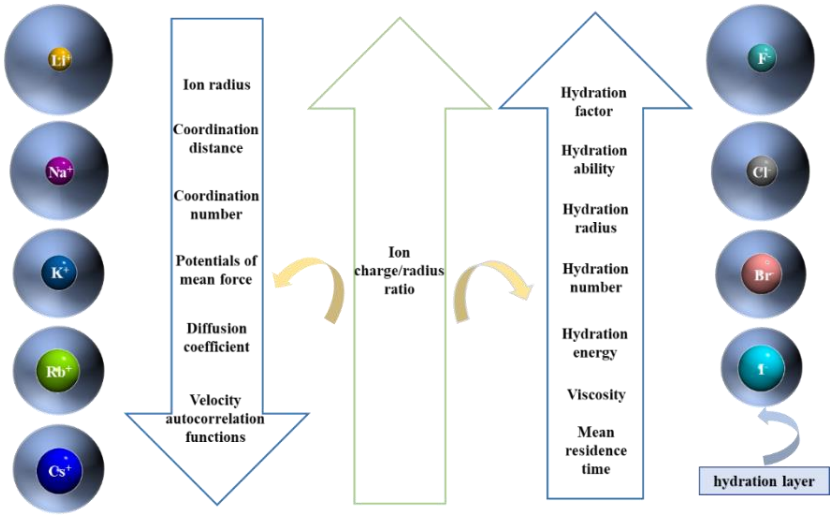

Figure 1. The variation rule of hydration characteristics with ionic charge radius ratio.

Acknowledgements: This work was financially supported by the National Natural Science Foundation of China (No.201973106) and the Innovation Platform Construction Project of Qinghai Province (2019-ZJ-T03).